



Document Number: H2020-ICT-52/RISE-6G/D4.3

Project Name:  
**Reconfigurable Intelligent Sustainable Environments for 6G Wireless Networks  
(RISE-6G)**

## Deliverable D4.3

### Deployment and control strategies of RIS based connectivity (Final Specifications)

Date of delivery: 30/06/2023  
Start date of Project: 01/01/2021

Version: 6.0  
Duration: 36 months



**Document:** H2020-ICT-52/RISE-6G/D4.3

**Date:** 30/06/2023

**Status:** Final

**Security:** Public

**Version:** 1.0

## Deliverable D4.3

### Deployment and control strategies of RIS based connectivity (Final Specifications)

<b>Project Number:</b>	101017011
<b>Project Name:</b>	Reconfigurable Intelligent Sustainable Environments for 6G Wireless Networks

<b>Document Number:</b>	H2020-ICT-52/RISE-6G/D4.3
<b>Document Title:</b>	Deployment and control strategies of RIS based connectivity (Final Specifications)
<b>Editor(s):</b>	Placido Mursia, Francesco Devoti, and Vincenzo Sciancalepore (NEC)
<b>Authors:</b>	Placido Mursia (NEC), Francesco Devoti (NEC), Vincenzo Sciancalepore (NEC), Fabio Saggese (AAU), Petar Popovski (AAU), Radosław Kotaba (AAU), Victor Croisfelt (AAU), Marco Di Renzo (CNRS), Nour Awarkeh (CNRS), Sumin Jeong (CNRS), Hajar El Hassani (CNRS), Kyriakos Stylianopoulos (NKUA), George Alexandropoulos (NKUA), Paolo Di Lorenzo (CNIT), Francesca Costanzo (CNIT), Sergio Barbarossa (CNIT), Emilio Calvanese Strinati (CEA)
<b>Dissemination Level:</b>	PU
<b>Contractual Date of Delivery:</b>	30/06/2023
<b>Security:</b>	Public
<b>Status:</b>	Final
<b>Version:</b>	6.0
<b>File Name:</b>	RISE-6G_WP4_D4.3_Final.docx



**Document:** H2020-ICT-52/RISE-6G/D4.3

**Date:** 30/06/2023

**Status:** Final

**Security:** Public

**Version:** 1.0

## Abstract

This deliverable provides the results of the RISE-6G proposals on architectures, control, signaling, and data flow related to work package 4 “RIS for Enhanced Connectivity and Reliability”, as well as final specifications and performance evaluations of these proposals.

## Keywords

*Beyond-5G; 6G; RIS; Scenarios; Architectures; Connectivity; Edge computing*



## Contents

<b>1</b>	<b>Introduction .....</b>	<b>11</b>
1.1	Deliverable objectives .....	11
1.2	Deliverable structure .....	11
1.3	Definitions and taxonomy.....	12
<b>2</b>	<b>Metrics and KPIs .....</b>	<b>15</b>
2.1	KPIs for communication channels.....	15
2.1.1	Latency .....	15
2.1.2	Spectral efficiency, throughput and goodput.....	16
2.1.3	Reliability .....	17
2.1.4	Bit Error Rate and Bit Error Ratio.....	17
2.1.5	Energy efficiency .....	17
2.1.6	Channel estimation accuracy.....	17
2.2	KPIs for control channels.....	17
2.2.1	Control Latency.....	18
2.2.2	Control Reliability.....	18
2.3	KPIs for quasi-active and active RISs .....	18
<b>3</b>	<b>Deployment strategies for network architecture .....</b>	<b>19</b>
3.1	Boosted communication and enhanced coverage.....	19
3.2	Static versus Nomadic.....	20
3.3	Edge computing.....	21
3.4	Deployment based on Artificial Intelligence.....	21
3.5	Centralized vs distributed RIS deployment.....	23
3.6	Perspective with overall RISE architecture.....	23
<b>4</b>	<b>RIS Control Plane.....</b>	<b>23</b>
4.1	RIS-aided networks with controlled RIS (explicit CC) .....	23
4.2	Control messages toward the RIS.....	24
4.3	RIS-aided networks with autonomous RIS (implicit CC).....	25
4.4	UE control messages in RIS-aided networks .....	26
<b>5</b>	<b>RIS protocol structures .....</b>	<b>26</b>
5.1	Algorithmic requirement for RIS operation.....	26
5.1.1	Channel estimation procedures.....	27
5.1.2	Computational resources .....	27
5.1.3	KPI measurement .....	27
5.2	Access procedures for RIS-empowered systems .....	28
5.2.1	RIS configuration after deployment .....	28
5.2.2	UE initial access .....	28
5.3	RAN protocol structure.....	29
5.3.1	CSI-based structure .....	29
5.3.2	Codebook-based structure .....	30
<b>6</b>	<b>RISE-6G architecture and control proposal for RIS-aided communication.....</b>	<b>30</b>
6.1	Summary of the contributions .....	30



<b>6.2</b>	<b>RIS-Aware Indoor Network Planning .....</b>	<b>32</b>
6.2.1	Motivation and context.....	32
6.2.2	Overall system description .....	33
6.2.3	Results and outcomes .....	34
6.2.4	Relation to other RISE-6G contributions .....	34
<b>6.3</b>	<b>RIS-Enabled Beamforming for Massive IoT Access.....</b>	<b>34</b>
6.3.1	Motivation and context.....	34
6.3.2	Overall system description .....	35
6.3.3	Results and outcomes .....	36
6.3.4	Relation to other RISE-6G contributions .....	36
<b>6.4</b>	<b>RIS-Empowered UAV Communications for Robust and Reliable Air-to-Ground Networks .....</b>	<b>37</b>
6.4.1	Motivation and context.....	37
6.4.2	Overall system description .....	38
6.4.3	Results and outcomes .....	40
6.4.4	Relation to other RISE-6G contributions .....	41
<b>6.5</b>	<b>Multi-UE channel estimation framework.....</b>	<b>41</b>
6.5.1	Motivation and context.....	41
6.5.2	Overall system description .....	42
6.5.3	Results and outcomes .....	43
6.5.4	Relation to other RISE-6G contributions .....	43
<b>6.6</b>	<b>Centralised multi-UE multi-RIS optimisation within a channel coherence time.....</b>	<b>44</b>
6.6.1	Motivation and context.....	44
6.6.2	Overall system description .....	44
6.6.3	Results and outcomes .....	46
6.6.4	Relation to other RISE-6G contributions .....	46
<b>6.7</b>	<b>Multi-UE codebook-based framework.....</b>	<b>46</b>
6.7.1	Motivation and context.....	46
6.7.2	Overall system description .....	47
6.7.3	Results and outcomes .....	47
6.7.4	Relation to other RISE-6G contributions .....	48
<b>6.8</b>	<b>Random access algorithm for RIS-aided communications .....</b>	<b>48</b>
6.8.1	Motivation and context.....	48
6.8.2	Overall system description .....	48
6.8.3	Results and outcomes .....	50
6.8.4	Relation to other RISE-6G contributions .....	51
<b>6.9</b>	<b>Multiple access protocol for combinations of static and mobile UEs.....</b>	<b>51</b>
6.9.1	Motivation and context.....	51
6.9.2	Overall system description .....	51
6.9.3	Results and outcomes .....	53
6.9.4	Relation to other RISE-6G contributions .....	53
<b>6.10</b>	<b>A Self-Configuring RIS Solution Towards 6G .....</b>	<b>53</b>
6.10.1	Motivation and context.....	53
6.10.2	Overall system description .....	54
6.10.3	Results and outcomes .....	55
6.10.4	Relation to other RISE-6G contributions.....	56
<b>6.11</b>	<b>RIS-Empowered MEC.....</b>	<b>56</b>
6.11.1	Motivation and context.....	56
6.11.2	Overall system description .....	56
6.11.3	Results and outcomes .....	59
6.11.4	Relation to other RISE-6G contributions.....	61
<b>6.12</b>	<b>Reconfigurable Intelligent Surfaces With Outdated Channel State Information: Centralized vs Decentralized Deployments .....</b>	<b>61</b>



6.12.1	Motivation and context .....	61
6.12.2	Overall system description .....	61
6.12.3	Results and outcomes .....	63
6.12.4	Relation to other RISE-6G contributions.....	63
<b>6.13</b>	<b>Channel estimation with simultaneous reflecting and sensing RIS.....</b>	<b>64</b>
6.13.1	Motivation and context .....	64
6.13.2	Overall system description .....	64
6.13.3	Results and outcomes .....	65
6.13.4	Relation to other RISE-6G contributions.....	65
<b>6.14</b>	<b>Static RIS tuning in rich scattering environments.....</b>	<b>66</b>
6.14.1	Motivation and context .....	66
6.14.2	Overall system description .....	66
6.14.3	Results and outcomes .....	68
6.14.4	Relation to other RISE-6G contributions.....	68
<b>6.15</b>	<b>Autonomous RIS solution with Energy harvesting and Self-configuration.....</b>	<b>68</b>
6.15.1	Motivation and context .....	68
6.15.2	Overall system description .....	68
6.15.3	Results and outcomes .....	69
6.15.4	Relation to other RISE-6G contributions.....	70
<b>7</b>	<b>Conclusions and outlook.....</b>	<b>71</b>
	<b>References.....</b>	<b>72</b>



## List of Figures

Figure 1-1: Areas covered in this deliverable and relations to D4.4. ....	12
Figure 3-1: Indoor RIS deployment scenario. ....	19
Figure 3-2: Different considerations and trade-offs in nomadic RIS deployment strategies, as highlighted from the analysis carried out in [DMS22]. ....	20
Figure 3-3: Online deployment of AI as a multiple RIS and BS orchestrator [ASH22]. In that scenario, the orchestrator observes the global CSI, determines the RIS configurations and beamforming vectors, and receives the SINR KPI which is maximised over time. ....	22
Figure 4-1: Long control payload for RIS configuration change ....	25
Figure 4-2: Short control payload for RIS configuration change ....	25
Figure 6-1: Summary of WP4 contributions in terms of communication interfaces. ....	32
Figure 6-2: Geometrical representation of the considered planning scenario. ....	33
Figure 6-3: SNR heatmap without RIS (left-hand side) and with 4 RISs represented by red squares (right-hand side). ....	34
Figure 6-4: Multi-UE RIS-empowered wireless network scenario. ....	35
Figure 6-5: Average sum rate obtained with the proposed RISMA algorithm and with conventional MMSE and ZF precoding versus the radius of the network area and for different values of transmit power. ....	36
Figure 6-6: Figure 37: Nomadic RIS on-board UAV scenario. ....	37
Figure 6-7: Physical scenario of deployment and nature of transactions. ....	38
Figure 6-8: Message sequence chart of nomadic RIS for different maneuvering options. ....	39
Figure 6-9: Frame structure for nomadic RIS and different maneuvering options. ....	40
Figure 6-10: Average minimum SNR over the target area obtained with RiFe and with an agnostic solution for different number of RIS elements. ....	40
Figure 6-11: Achievable rate and associated reconfiguration overhead for a nomadic UAV scenario with EO. ....	41
Figure 6-12: General deployment and signal diagram for CE with a reflecting RIS. ....	42
Figure 6-13: Block diagram for the general CE procedure with reflecting RISs. ....	43
Figure 6-14: Time diagram of the signalling process of the general CE framework with reflecting RISs. ....	43
Figure 6-15: System and signal model of the centralised RIS orchestration scheme. ....	44
Figure 6-16: Time diagram of the centralised RIS optimisation architecture within a channel coherence time. ....	45
Figure 6-17: Block diagram of a coherence block for the centralised RIS control deployment strategy ....	46
Figure 6-18: Performance comparison between CE-based (OPT-CE) and codebook-based (CB-BSW). ....	48
Figure 6-19: Impact of CC reliability on the overall performance for out-of-band (OB-CC) and in-band (IB-CC) CCs. The values of $\lambda_r$ and $\lambda_u$ represent the average SNR of the control messages at the RIS RX and UEs needed to achieve a certain probability of correct control pcc. ....	48
Figure 6-20: Physical scenario of deployment and nature of transactions. ....	49
Figure 6-21: Message sequence chart of random access algorithm for RIS-aided communications. ....	50



Figure 6-22: Time diagram for random access procedure in RIS-aided networks.....	50
Figure 6-23: Expected overall throughput vs. the channel load (i.e., UE active during an access). .....	51
Figure 6-24: The MAC protocol of the proposed NGMA framework as a frame structure. ....	52
Figure 6-25: Physical scenario of deployment and nature of transactions. ....	54
Figure 6-26: autonomous RIS implicit CC message sequence chart.....	55
Figure 6-27: autonomous RIS implicit CC frame structure. ....	55
Figure 6-28: Network performance as a function of the probe/reflection trade-off. In order: NMSE of the CE at the BS; Average signal-to-interference-ratio; Average SE achieved. ....	56
Figure 6-29 Physical scenario of deployment for RIS-Empowered MEC .....	57
Figure 6-30 Message sequence chart for RIS-Empowerd MEC .....	58
Figure 6-31 Time diagram for RIS-Empowerd MEC .....	59
Figure 6-32 (Left) Average E2E delay versus Average system energy consumption, for different scenarios. (Right) Average UE Energy consumption versus number of blocks composing the RIS, for different number of quantization bits. ....	60
Figure 6-33 (Left) Delay-Energy trade-off for different offloading strategies. (Right) Average transmit power versus AP blocking probability .....	60
Figure 6-34 (Left) Average power consumption versus average delay, for different strategies. (Right) Survivor function.....	61
Figure 6-35: Physical scenario of deployment and nature of transactions. ....	62
Figure 6-36: Message sequence chart for CE with RIS.....	63
Figure 6-37: EC versus P for different values of K0 for centralized and distributed RIS deployments. 63	
Figure 6-39: CE performance of the proposed methodology utilising a quasi-active RIS. (left) Trade-off of estimation errors between the BS-RIS and the BS-UE links across different configurations. (right) Estimation of the cascaded channel over increasing SNR values [ZSA23]. ....	65
Figure 6-40: Deployment architecture of the static RIS tuning methodology.....	66
Figure 6-41: Time diagram of the static RIS optimisation deployment strategy. ....	67
Figure 6-42: Data flow of the static RIS tuning methodology. ....	67
Figure 43: Reference diagram of HRIS with EH capabilities. ....	69
Figure 44: EH performance as a function of the number of HRIS elements N. The average harvested power is shown with different levels of traffic $\zeta$ and different phase shifters quantization levels Q. The average consumed function is shown with different values of energy consumption of the PIN diodes PON and different phase shifter quantization levels Q.....	70
Figure 45: Loss of charge probability against the battery capacity. N = 40 meta-atoms, Q = 2. The scenario includes K = 75 users with traffic $\zeta = 0.5$ .....	70





## List of Tables

Table 1: RIS deployment taxonomy.....	13
Table 2: RIS control channel taxonomy.....	13
Table 3: RIS hardware taxonomy.....	13
Table 4: RIS operation taxonomy.....	14
Table 5: Summary of WP4 contributions.....	30



## List of Acronyms

5G	5 <sup>th</sup> Generation
AP	Access Point
BER	Bit Error Ratio
BS	Base Station
CAPEX	CAPital EXpenditure
CC	Control Channel
CE	Channel Estimation
CSI	Channel State Information
DL	Downlink
E2E	End-to-End
EC	Ergodic Capacity
EH	Energy Harvesting
EM	Electromagnetic
EMFE	ElectroMagnetic Field Exposure
ES	Edge Server
HRIS	Quasi-active RIS
KPI	Key-Performance Indicator
LoS	Line-of-Sight
MEC	Mobile Edge Computing
MIMO	Multiple Inputs Multiple Outputs
MSE	Mean Squared Error
NGMA	Next Generation Multiple Access
NMSE	Normalised Mean Squared Error
PL	Physical Layer
RAN	Radio Access Network
RF	Radio Frequency
RIC	RAN Intelligent Controller
RIS	Reconfigurable Intelligent Surface
RISC	RIS controller
RISO	RIS Orchestrator
RX	Receiver
SINR	Signal to Interference plus Noise Ratio
SISO	Single-Input Single-Output
SMSE	Sum Mean Squared Error
SNR	Signal to Noise Ratio
TX	Transmitter
UAV	Unmanned Aerial Vehicle
UE	User Equipment
UL	Uplink



## 1 Introduction

RISE-6G is a 5G-PPP project funded by the European Commission under the H2020 framework. The project focuses on designing and prototyping radical technological advances based on reconfigurable intelligent surfaces (RISs), enabling boosted connectivity, localisation, and sensing performance, as well as dynamic adaptation to the varying environmental requirements on electromagnetic (EM) field emissions, energy efficiency, and secrecy. The main objectives of RISE-6G are: (i) definition of novel architectures and control strategies incorporating multiple RISs; (ii) study of the fundamental limits of RIS technology based on realistic and validated radio wave propagation models; (iii) design of algorithmic frameworks enabling high-capacity connectivity, energy efficiency, low Electromagnetic Field exposure (EMFE), localisation accuracy, and edge computing based on RIS-empowered wireless environments; (iv) prototyping the proposed innovation via two complementary field trials at vertical facilities.

Within RISE-6G, work package 4 (WP4) considers the use of RISs for improved wireless connectivity for legacy frequencies and higher-frequency bands. The aim of WP4 is four-fold: (i) Design RISE network architectures and deployment strategies including RIS control signalling for enhanced connectivity; (ii) Establish the fundamentals of communication for RIS-empowered systems; (iii) Design and optimise protocols and methods for RIS control and resource allocation to support high reliability, coverage, low-latency, and high two-way data rate; (iv) Design joint resource allocation and offloading strategies to unlock seamless, reliable, distributed, RIS-empowered edge computing services.

### 1.1 Deliverable objectives

In the present deliverable, we report the research work carried out by the consortium of RISE-6G on deployment and control strategies of RIS-aided smart radio environments. The research findings reported in the present deliverable represent the logical development of the initial specifications reported in deliverable D4.1 titled “Deployment and control strategies of RIS based connectivity (Intermediary Specifications)”. Indeed, the results reported in the present deliverable constitute final specifications that will serve as the RISE-6G perspective and guidelines on this topic.

In this regard, the objectives of the present deliverable are summarized as follows:

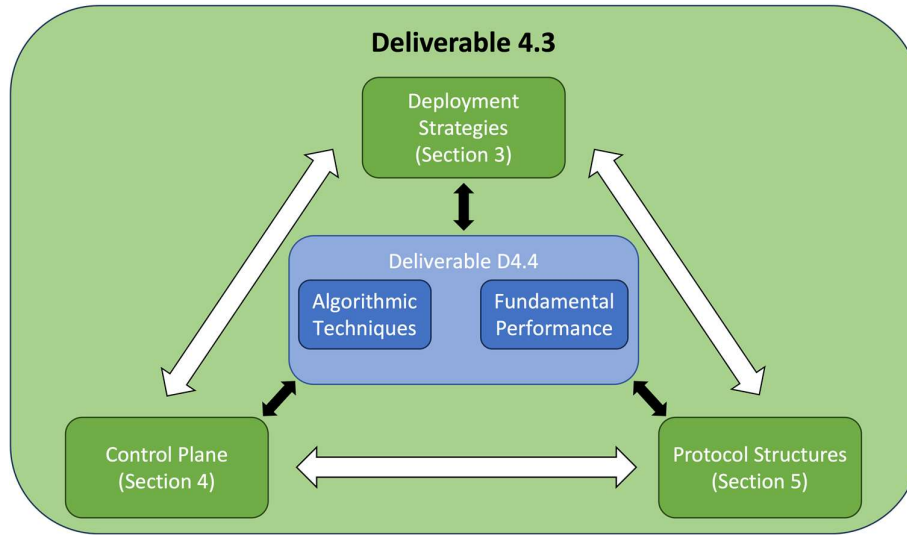
- (1) To report final specifications and associated results on deployment strategies and architectural building blocks for RIS-aided networks, which account for different relevant Key-Performance Indicators (KPIs).
- (2) To report final specifications and associated results on the design and optimisation of the RIS control plane.
- (3) To report final specifications and associated results on the design and optimisation of control signalling protocols, channel estimation (CE) algorithms, resource allocation and access procedures for RIS-empowered systems to support the efficient deployment of RISs in smart radio environments.

This deliverable exploits the RISE network building blocks as defined in deliverable D2.5 “RISE network architectures and deployment strategies analysis: first result”. Moreover, the findings reported herein are in accordance with architectural and deployment aspects developed in D5.3 and D6.3 (WP5 and WP6, respectively), which are related to mapping and localisation, and energy efficiency, EMFE reduction, and secrecy, respectively.

### 1.2 Deliverable structure

This document comprises the following sections. In Section 1.3, we provide the basic terminology used throughout the document and a taxonomy of the RIS, considering aspects related to hardware, control, and operation mode. Section 2 introduces the KPIs that are relevant to the design of RIS control strategies and the deployment of connectivity-enhancing RIS-empowered networks. Section 3 describes final specifications on different RIS deployment strategies for different associated relevant KPIs, as well as architectural building blocks for RIS-empowered communications. In this regard, four alternative

deployment strategies are proposed in RISE-6G, which consider both centralized and distributed RIS deployments with different KPIs and scenarios involving enhanced coverage, static and nomadic integration of RISs in wireless networks, RIS-empowered mobile edge computing (MEC), and deployments that rely on artificial intelligence (AI) tools. Section 4 tackles the design and optimization of the RIS control plane, which is fundamentally subdivided into the case of explicit control channel (Controlled RIS) and implicit control channel (autonomous RIS). Section 5 reviews the final specifications on RIS protocol structures and associated signaling, considering CE, allocation of transmission resources and adaptation of the transmission parameters, as well as (random) access procedures. In Section 6, we describe recommendations for the overall RISE-6G architecture by providing the deployment, data flow and signaling diagrams of each relevant RISE-6G contribution. Finally, Section 7 concludes the deliverable. The interplay between the topics of this deliverable as well as the topics to be covered by D4.4 are illustrated in Figure 1-1.



**Figure 1-1: Areas covered in this deliverable and relations to D4.4.**

### 1.3 Definitions and taxonomy

In this section, we provide the main definitions and taxonomy used throughout the rest of the document. In this regard, we identify four key entities in RIS-empowered networks, which are detailed as follows. The following taxonomy is ordered according to increasing complexity and computational capabilities. The final taxonomy will be devised in D2.6.

**RIS:** it is the device based on reflect-array or meta-material technology that is directly controlled by an associated RIS actuator. In some scenarios, the RIS actuator may be embedded into the RIS device. In such a case, we envision a resulting new RIS device directly controlled by the RIS controller (RISC) function.

**RIS actuator (RISA):** it is the element in charge of actuating the logical commands received by the RISC, i.e., of translating them into physical configurations to be applied to the RIS device. In particular, such configurations might be envisioned as phase shifts or ad-hoc meta-material state changes. In addition, the RIS actuator can provide feedback or limited sensing input when considering different RIS devices. The RISA is controlled by the RISC.

**RIS controller (RISC):** the controller associated to an RIS actuator or an RIS function. It is responsible for generating the logical commands associated to the switching operations between the



configurations/states of the RIS elements (e.g., predefined phase shifts); RISCs may have different levels of complexity and capabilities and can embed third-party apps to implement smart algorithms. An RISC may either be controlled by other elements in the network, in which case it simply acts as an interface that configures the RIS elements based on external explicit instructions (Controlled RIS), or it may operate on its own (Autonomous RIS).

**RIS orchestrator (RISO):** the orchestrator is placed on a higher (hierarchical) layer and it coordinates multiple RISCs.

Unless otherwise stated, we refer to RIS as the overall device, thus implying that optimization and control functions are carried out at the RISC and RISA depending on the required time granularity and computational complexity.

In RISE-6G, we consider two types of RIS deployment and control channels (CCs) as reported in Table 1 and Table 2, respectively. Moreover, the RIS hardware and operation taxonomy is categorized in three different cases as reported in Table 3 and Table 4, respectively.

**Table 1: RIS deployment taxonomy.**

Deployment	Description
Static	The RIS is deployed in a fixed position, which is assumed to be known and does not change over time.
Nomadic	The RIS is deployed on a moving platform (e.g., unmanned aerial vehicles (UAVs), cars, etc.) whose location varies over time. The location of the RIS may be unknown or tracked with some uncertainty.

**Table 2: RIS control channel taxonomy.**

Control Channel		Description
Explicit	Out-of-band	Any communication channel, either wireless or wired, which does not consume resources from the primary communication channel that is influenced by the RIS; examples include: wired channel, wireless channel in a different frequency band, free space optical, etc. This allows for simpler CC design, but at the cost of possibly lower spectral efficiency.
	In-band	The CC employs resources overlapping RIS operational spectrum resources, so it does influence the operation of the RIS. This implies a more complex CC design, but with possibly higher spectral efficiency.
Implicit		There is no dedicated CC or signal over which explicit instructions are sent to the RISC (but the synchronization signal). As such, all decisions wrt. RIS(A) operations must be made locally by the RISC; however, these decisions can be based on other received and interpreted signals (e.g. pilot symbols, user equipment (UE), scheduling information) which implicitly (indirectly) control the behavior of the RIS.

**Table 3: RIS hardware taxonomy.**

Hardware category	Description	Capabilities
Nearly-passive	No RF chains, power amplifiers, only ultra-low-power elements to change the states of the RIS.	Changing the state of its elements.



<b>Quasi-active</b>	Includes up to N receiving RF chains, where N is the number of tunable elements.	Changing the state of its elements; can collect measurements in baseband for performing sensing/parameters estimation (in time orthogonal manner with reflection or simultaneously); can also have processing capabilities to perform localisation, CE, etc.
<b>Active</b>	Includes N transmitting RF chains, where N is the number of tunable elements.	Changing the state of its elements; can also perform reflection amplification or transmit their own signals.

**Table 4: RIS operation taxonomy.**

<b>Controlled RIS</b>	<b>Autonomous RIS</b>	<b>Shared RIS</b>
RIS operations are controlled by an external entity providing the main computational processing, and informing the RISC functions through the explicit CC.	RIS operations are defined by the RISC on its own, without involving any external entity, even though an explicit CC may be present for communicating synchronization or feedback information.	RIS may be shared among multiple entities. This requires requires distributed control and coordination, which can be carried out through explicit and/or implicit CCs.

**Disclaimer regarding RISA/RISC/RISO concepts.**

RISE-6G project builds a new architecture for RISE networks with the following stepped approach:

- Step 1: during the first half of the project, WP4/5/6 have reported intermediary requirements in terms of architecture and control signalling to support their innovations, in D4.1/5.1/6.1, respectively.
- Step 2: all the aforementioned requirements have been used to derive an intermediary RISE network architecture in D2.5.
- Step 3: During the second half of the project, D4.1/5.1/6.1 are updated to D4.3, D5.3 and D6.3) to report the final requirements in terms of architecture and control signalling, taking into account latest and additional innovations.
- Step 4: at M30 of the project, almost all HW RIS prototypes of the project are made available to the consortium. The project lists the different practical ways to control a RIS. The project lists the different practical ways to split the control of the RIS in a functional and physical architecture.
- Step 5: D2.6 provides the final RISE network architecture, taking into account:
  - o requirements on architecture and control signalling to support innovations from WP4/5/6, from step 3;
  - o the analysis of practical splits based on existing RIS prototypes, from step 4;

As a consequence, the concepts linked to the split of control in the functional and/or physical architecture, such as RIS actuator (RISA), RIS controller (RISC) and/or RIS Orchestrator (RISO), will reach their final definitions only in step 5.

Therefore, the definitions of these concepts are local to each deliverable preceding D2.6 and may vary between deliverables preceding D2.6.



## 2 Metrics and KPIs

### 2.1 KPIs for communication channels

This section introduces the KPIs that are relevant to the design of RIS control strategies and the deployment of connectivity-enhancing RIS-empowered networks. There is a close correspondence with what is described in Deliverables D2.2 and D2.4 of this project regarding the general KPI definitions. However, this document includes a more detailed description of the metrics specifically relevant to WP4, while introducing novel specifications for control signalling.

The metrics presented below constitute ubiquitous performance indicators in wireless communications, which, in most cases, have been redefined or extended to account for the introduction of the RIS in the communication system. At the same time, special highlight is given to the KPIs introduced to accommodate specific contributions of this deliverable, such as for control signalling and MEC operations)

#### 2.1.1 Latency

In a communications system, *latency* expresses the time delay between the initiation of an event, such as packet transmission, and the instant at which the event takes an effect at a remote point, such as packet reception. It is one of the key performance metrics in the current and next-generation communication systems. Indeed, 6G specifications target end-to-end (E2E) latency objective that can go down to 10 $\mu$ s [GRT21]; however, most of the applications will require latency guarantees within tens of milliseconds. From a wireless system engineering perspective, we consider the Physical Layer (PL) latency, which is given by the sum of the following components [XH21]:

$$T_{PL} = T_{que} + T_{ttt} + T_{proc} + T_{prop} + T_{retr}$$

where

- $T_{que}$  is the queuing latency arising from the waiting time of the current packet until the transmission of the previous packet is completed.
- $T_{ttt}$  (time-to-transmission) is the time needed for the packet to be forwarded to the physical link.
- $T_{proc}$  denotes the processing latency which accounts for the operations applied to the transmitted data (e.g., encoding/decoding, precoding/combining, modulation/demodulation, channel interleaving and estimation, scrambling, data and control multiplexing).
- $T_{prop}$  expresses the propagation time of the EM waves through the channel.
- $T_{retr}$  captures the delay induced by retransmissions in case of packet loss when low-reliability links are involved. We remark that this is a composite measure that includes some of the aforementioned quantities, such as  $T_{prop}$ . In this context, we consider it as a single variable for simplicity though its value can be derived similarly as the case of a single transmission.

In the context of RIS-based connectivity, the  $T_{proc}$  component is of particular interest since it is directly affected by the deployment and control strategies adopted. Furthermore, depending on the system under examination, specific sub-components of the processing latency can be defined. In the sequel, we also highlight the E2E latency in the MEC context, which depends on the nature of the computation offloading.

#### *Static computation offloading*

*Static computation offloading* deals with ephemeral applications with intermittent communication, where mobile UEs send a single computation request, typically also specifying a service time. Let  $A_k(t)$  be the number of input bits required by the application run by UE  $k$  at time  $t$ , and let  $w_k(t)$  be the number of Central Processing Unit (CPU) cycles associated with the computing task. Then, the overall E2E delay of UE  $k$  is composed of three terms: (i) an uplink (UL) communication time  $\Delta_k^u(t)$ , needed by the device to send the input bits to the base station (BS); (ii) a computation time  $\Delta_k^c(t)$ , needed by the Edge Server



(ES) to process the input bits and run the specific application; (iii) a DL communication time  $\Delta_k^d(t)$ , needed by the BS to send the result of computation back to the UE(s). In summary, the overall E2E latency at time  $t$  is given by:

$$\Delta_k(t) = \Delta_k^u(t) + \Delta_k^c(t) + \Delta_k^d(t) = \frac{A_k(t)}{R_k(t)} + \frac{w_k(t)}{f_k(t)} + \frac{B_k(t)}{R_k^d(t)}$$

where  $R_k(t)$  is the UL rate from UE  $k$  to the BS,  $f_k(t)$  is the CPU frequency allocated by the ES to UE  $k$ ,  $R_k^d(t)$  is the downlink (DL) rate from the BS to UE  $k$ , and  $B_k(t)$  is the number of output bits of the application run by the ES on behalf of UE  $k$ . In static computation offloading, communication and computation resources are orchestrated to guarantee that the overall E2E delay  $\Delta_k(t)$  is less than or equal to an application-dependent requirement, say  $L_k$  for all  $t$ .

### Dynamic computation offloading

In *dynamic computation offloading*, each device continuously generates data  $A_k(t)$  to be processed at a certain rate; for example, a transmission of a video recorded by a UE to be processed by the ES for pattern recognition or anomaly detection. Then, a queueing system is used to model and control the dynamic data generation, transmission, and processing. At each time slot  $t$ , each UE buffers data in a local queue  $Q_k^l(t)$  and transmits them to the access point (AP) at the transmission rate  $R_k(t)$ . The local queue update follows the rule:

$$Q_k^l(t+1) = \max(0, Q_k^l(t) - \tau R_k(t)) + A_k(t)$$

where  $\tau$  is the duration of the time-slot used for scheduling the resources.

Then, the BS receives data from each device  $k$  and sends the data to the ES, which processes  $J_k$  bits-per-cycle, where  $J_k$  is a parameter that depends on the application offloaded by device  $k$ . Thus, the computation queue at the ES evolves as:

$$Q_k^c(t+1) = \max(0, Q_k^c(t) - \tau f_k(t) J_k) + \min(Q_k^l(t), \tau R_k(t))$$

Finally, the BS sends back to each UE the bits resulting from the computation, draining a DL communication queue that evolves as:

$$Q_k^d(t+1) = \max(0, Q_k^d(t) - \tau R_k^d(t)) + c_k \min(Q_k^c(t), \tau f_k(t) J_k)$$

where  $c_k$  denotes the ratio between output and input bits of the application required by UE  $k$ . Thus, the E2E delay experienced by offloaded data is related to the sum of the three queues

$$Q_k^{tot}(t) = Q_k^l(t) + Q_k^c(t) + Q_k^d(t).$$

From Little's law, given a data arrival rate  $\bar{A}_k = \mathbb{E}[A_k(t)]$ , (where  $\mathbb{E}[\cdot]$  is the expectation) the average latency experienced by a new data unit from its generation to its computation at the ES is:

$$\bar{D}_k = \lim_{T \rightarrow \infty} \frac{1}{T} \sum_{t=1}^T \mathbb{E} \left[ \frac{Q_k^{tot}(t)}{\bar{A}_k} \right].$$

Thus, in this dynamic context, an average E2E delay constraint can be written as:

$$\lim_{T \rightarrow \infty} \frac{1}{T} \sum_{t=1}^T \mathbb{E}[Q_k^{tot}(t)] \leq Q_k^{avg} = D_k^{avg} \bar{A}_k$$

More sophisticated probabilistic constraints can also be imposed on the maximum tolerable delay.

### 2.1.2 Spectral efficiency, throughput and goodput

In this sub-section, we provide an example of definition of the *spectral efficiency (SE)* metric, which concerns the rate of reliably transmitted information over the allocated communication bandwidth  $B$ . The



central concept behind spectral efficiency is the (received) Signal to Noise Ratio (SNR) which expresses the ratio between the power of the transmitted signal as it reaches the UE, over the power of the background noise. The presence of the RIS affects the received power of the E2E channel by reflecting the impinging EM waves so that they form beams of concentrated power to desired locations. For multi-UE communications, this idea extends to the Signal to Interference plus Noise Ratio (SINR), which also captures the interference signals appearing due to the simultaneous communication of multiple ends. Formally, the *achievable SE* with respect to a UE depends on the UE's SINR. For instance, the achievable SE with respect to a UE  $k$  is given by

$$SE_k = \log_2(1 + \text{SINR}_k) \quad (\text{bits/s/Hz})$$

and the *sum-rate over the allocated bandwidth* (i.e., the sum of individual rates for all UEs) reads as:

$$\mathcal{R} = \sum_k SE_k$$

Furthermore, the *throughput* of the considered system is finally given by  $T = B\mathcal{R}$ .

Finally, the *goodput* of the considered system is given by  $G = \eta T$ , where  $\eta$  is an efficiency term between 0 and 1 accounting for the resources in time used for overhead operations, such as channel estimation procedures. For example, if 50% of the available time is reserved for channel estimation, we have  $\eta = 0.5$ .

### 2.1.3 Reliability

We define the notion of *reliability* of the communication by considering a given minimum SINR threshold denoted as  $\theta$ , which is necessary to decode the incoming signal. This is also referred to as *coverage probability*. We define the set of UEs whose received SINR is greater than  $\theta$  as

$$\mathcal{U} = \{k : \text{SINR}_k \geq \theta\}$$

RIS-Enabled systems are expected to enlarge the network area in which the received SINR of a given UE is above a given threshold, and thus sufficient for successful decoding of the incoming signal.

### 2.1.4 Bit Error Rate and Bit Error Ratio

Considering a digital transmission, the bit error rate defines the number of bits received incorrectly by the end node per unit time. The normalized version of this metric, the *Bit Error Ratio* (BER) concerns the number of incorrect bits as a proportion of the total number of bits transmitted.

### 2.1.5 Energy efficiency

The *Energy Efficiency* (EE) for a DL communication from a BS to a UE is defined as follows:

$$EE = \mathcal{R}/P \quad (\text{bits/s/Hz/Watt})$$

where  $\mathcal{R}$  is the sum data spectral efficiency and  $P$  is the total power consumption.

### 2.1.6 Channel estimation accuracy

For the specific problem of CE, we consider the *Normalized Mean Squared Error* (NMSE) to assess the performance of the estimation process. Specifically, NMSE (in dB) is defined as:

$$\text{NMSE} = \mathbb{E} \left[ 10 \log_{10} \frac{\|\mathbf{H} - \hat{\mathbf{H}}\|_F^2}{\|\mathbf{H}\|_F^2} \right]$$

where  $\mathbf{H}$  and  $\hat{\mathbf{H}}$  are the true and estimated channel matrices, respectively, and  $\|\cdot\|_F$  is the Frobenius norm.

## 2.2 KPIs for control channels

The design of the CC of the RIS can affect the performance of the communication system. To that end, it is important to define relevant performance indicators assessing the efficiency of the investigated control methodologies both as standalone components, as well as integrated parts of the envisioned deployment strategies.

Depending on the type of the CC, different computational resources are employed by the control mechanism that may consume part of the available bandwidth or transmission frame. As a result, the KPIs presented in the previous section can be exploited to evaluate the overall performance of a system with integrated control strategies, by considering the utility of the resources allocated to the data transmission part of the system, while treating the control signals as an overhead.

### 2.2.1 Control Latency

Extending the definition of section 2.1.1, we define the **control latency**  $T_{contr}$  as the time delay from the time instant when the configuration of the RIS (or a change from a previous configuration) is specified, to the instant after the surface has changed its phase-shifting state. It can be expressed as:

$$T_{contr} = T_{PL}^{contr} + T_{conf}$$

where:

- $T_{PL}^{contr}$  denotes the PL latency, as described in section 2.1.1, here concerning only the control signal. The nature of this delay depends heavily on the type of CC and RIS method of operation. When wireless or wired out-of-band control infrastructure is available, (i) the processing delays are lower, (ii)  $T_{prop}$  concerns the propagation of the information bearing (typically electronic) signal, and (iii) there are hardly retransmissions due to the increased reliability of the medium. For out-of-band and in-band CCs, this delay is approximately identical to the latency experienced by the data stream. When considering autonomous RISs this term can be ignored.
- $T_{conf}$  expresses the configuration adaptability of the surface, i.e., the time delay needed for the surface to update the states of its elements. This delay depends on the computation capacity of the RIS. More importantly, the architecture and manufacturing of the surface affect the state-transition intervals of the individual elements. The quantification of this behavior requires more investigation since it depends on the integrated meta-material elements, and it falls therefore under the objective of Work Package 3 of this project. As previously mentioned, the expected time granularity is 10-50 ms. Nevertheless, it is worth mentioning that it is conceivable for delays to be introduced when changing the complete configuration (i.e., the state of all the elements) of large surfaces.

Let it be noted that the definition of the control latency neither includes any of the delays caused by the algorithmic part of the configuration selection nor the time needed for its execution. The algorithmic aspects are discussed per case in the relevant sections of the control strategies and algorithmic requirements. The exact execution-time delays depend on the software and hardware selected for the system implementation, which falls out of the scope of this deliverable.

### 2.2.2 Control Reliability

The reliability of the control signals can be measured with the aforementioned BER and reliability KPIs of the previous section. Note that, in both cases, the receiving end of this case is the RIS, instead of the intended UEs. Therefore, it is likely that the KPI values for the control signals differ substantially from the KPI values of the E2E communication. Ultra-high control reliability is a principal objective in the deployment of RIS based solutions.

## 2.3 KPIs for quasi-active and active RISs

For RIS hardware architectures with receive- and transmit-RF-chains [AAS21], [ASA21], [JAB22], [WHA21] special KPIs are introduced to reflect the multiple objectives of the surfaces. Those depend on the exact operation and/or application of the RIS, namely:

- The NMSE metric can be employed for performance evaluation also for sensing RISs that perform parameter or CE.

- For surfaces capable of performing reflection and amplification, the communication performance metrics of section 2.1 can be applied.
- When considering surfaces that transmit their own information to facilitate improved control algorithms, the same KPIs are to be applied for evaluation. In this case, only the communication link between the RIS and the network's computational infrastructure is to be taken into consideration, rather than the E2E communication system.

### 3 Deployment strategies for network architecture

The first problem to be addressed when designing architectures and strategies of any new network element is its deployment in the environment. Indeed, the location of the RISs determines how they should be physically interconnected with the rest of the network and what is their optimal configuration at a given time instant. RISs require ad-hoc design, deployment, and management operations to be fully exploited. Indeed, while RISs properly steer the reflected beams towards specific desired directions, it can still cause interference unwanted spatial points and areas, unless properly handled. This issue exacerbates the overall deployment complexity calling for advanced optimisation techniques to strike the optimal trade-off between RISs density and the corresponding spurious detrimental interference.

In the literature, the BSs deployment problem has been exhaustively investigated in a single link, but not at the network level. However, most existing works are based on the isotropic antenna radiation assumption at the BS, making the problem easy-to-solve via graph-coloring algorithms or convex programming approaches. When dealing with directive transmissions — e.g., mmWaves above 6 GHz — a new degree of freedom is introduced: the beam orientation. Specifically, BSs operating at mmWaves must be properly placed and electronically oriented to effectively point the radiated beam towards specific locations leveraging on the available channel state information (CSI). Nonetheless, an ideal RISs deployment is harder to achieve. On the one hand, the optimal RISs deployment requires a priori information on the applied RISs configurations; on the other hand, the optimal RISs configurations can be obtained only upon fixing the BSs and RISs positions. To overcome this issue and make the analysis tractable, simplistic assumptions on agnostic RISs optimisation can be done [MFC21]. However, a full exploitation of the RISs capability to improve network performance requires advanced modelling and optimization, as detailed below.

#### 3.1 Boosted communication and enhanced coverage

The deployment problem is tightly coupled with the RIS application scenario. In the context of indoor scenarios, RISs are considered as the best candidate to solve the mobile dead-zone problem by enabling very-dense RIS-based network deployment at low capital expenditure (CAPEX). For instance, in Figure

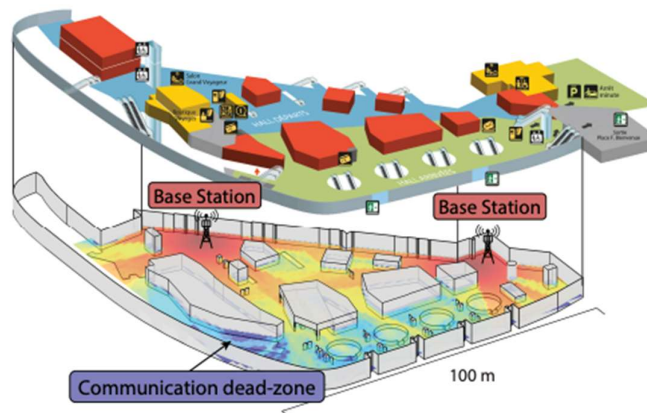


Figure 3-1: Indoor RIS deployment scenario.

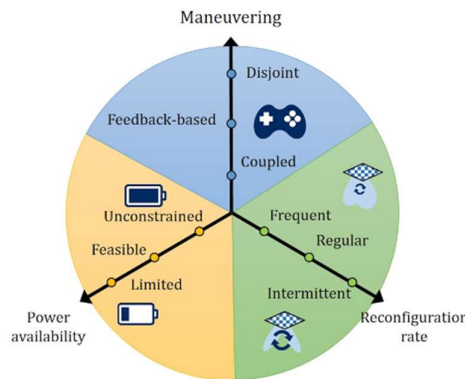
3-1, we illustrate an existing network infrastructure in a real railway station, which however may fail to guarantee satisfactory performance within the entire environment. In such circumstances, ad-hoc RIS design and deployment strategies might be the correct answer to solve the dead-zone problem with a limited investment.

It is important to highlight that active beamforming via an antenna array at the transmitter (TX) side and passive beamforming in the channel via RIS can complement each other and provide even larger gains when they are both jointly optimised. In this regard, the choice of an objective function is of paramount importance, especially for massive access scenarios. Indeed, successful RIS deployments require agile and low-complexity algorithms to be run *online* at the RIS. To facilitate those considerations, this deliverable includes contributions that investigate deployment strategies designed for network planning (Section 6.2), massive access beamforming (Section 6.3), offline static RIS optimisation (Section 6.14), as well as online multi-RIS control and orchestration (Section 6.6).

### 3.2 Static versus Nomadic

RISs can be integrated in the wireless networks in two different ways, namely: *i) static* RIS, i.e., by mounting them on the facade of buildings to assist in the communication to/from the UEs; and *ii) nomadic* RIS, i.e., by mounting them on-board moving objects such as UAVs, HAP, FWA, or even cars/public transport. While the former category is well understood and developed in the literature, little is known about the latter category, which still requires to be explored. UAVs have attracted considerable interest owing to their agile deployments and the ability to establish a LoS link towards ground UEs thereby acting as flying APs avoiding obstacles that impair the overall communication quality [MSG21]. Such solutions, namely air-to-ground networks are proposed to bring back-up connectivity in natural disaster areas and/or leverage on advanced sensing and localisation techniques exploiting the cellular protocol stack to find missing people [ASC21].

In this context, RISs may be mounted as substitutes to bulky active components such as conventional BSs on board the flying device [SAH22]. By allowing the UAV to carry an inherently lightweight and passive device on board such as an RIS, nearly all the available power can be devoted to enlarging the range of operation, while simultaneously achieving highly selective beamforming [AJH20].



**Figure 3-2: Different considerations and trade-offs in nomadic RIS deployment strategies, as highlighted from the analysis carried out in [DMS22].**

A widely adopted assumption in the SoA control architectures is to consider the RIS-bearing platform as in a predefined location in space with negligible orientation and position variations during the communication phase, while its position is updated only within the displacement phase. However, such assumption does not hold in nomadic RIS scenarios, wherein the platform maneuvering, and several atmospheric phenomena can change its position and orientation even during the communication

operations, leading SoA solutions to be potentially inefficient — or even unfeasible — to operate in realistic conditions. For the case of UAVs, as they are hovering at a certain altitude, their motion is influenced by a deterministic component, which is due to the *intentional* maneuvering of the UAV, i.e., following a predefined trajectory, and a *random* component, due to unpredictable factors such as atmospheric conditions including wind, rain, and humidity, imprecise maneuvering, non-ideal UAV instrumentation, etc. Such movements result in translations and rotations of the surface of the on-board RIS, which in turn lead to misalignment of the transmit and reflected beams. This effect is further exacerbated by the highly directive nature of mmWaves beamforming at the RIS and can ultimately result in loss of connectivity at the UE-side. Moreover, the rapid variability of the meteorological phenomena and their difficult predictability in the short-term, make real-time RIS control impractical to overcome the UAV undesired movements effect.

### 3.3 Edge computing

With the advent of beyond 5<sup>th</sup> generation (5G) networks, mobile communication systems are evolving towards enabling a plethora of new services (including verticals), such as Industry 4.0, Internet of Things (IoT), and autonomous driving, building on the tight integration of communication, computation, caching, and control [NTH19], [MDB21]. In this context, a prominent role will be played by MEC, whose aim is to move cloud functionalities (e.g., computing and storage resources) at the edge of the wireless network to avoid the relatively long and highly variable delays necessary to reach centralised clouds [BSD14]. MEC-enabled networks allow UEs to offload computational tasks to nearby processing units or ESs, typically placed close to APs, in order to run the computation on the UEs' behalf. However, moving toward mmWave communications (and beyond), poor channel conditions due to mobility, dynamicity of the environment, and blocking events, might severely hinder the performance of MEC systems. In this context, a strong performance boost can be achieved empowering MEC with RISs, with the aim of increasing UL and DL capacities, and to counteract channel blocking effects in the case of directive mmWave communications [DMC21]. In such a dynamic context, the available resources (i.e., radio, RISs, computation, etc.) must be properly managed to provide the UEs with a satisfactory Quality of Service. Since the E2E delay includes a communication time and a computation time (cf. Sec. 2.1.1), the edge resources must be managed jointly, learning over time the best joint resource allocation in a dynamic and data-driven fashion. In this architecture, the ES has the primary role of computing resource, but also represents the central unit that performs online resource optimisation and RIS control. The contribution of Section 6.1.1 provides a detailed description of a MEC system aided by RISs and highlights the dynamic interplay between communication and computation aspects.

### 3.4 Deployment based on Artificial Intelligence

The main paradigms of algorithmic control of the deployed RISs and the various network components to achieve the target objectives rely on optimisation procedures based on precise modelling of the underlying system and wireless medium. While such approaches are ubiquitous in the community (see also Section 5.1), the recent advancements in machine learning and Artificial Intelligence (AI) offer a paradigm shift toward fully data-driven approaches. Under that prism, the deployed system learns to operate efficiently by relying on data collection and KPI-feedback signals.

The algorithmic details of such methodologies will be part of the focus of D4.4, however the deployment of AI-based techniques entails potential new considerations regarding the deployment of RISE systems. To that end, it is important to review the different roles of those techniques and highlight their modes of operation, benefits, and associated requirements.

Primarily, AI can be used to serve as a RIS controller, or more generally, RIS/network orchestrator. Generally, there are three distinct settings of machine learning approaches:

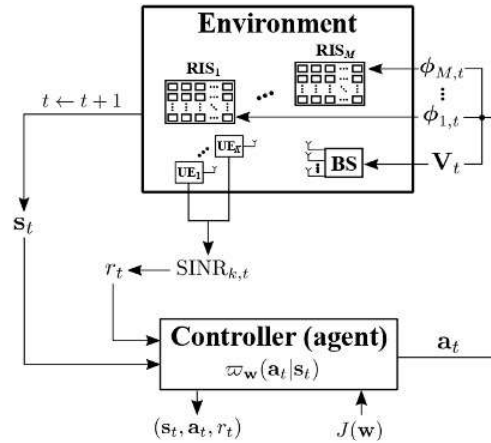
*Supervised training and deployment:* Once the infrastructure is set, the network needs to undergo a data collection stage, where implementation-specific measurements are taken, alongside quantifiable target/KPI/objective values. A machine learning model then undergoes a training phase to learn and



model the relations between measurements and KPI values. During the final deployment phase, the trained model can be incorporated in control schemes either directly (i.e., by learning optimal control decisions based on current measurements) or indirectly (i.e., by empowering other optimisation schemes). As an example, the contribution of Section 6.14 is designed to take advantage of a training phase to learn the statistics of a high-reverberant environment, which can then be used to arrive to a (static) on-average optimal RIS tuning. On the other hand, this deployment has the following shortcomings: (i) The data collection step implies that the network is not operational for specified durations, and (ii) if the statistics of the wireless environment vary from those the AI was trained on, effective performance is not guaranteed.

*Unsupervised deployment:* Machine learning algorithms are capable of solving optimisation problems, similar to traditional, model-based approaches. This type of methods require iterative training procedures on high-end hardware per optimisation instance. Such a deployment, thus, may not be capable of providing high levels of time granularity if placed as an RIS controller, or may be too costly to deploy on physical surfaces

*Online training and decision making:* A different category of controller implementation can offer “instantaneous” (i.e., low computational cost) decision making, without relying on a pre-determined training phase. Such methodologies are trained in a “trial-and-error” manner: For every control decision they are called to make, they observe current measurements of the environment, determine a desired decision (e.g., RIS profile) and rely on the system feeding them back the achieved KPI value to perform training, as illustrated in Figure 3-3. The computational complexity for the decision making process is



**Figure 3-3: Online deployment of AI as a multiple RIS and BS orchestrator [ASH22]. In that scenario, the orchestrator observes the global CSI, determines the RIS configurations and beamforming vectors, and receives the SINR KPI which is maximised over time.**

almost constant-time and the lifelong learning paradigm makes this setting applicable to cases of time variability or environmental changes. On the downside, the decisions taken by the controller at the beginning of the deployment are sub-optimal and prolonged periods may be required before satisfactory performance is achieved. Finally, the training procedure involves perpetually calculating the KPI values and making them available to the controller, which may involve additional infrastructural requirements. Moreover, in online training and decision making, the RISC can interact with the radio access network (RAN) intelligent controller (RIC) in the infrastructure and thus adjust its actions/states accordingly. Contribution 6.6 illustrates a generalised deployment framework that may serve as a setting for such online methodologies – to be presented in D4.4.

On the other hand, machine learning may have a supportive role in the overall system deployment and control by performing intermediate tasks that are to be taken advantage by the actual controlling entity. As an example, ML approaches may be employed for CE (see Section 5.1.1), predicting user mobility, traffic, or transmission patterns, or clustering users based on positions. While such a diverse spectrum of



applications entails per-case consideration, it is highlighted that employing machine learning models is expected to come with increased sets of computational and measurement requirements (which will be further elaborated in Section 5.1.2).

### 3.5 Centralized vs distributed RIS deployment

One important consideration when determining the appropriate deployment strategies of RIS-enabled networks is the dichotomy between centralised controller functionalities or decentralised operation. On the one hand, that choice may be directed by the deployment scenario (e.g. scenarios where each operator deploys their respective RIS – as illustrated in WP2 – inherently involve decentralised treatment). At the same time, this dichotomy becomes more important in scenarios where cooperation between RISCs toward a system-wide objective is needed. Inherently, decentralised approaches have the ability of scaling up, as well as adapting to network changes. However, they also require multiple computational components spread over the network as well as possible substantial increases in the control signalling required for their cooperation (see Section 4 below). Under this deliverable, a general framework for centralised deployment is illustrated in Contribution 6.6. Furthermore, Contribution 6.12 performs a study of centralised and decentralised RIS architectures and highlights important benefits and use-cases of each category. Finally, the concept of autonomous RISs, presented in Section 4.3 and elaborated under Contribution 6.10, may serve as a solution for distributed RIS deployment without the requirements of inter-RIS communication, and therefore increased CC utilisation.

### 3.6 Perspective with overall RISE architecture

The nature of the deployment strategies of the RISs requires careful consideration. The exact decision is dictated by a number of factors investigated by different activities under the RISE-6G project. The primary indicators that need to be taken into account when designing the architecture are highlighted below:

- Use-case and objective KPI (focus of D2.3, D2.4).
- RIS ownership, availability, and capabilities (focus of D2.6, D3.2).
- Wireless propagation environment characteristics (focus of D3.3).
- Computational resources, including physical entities, such as MEC, which can handle edge computation (see also Section 5.1.2).
- Achievable performance by the implementation of the control techniques (focus of D4.4).
- Control infrastructure and protocol structure (see also Sections 4 and 5).
- Considerations of parallel KPIs regarding localisation, sensing, EMFE and secrecy (objectives of WP5 and WP6).

Sections 4 and 5 below further elaborate on particular requirements for RIS-based connectivity by highlighting various architectural components. The contributions of Section 6 present standalone studies of a diverse set of deployment choice, which are designed to provide a unified view of the algorithmic advancements and performance analysis that will be presented in D4.4.

## 4 RIS Control Plane

In this section, considerations on the control messages exchanged with the RIS are given. Both explicit and implicit CCs are considered. Finally, the impact of the RIS on the UEs CC is discussed.

### 4.1 RIS-aided networks with controlled RIS (explicit CC)

When employing controlled RISs, it is essential to design an enhanced framework to control the RISs operations. Since the RIS is typically conceived as a lightweight easy-to-deploy device, the data processing related to any optimisation task is carried out at an external entity, e.g., the BS-side controller,

which is part of the traditional mobile communication network. Such a unit is in charge of detecting active UEs and collecting the associated channel measurements. The relevant CSI must be generated at a rate that must be adapted to the local mobility pattern of both UEs and RISs. Real-time manoeuvring instructions and RIS sensors' output may also be incorporated in the optimisation of the communication process, if available.

The optimised RIS configuration, both for CSI acquisition/activity detection or communication purposes, is sent-out by the network to the RIS controller via the available CC. Moreover, in the case of nomadic RIS, the network-side controller informs the RIS of its BS association. An anticipated drawback of such a solution is the use of precious time/frequency resources to be devoted to the CC. In particular, the explicit CC can be either *in-band* or *out-of-band* [SCK23]. In the former case, the control messages employ resources overlapping the one used for communication. Such a solution allows for the use of the existing CCs resulting in a cheaper CC design but increases the amount of communication overhead. Indeed, the messages intended to the UEs and the RISs need to be transmitted on the same channel, requiring orthogonal allocation in the pool of shared resources. On the other hand, employing the out-of-band channel, a dedicated pool of resources is reserved for control messages intended for RIS. This can happen through a wired connection between the RIS hardware and the network or, alternatively, another wireless interface that uses a band different from the one controlled by the RIS. The control messages can be considered totally separated to the one intended for the UEs and hence can be transmitted without influencing the communication overhead, at the cost of having a larger capital expense for the system.

The type of CC also affects the reliability of delivering control messages. In particular, the out-of-band channel is generally more robust to errors, and hence more reliable. Conversely, an in-band channel is less reliable, and might generate more erroneous control events. Finally, we remark that the amount of control information to send plays a fundamental role in the reliability of the CC: communication paradigms and algorithms that need less exchange of control information are inherently more reliable, regardless the specific design of the CC. In Section 6.7, the impact of CC on the reliability is shown for two different protocol paradigms. More details can be found in [SCK23].

## 4.2 Control messages toward the RIS

A controlled RIS operates according to the instruction provided by a decision maker by means of specific control messages. In general, signalling related to frame synchronization must be performed so that the RIS is able to act synchronously with the network. These kinds of messages can follow the actual standard of communication, not requiring a specific design.

On the other hand, specific control messages should be designed to inform the RIS to change configuration, when this is evaluated by the network designer. Considering a multi-RIS environment, a control message should have two main parts, a RIS control ID and a control payload [SCK23]. The former contains the information on the RIS whose control message is intended to, while the latter contains the instruction on the configuration change. A possible control payload should have at least the following fields:

- *Element ID*: the information on the group of RIS elements that needs to change their phase shift profile. This can be avoided if the RIS always reconfigure all its elements.
- *Configuration profile*: either phase or amplitude parameter (or both) of the elements involved in the configuration change. The resolution of the RIS, i.e., the number of levels that each RIS element can take, directly affects the length of this field. It should be noted that in the system there might be multiple RISs with different resolutions, which will entail configuration packets of variable lengths.

Moreover, assuming that the RIS has memory capabilities – in the actuator, controller or orchestrator –, it can store some configurations in a look-up table, and additional fields can be considered into the control payload:

- *Overwrite*: flag denoting whether the provided configuration should be saved locally in the look-up table at the RIS controller.



- *Configuration no.:* if *Overwrite* = “true”, it denotes the index in the look-up table under which the configuration is stored; since the number of possible configurations is potentially huge, only a limited subset might be preserved.

If a configuration profile is stored into the look-up table, it may be convenient to inform the controller to load it, transmitting only the Configuration number, thus reducing the required control information. Hence, the control payload can be either in the “long” or in the “short” format. To enable this possibility, a flag informing the Type of control packet should be inserted in the header of the frame. Figure 4-1 and Figure 4-2 show a representation of both short and long control frames. We remark that the use of short packets is the preferred choice to increase the reliability of the control transmission, particularly useful for in-band CCs.

Type	Element ID	Configuration profile	...	Overwrite	Configuration no.
------	------------	-----------------------	-----	-----------	-------------------

**Figure 4-1: Long control payload for RIS configuration change**

Type	Configuration no.
------	-------------------

**Figure 4-2: Short control payload for RIS configuration change**

Finally, other types of control information are required if the RIS device can locally run an optimisation procedure. In this case, the information required depends on the specifications of the optimisation algorithm. In general, we can divide the requirements in two:

- Channel and environment information, if the algorithm is based on CSI for controlling the propagation environment.
- Measurement of KPIs (e.g., SINR at the receivers (RXs)), if the algorithm modifies the policy after checking the results in the environment; this is particularly suitable for machine learning approaches involving feedback, such as reinforcement learning techniques [SAH22], [TKB22].

For this type of information, the CC can be designed according to the transmission of CSI and KPI data, as a conventional CC used in the 5G NR standard. Here, particular attention to the channel reliability must be considered, especially for in-band CCs.

### 4.3 RIS-aided networks with autonomous RIS (implicit CC)

In the case of autonomous RIS, we assume that the device has sensing capabilities but cannot receive packetized control messages used explicitly to control its operation; otherwise, in presence of dedicated control messages, we can treat the scenario as the one with controlled RIS with an explicit in-band channel. Therefore, only the implicit CC is considered in this section. Due to its sensing capabilities, the RIS device is usually able to acquire the CSI locally [AV20], and to self-optimize the RIS profile [ADS22]. The local CSI acquisition separates the RIS configuration problem from the optimisation of the BS communication parameters, such as beamforming, power, resource allocation, etc. It is worth pointing out that without a CC between the network and the RIS the presence of the RIS is transparent to the rest of the network from the control point of view. Indeed, once the RIS is configured, the BS can detect additional, potentially enhanced, multipath components provided by the RIS through standard channel sounding operations and exploit their availability with a proper beamforming optimisation. Therefore, implicit control strategies facilitate agile deployment and configuration of the RIS devices, which are essential features to easily integrate the RIS technology into existing networks and standards and expedite the penetration of the RIS devices in the market. As a side-effect, the RIS hardware needs to have the capability to process the incoming signal to acquire local CSI, therefore either quasi-active or active RIS hardware is necessary [ASA21]. Moreover, an orchestration framework needs to be considered to let the

RIS work without disrupting the network operations [CDS23]. Indeed, when acquiring the local CSI, the RIS might shape the propagation environment and mislead other processes performed in the network, e.g., the CSI acquisition at the BS. In this document, Section 6.10 presents a possible orchestration framework for autonomous RIS, while Section 6.13 presents the methodologies for local CE using this kind of hardware.

Finally, it is worth mentioning that the RIS still needs to be connected to the CCs to receive synchronization frame messages, and other information related to the overall data scheduling. Nevertheless, it only needs to listen to these messages, and thus can be considered to act as a UE from the network perspective and so work in a transparent manner [CDS23].

#### 4.4 UE control messages in RIS-aided networks

We remark that also the UEs CCs might be affected by the deployment of the RIS. In particular, when deploying RISs to extend coverage, it might be possible that also the control messages need to be boosted by the RIS to reach the intended UEs. In these scenarios, an RIS needs to have a *control configuration* able to support the reflection of control messages toward the area of coverage. Usually, this requires a widebeam configuration able to support transmit low rate packets in a wide area. For example, this configuration design can be obtained by means of hierarchical beamforming [AJS22]. It is worth mentioning that the RIS should automatically load the control configuration anytime the RIS is in an idle state, i.e., is waiting for control decision from the RIS or another decision-maker in the network [SCK23]. In this way, the RIS can help the delivery of control messages whenever is not performing other explicit operations. Finally, remark that the previous consideration can be applied for different RIS hardware. Both controlled or autonomous RIS can employ the control configuration to boost UE control messages. Likewise, nearly-passive, quasi-active and active RISs might be equipped with such configuration; the working principle is the same, the difference lies in the capability of performing sensing the environment to decide if load the control configuration (quasi-active) or the ability of enhancing the incoming signal (active).

### 5 RIS protocol structures

This section presents the different protocol designs applicable to RIS-aided systems, discussing the specific algorithmic requirements brought by the RISs deployment, the novel considerations to address for the access procedures, and the general RAN structure for scheduled UEs.

#### 5.1 Algorithmic requirement for RIS operation

The algorithmic requirements for RIS-aided communications are generally related to CE, scheduling, and configuration optimization. Nevertheless, the specifics and who bears the responsibility depends on whether the RIS operates autonomously or is being explicitly controlled, with the latter typically offering more capabilities and flexibility at the cost of higher control overhead. The considerations are given in the following:

- *Controlled RIS* – in non-autonomous RIS, i.e., managed by an external entity, the algorithmic requirements are primarily placed on the respective decision maker. One such requirement calls for novel CE procedures that consider the specifics of composite channels (explained in more detail below). Other algorithmic aspects are related to resource allocation and scheduling techniques that are RIS-aware. Whenever feasible, the objective should be to jointly optimise RIS configuration and the transmission parameters of BS/multiple UEs. Further algorithmic nuances appear when RIS needs to be shared by multiple operators/stake holders. In that case, additional constraints on the scheduling as well as cross-interference (related to the bandwidth-of-influence) need to be taken into account.
- *Autonomous RIS* – when RIS operates autonomously (either natively or as one of its modes, i.e. upon being instructed by the external controller to act autonomously until further notice), the algorithmic requirements include: capability to obtain and process channel measurements locally (as discussed in Section 4.3); ability to determine appropriate configuration based on locally

implemented algorithm (through e.g. machine learning or other optimisation techniques); being able (to some extent) to infer the communication objective and self-adjust, e.g., by detecting pilots specific to localisation and/or sensing, it might use different set of configurations to facilitate those procedures.

### 5.1.1 Channel estimation procedures

A big portion of the algorithms designed for RIS control and orchestration are designed to exploit CSI to achieve their intended objectives. In fact, the problem of reliably estimating information about channels when RISs are introduced is more challenging [JAB22], [ZZD22]. First, it involves the estimation of multiple channels simultaneously (the direct channel between the BS and each UE, the channel between the RIS and BS, and the channel between the RIS and each UE). Moreover, the dimension of the channel matrices for estimation increases with the number of RIS elements. In addition, the standard E2E pilot-exchange method results to measure of the cascaded channel instead of the aforementioned links. Last, the near-field CE problem needs to be taken into consideration, which is a fundamentally different process. This task becomes more complex when the deployed RISs are equipped with massive elements with non-linear hardware impairments [HHA20]. The unavoidable hardware error decreases the accuracy of CE, and the beam squint phenomenon occurs in wideband channels. To that end, the deployment strategies and control protocols of RIS based environments must take the CE step into consideration.

In general, the CE process involves the transmission of (predominantly known) pilot symbols or information from the sending node to the RX, at which end, an estimation process is performed. When RISs are involved, multiple pilots are sent, while the RIS changes its configuration to collect descriptive data about the channel. Such a protocol is described as a separate contribution in Section 6.5 for single RIS deployment, and expanded for multi-RIS deployment in Section 6.6. From a CC perspective, the RIS may either change its configuration autonomously, provided sufficient synchronisation (implicit CC), or may be controlled to desirable configurations during the estimation process (explicit CC – either in-band or out-of-band). It is important to mention that many RIS control algorithms rely heavily on the knowledge of the separate component channels. To that end, the CE data flow might need to account for the estimation of the separate channels, for example turning off the RIS to estimate the direct paths between BS and UE, as described in Sections 6.5 and 6.6. With the same scope, other algorithms might make use of the sparsity of the channels to perform CE, as in [NTH19] – specific algorithms will be presented in Deliverable 4.4. Moreover, quasi-active RISs can employ their sensing capabilities to estimate the individual BS-RIS or UE-RIS links [ADS22] [CDS23].

Finally, let it be noted that a parametric CE procedure is an alternative to the direct measurement estimation using pilot exchanges. In this context, the CE task of the RIS communication protocol involves measuring certain components of the network (e.g., angles of departure from the sender to the RX), which can be exploited under sensing frameworks. As such, those methods will be predominantly studied in Work Package 5 of this project.

### 5.1.2 Computational resources

The algorithmic control of the RISs necessitates several additional requirements. At first, the network needs to be empowered with computational capabilities. The specific requirements of the computational infrastructure depend on the exact application scenario, although in principle, the computation may happen at either communication end, the BS, or at the RIS controller, perhaps aided by a MEC server. The consideration on RIS-aided MEC operation are given in Section 6.11.

Another consideration of multi-UE systems is whether the employed algorithms are designed in a distributed or in a centralised manner. The latter case has the potential for higher performance, but it requires additive information exchange operations between the involved nodes.

### 5.1.3 KPI measurement

An important consideration of RISE environments is the ability to compute the metric of interest at certain instances. The reason behind this is twofold. On one hand, the resulted KPIs can be used to evaluate the



performance of different proposed algorithms and strategies. More importantly, autonomous deployment strategies (such as the contribution of Section 6.10) mostly rely on continuous observations of the current KPI value, as a feedback signal. This entails both a measuring and a signaling overhead.

For the metrics considered here, the receiving end node is capable of individually performing the computation of the current metric value without the need for explicit communication with the sender (or with only minimal communication that can be carried out during the access phase). Moreover, the metric values can also be computed without complex infrastructure requirements (e.g., channel measuring or sensing). On the other hand, the KPI measurement may introduce a signaling overhead since the measured values need to be transmitted to the computation-capable part of the network [CDS23], [SCK23].

## 5.2 Access procedures for RIS-empowered systems

The presence of a RIS in a network influences the access procedures considered. Firstly, the RIS needs to be setup to access to the network control information. Moreover, the increased spatial dimension the RIS provides can be exploited to design novel UEs access procedures.

### 5.2.1 RIS configuration after deployment

A new deployed RIS needs to connect to the network for control messages exchange. The kind of connection depends on the kind of CC required. For a wired connection, dedicated infrastructure connection is made between a decision maker and the RIS device. Control information might be shared by means of proprietary communication protocol. When wireless connected, the RIS should access to the network CC, and listen to the synchronization and identification messages to act according to the network. If the CC is implicit, the RIS can act transparently, acquiring information on the data frame structure; if the CC is explicit, the RIS needs to establish a connection with the decision maker through a standard handshaking procedure set by the network.

In presence of nearly-passive RIS, the wireless connection calls for a specific RF hardware to be co-located to receive control messages – usually connected to the RIS. Instead, in presence of quasi-active or active RIS this extra hardware is not required, due to the device sensing capabilities. However, the RIS must locally know a configuration profile to use when receiving control packets. Otherwise, the control packets may be lost due to unfavourable channel conditions [SCK23].

### 5.2.2 UE initial access

For the UEs initial access in absence of any information, the procedure may be done sweeping through a set of possible configurations of the RIS [CSL22], [CSL23]. Through the transmission of DL pilots, we let the UEs sense and learn which configuration provides an acceptable SNR. Using this information, each UEs can send pilot signals during the access (UL) phase in the attempt to access the network. A detailed explanation of the exchanged data for performing the access is given in Section 6.8. Moreover, Section 6.9 presents a refined version of an access protocol able to consider a multi-RIS environment with large numbers of both static and non static UEs by introducing RIS-sharing policies.

Regardless the method employed, the correct implementation of the access protocol requires a careful design of the pool of configuration used. These must be planned considering both the coverage of the area of interest and the time needed for training and access phases. A high number of configurations translate into a larger covered area, but also into a higher time needed for sweeping through them, possibly reducing the overall throughput. A trade-off must be found depending on the scenario at hand. We remark that the use of configuration having large beamwidth (e.g., as [AJS22]) might be beneficial for this task, especially when expecting a low number of UEs accessing at once. A more selective beamformer gives advantage for crowded scenarios, being able to separate them in space, thus reducing the collision probability [CSL23].

### 5.3 RAN protocol structure

After the RISs have been deployed in the scenario, and the relevant access procedures described in Section 5.2 have been performed, the RAN protocol under consideration can take place. While different protocols have different structure, it is possible to describe the general phases a RAN protocol is subjected to in a RISE system [SCK23].

- *Setup phase:* in this phase, the decision maker informs the other entities about the relevant information of the task at hand. For example, the length of the data frame, and the used transmission method needs to be shared to the RIS and the UE. This is a *control phase*, i.e., a phase in which only control messages are sent, and it is subject to all the considerations on the control plane given in Section 4. This phase can be performed once per communication task, or repeated if some information needs to be updated with a certain frequency. For example, while the frame duration might be considered static for the communication task at hand [SCK23], the information about the status of the queue in MEC offloading operations needs to be continuously transmitted to the decision maker that needs to act accordingly [DMC21].
- *Algorithmic phase:* in this phase all the operations needed to set the transmission parameters are performed. A (non-exhaustive) list of operations includes CE, resource allocation, RIS configuration optimization, BS beamforming evaluation, etc. This phase is task and protocol dependent. Usually, this phase uses the data channels, but some minor control messages might be sent during this phase. It is worth noting that a larger time used for evaluating the communication parameters implies a larger communication overhead [SCK23].
- *Acknowledgement phase:* here, the decision maker transmits control messages to inform the devices about the relevant parameter of communication evaluated in the Algorithmic phase, e.g., informing the RIS about the configuration to use for the data transmission. We remark that in the presence of an autonomous RIS this phase does not involve the RIS, which optimises its own configuration and/or transmission parameter locally. This is a control phase, as the Setup phase, and hence all the considerations on the control plane given in Section 4 are relevant.
- *Payload phase:* this phase comprises the transmission of payload data of the devices involved in the communication task. It is intended that the communication parameters are set previously.

Usually, the system needs to perform all the aforementioned phases every coherence time of the channel; indeed, for any realisation of the channel, the communication parameters need to be evaluated and set before the actual payload transmission. Nevertheless, depending on the scenario at hand, some of the phases might not be present, or some of them might be repeated more than once. For example, the Setup phase might be present once to configure the frame structure and time, and be repeated only when the frame needs to be changed. Other cases might require iterations of Algorithmic and Acknowledgement phases, if the optimization of communication parameters requires the exchange of information between devices. The organisation in phases of the protocol structure is a tool that is useful to evaluate the performance of the various protocols, including the overhead generated by the optimization of the network to the usual communication performance [SCK23], [CSL23][CDS23].

In the following, the description of the phases for two examples of communication protocol for controlled RISs and explicit CC are given.

#### 5.3.1 CSI-based structure

This RAN structure refers to the classical multiplexing transmission of wireless networks: the CSI is acquired and the transmission parameters are adapted to maximise the communication performance metric at hand, e.g., the spectral efficiency. For this protocol, the CE procedure is the fundamental step, whose description can be found in Section 6.5. Hence, the Setup phase comprises the transmission of the information to correctly perform CE. This includes at least: the assignment of (possibly orthogonal) pilot sequence to each UE, the RIS configurations to sweep through during the process, and the duration of the CE process. The algorithmic phase comprises the CE process, the optimization of the RIS phase shift





profile, and the resource allocation processes. The acknowledgement phase includes at least the transmission of the optimised configuration to the RIS, and the time-frequency allocation grid to the UEs. Accordingly, the overall communication performance is subject to a trade-off: the longer the Algorithmic phase - due to longer CE or resource allocation processes - the more reliable is the communication parameter setting. However, this also reduces the time left for the Payload phase, and hence the overall communication performance.

### 5.3.2 Codebook-based structure

This RAN structure refers to the classical diversity transmission of wireless networks: the communication is done with a predefined data rate and the sender hopes that the channel will support the rate. In RIS-aided communications, the main point is to find a configuration that is able to boost the E2E SNR so as to increase the chances that the signal is received. Therefore, for this protocol, the selection of the configuration from a predefined codebook is the fundamental step, whose description can be found in Section 6.7. In this case, the Setup phase comprises the transmission of the information to correctly perform configuration selection, including: the codebook of configurations to test, and the assignment of (possibly orthogonal) pilot sequence to each UE for KPI measurement. The algorithmic phase comprises only the configuration selection process. The acknowledgement phase includes at least the transmission of the selected configuration to the RIS, and the time-frequency allocation grid to the UEs. The same trade-off of the CSI-based transmission is present here. Nevertheless, the codebook-based Algorithmic phase duration is inherently shorter, due to the lack of CE and resource allocation processes. On the other hand, it is less probable that the configuration selected will provide the same gain as an optimised one, resulting in a reduction of performance with respect to the CSI-based protocol [SCK23].

## 6 RISE-6G architecture and control proposal for RIS-aided communication

### 6.1 Summary of the contributions

In this section, we describe in detail each relevant WP4 contribution on deployment and control strategies. The main architectural characteristics of such RISE-6G WP4 contributions are summarized in Table 5 below. We remark that in this context we refer to contributions that exploit statistical CSI, i.e., slowly-varying CSI, with the term *statistical timeline*. Moreover, in Figure 6-1 we summarize all considered interfaces and connections between the various entities in the network for the reported contributions.

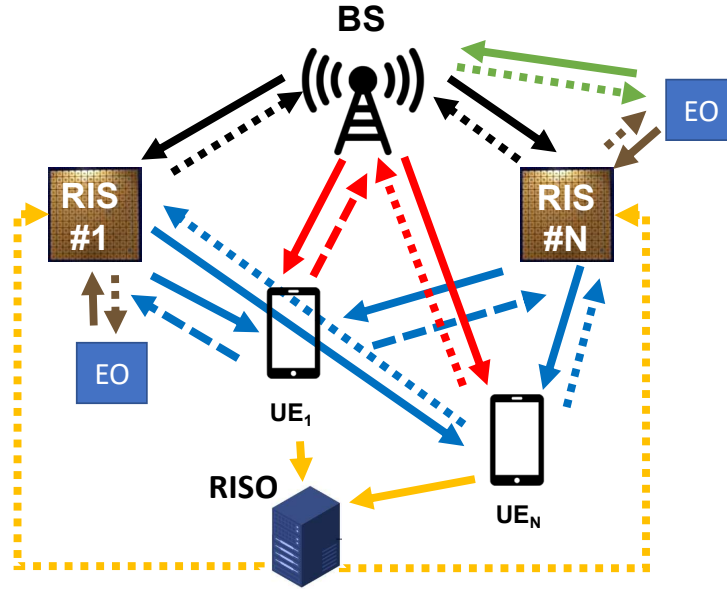
Table 5: Summary of WP4 contributions.

Contrib.	# BS	# RIS	# UE	RIS mobility	Freq. band	RIS hardware	RIS operation	RIS CC	UE mobility	Timeline	Relevant section
6.2	Multiple	Multiple	One	No	Sub-6GHz	Nearly-passive	Controlled	Explicit, out-of-band	No	Offline	3.1
6.3	One	One	Multiple	No	mmWave	Nearly-passive	Controlled	Explicit, out-of-band	No	Within channel coherence	3.1
6.4	One	One	Multiple	Yes	Sub-6GHz	Nearly-passive	Controlled	Explicit, out-of-band	Yes	Statistical	3.2



<b>6.5</b>	One	One	Multiple	No	Sub-6GHz, mmWave	Nearly-passive	Controlled	Explicit, in-band and out-of-band	No	Within channel coherence	5.1.1
<b>6.6</b>	One	Multiple	Multiple	No	Any	Nearly-passive	Controlled	Explicit, out-of-band	Low mobility	Within channel coherence	3.5
<b>6.7</b>	One	One	Multiple	No	Sub-6GHz and mmWave	Nearly-passive	Controlled	Explicit, in-band and out-of-band	No	Within channel coherence	3.1
<b>6.8</b>	One	One	Multiple	No	Any	Nearly-passive	Controlled	Explicit, out-of-band	Low mobility	Within channel coherence	5.2.2
<b>6.9</b>	One	Multiple	Multiple	No	Sub-6GHz	Nearly-passive	Controlled	Explicit, in-band and out-of-band	Yes	Within channel coherence	5.2.2
<b>6.10</b>	One	One	Multiple	No	Any	Quasi-active	Autonomous	Implicit	Low mobility	Within channel coherence	4.3
<b>6.11</b>	One	Multiple/One	Multiple/One	No	Any/mmWave	Nearly-passive	Controlled	Explicit out-of-band/ Implicit	Low mobility	Within channel coherence	3.3
<b>6.12</b>	One	Multiple/One	One	No	Any	Nearly-passive	Controlled	Explicit out-of-band	No	Slower than channel coherence	3.5
<b>6.13</b>	One	One	Multiple	No	Any	Quasi-active	Controlled	Explicit out-of-band	Low mobility	Within channel coherence	5.1.1
<b>6.14</b>	One	One	One	No	Sub-6GHz	Nearly-passive	Controlled	Implicit	No	Statistical	3.4

6.15	On e	On e	Mu ltiple	No	Any	Nearly-passive	Autono mous	Implic it	Low mobili ty	Within channel coheren ce	4.3
------	------	------	-----------	----	-----	----------------	-------------	-----------	---------------	---------------------------	-----



Arrow	interface	6.2	6.3	6.4	6.5	6.6	6.7	6.8	6.9	6.10	6.11	6.12	6.13	6.14	6.15
→	BS-to-RIS	X	X	X	X	X	X	X	X	X	X	X	X	X	X
...	RIS-to-BS			X	X		X	X			X		X		
→	BS-to-UE	X	X	X	X	X	X		X	X	X	X	X	X	X
...	UE-to-BS				X		X		X	X	X				X
→	RIS-to-UE	X	X	X		X		X	X	X	X	X	X	X	X
...	UE-to-RIS				X		X	X	X	X	X		X		X
→	UE-to-RISO	X	X			X								X	
...	RISO-to-RIS	X	X			X			X						
→	EO-to-BS			X											
...	BS-to-EO			X											
→	EO-to-RIS			X											
...	RIS-to-EO			X											

Figure 6-1: Summary of WP4 contributions in terms of communication interfaces.

## 6.2 RIS-Aware Indoor Network Planning

### 6.2.1 Motivation and context

As stated above, a key element towards successful integration of RISs in wireless network is to understand the problem of optimizing its deployment. In this contribution, we develop a mathematical framework analyzing the problem of enhancing the coverage of a wireless network wherein  $N_{BS}$  multi-antenna BSs (in fixed position) and  $N$  multi-antenna nearly-passive RISs may be applied (locations to be optimized)



in order to serve a given target area of interest. We assume that the direct link between such area and the BSs is blocked, causing the so-called “communication dead-zones”. Furthermore, we assume that each RIS is used and controlled by a single BS via a separate (wired or wireless) control link. The considered scenario is depicted in Figure 6-2.

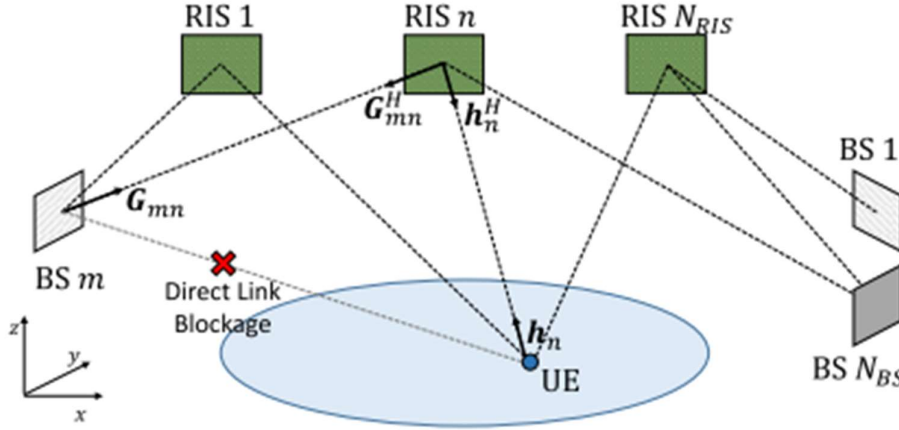


Figure 6-2: Geometrical representation of the considered planning scenario.

In [AES22], we present an iterative algorithm, dubbed as RISA, aiming at optimizing the active beamforming vectors at the BSs, as well as the RIS configurations and locations within a specific candidate set. The resulting optimisation problem is highly non-convex and extremely difficult to tackle due to the intricate coupling between the BSs-RISs and BSs-UE associations, and the joint active-passive beamforming configurations throughout the network. Our proposed solution, assumes a cellular-like architecture in which each RIS provides coverage to one contiguous subarea, thus avoiding any overlap among the RISs. As a result, we obtain the optimized association between serving BS, RIS and UE. Moreover, this approach does not have any impractical assumption on the available CSI but assumes only geometric information on the scenario.

## 6.2.2 Overall system description

### *Deployment scenario, signalling and data flow*

The considered deployment scenario is the one of a multi-RIS single-UE scenario with centralized processing and static RIS deployment, as described in Section 6.6. Hence, the associated methodology and control considerations can be derived from the associated figures.

### *Methodology and control considerations*

As described above, for the sake of analytical tractability, we assume that the RISs are deployed only at specific locations, namely candidate sites. Note that this is a realistic requirement, since network operators are required to meet logistical, administrative, and physical constraints in real-life scenarios. Similarly, the target area is also sampled into a series of test points, representing possible locations of a UE. We then formulate the problem of maximizing the worst SNR among all possible UE locations.

Given the complexity of treating such non-convex problem, we decouple the RISs and BSs beamforming configurations from the planning problem itself by configuring each RIS to provide coverage to one contiguous subarea, assuming that each BS radiates all its available power towards each of its associated RISs in a time-division multiple access (TDMA) fashion. The RIS configuration can then be obtained by means of 3D beam broadening and flattening as described in [HYS20], while the BS precoder is set to maximum ratio transmission on the equivalent channel. The RIS deployment problem is solved by block-coordinate ascent and fractional programming relaxation.

Note that this contribution deals mainly with the task of offline network planning and deployment, and is agnostic of the control signalling framework that is later adapted to it. Moreover, when evaluating the system performance for a given RIS candidate deployment strategy, this method assumes a centralized optimization and a lossless out-of-band (explicit) CC with the BS. However, it would also be possible to integrate specific requirements in the design of the deployment optimization algorithm so as to meet given KPIs (e.g., capacity of the CC).

### 6.2.3 Results and outcomes

In order to verify the effectiveness of the proposed solution, and in accordance with the envisioned proof-of-concept in WP7, we consider a realistic indoor scenario, namely the Rennes train station in France, which is depicted in Figure 6-3. Here, on the left-hand side we show the SNR heatmap without the RIS, whereas on the right-hand side for the case of 4 RISs, located at the square dots.

Such relevant scenario clearly demonstrates how our approach achieves outstanding results to improve the existing cellular infrastructure of one of the major European operators and solve the dead-zone problem.

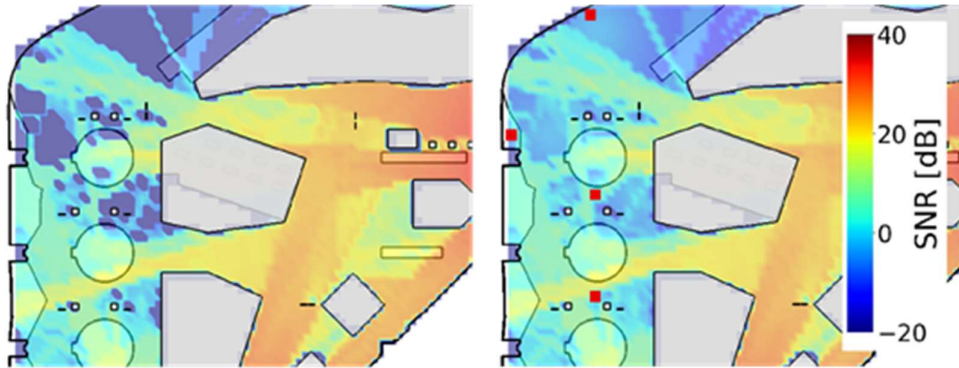


Figure 6-3: SNR heatmap without RIS (left-hand side) and with 4 RISs represented by red squares (right-hand side).

### 6.2.4 Relation to other RISE-6G contributions

This method provides a useful tool to optimise RIS deployment for many relevant practical scenarios. The design of a control signaling framework (as described in this deliverable) may be based on the initial RIS deployment, which is obtained via this method. Conversely, specific control framework requirements as described in Sections 4 and 5 may be taken into account to modify the utility function of this method so as to meet given KPIs.

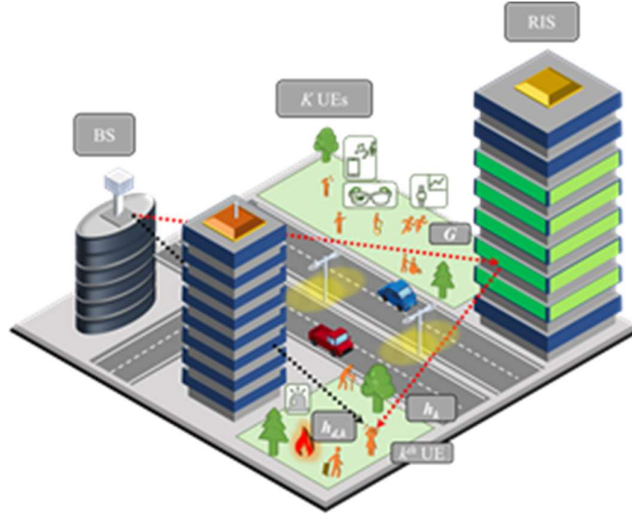
## 6.3 RIS-Enabled Beamforming for Massive IoT Access

### 6.3.1 Motivation and context

In this contribution, given a specific BS and RIS deployment, we study the fundamental problem of jointly optimizing the active beamforming at the BS and the passive beamforming at the RIS in order to maximize the system performance. In particular, we consider a dense scenario, dubbed as *IoT massive access*, wherein a large number of single-antenna UEs are deployed as shown in Figure 6-4. Hence, the objective is to find a simple and scalable solution to such a complex problem to allow efficient and fast online system optimization. We assume that the BS is equipped with  $M$  antennas and serves a set

of  $K$  single-antenna UEs. The connection is established with the aid of a nearly-passive RIS installed on the building glasses consisting of  $N$  equivalent antenna elements. The BS communicates to each UE in the DL via a direct link which comprises of several multipath, as well as a multipath link via the RIS. All channels follow a quasi-static flat-fading model and thus remain constant over the transmission time of a codeword. We further assume that perfect CSI is available at the BS. The BS operates in time-division duplexing mode, such that the UL and DL channels are reciprocal.

In [MDS21], we present RISMA, a RIS-empowered MultiUE Alternating optimisation algorithm that jointly optimises the beamforming strategy at BS and the RIS parameters to provide high-bandwidth low-cost connectivity in massive IoT scenarios. The key element of such system is the choice of the SMSE as objective function, which possesses the unique characteristic of being bi-convex, i.e., convex in the two optimization variables separately, namely the active beamforming at the BS, and the passive beamforming at the RIS. In marked contrast with prior work, RISMA exploits the convex nature of the problem at hand in the two optimisation variables separately to ensure scalability, efficiency, and provable convergence without the need of setting any system parameter.



**Figure 6-4: Multi-UE RIS-empowered wireless network scenario.**

### 6.3.2 Overall system description

#### *Deployment scenario, signalling and data flow*

We assume a general multi-UE single-RIS static deployment scenario where the system optimization is carried out in a centralized manner within the network. Hence, the associated deployment scenario and control message exchanges can be easily generalized starting from Section 6.6 and associated figures.

#### *Methodology and control considerations*

As stated above, this contribution considers the SMSE of all UEs as the main network utility function. For a given configuration of the RIS, the considered system in the DL is a broadcast channel and duality between broadcast and UL multiple access channel holds, which implies that the classical relation between MSE and maximum SINR of each UE holds for linear filters [HJU09]. The problem of minimising the SMSE via joint optimization of the BS and RIS beamforming vectors is however non-convex and challenging. In this regard, we propose to use an alternating optimization-based algorithm where the two optimization variables are iteratively updated. At each step, the partial objective function is convex in the given optimization variable and can thus be solved in closed form by studying the associated KKT conditions.

Moreover, RISMA is adapted to accommodate practical constraints when using realistic RIS hardware, which is modelled as comprised of antenna elements that can be activated in a binary fashion and that can assume only phase-shifting values from a discrete set. To address this scenario, we propose Lo-RISMA, which decouples the optimisation of the binary activation coefficients and the quantized phase shifts. The former is optimised via semi-definite relaxation while the latter are projected onto the quantized space.

This contribution assumes that both BS and RIS configurations are optimized in a centralized manner, by exploiting the knowledge of the CSI in the scenario. Moreover, we assume the existence of lossless out-of-band (explicit) CC with the BS, such that the optimized configuration can be communicated error-free within a channel coherence time. We refer to the control framework described in Section 6.6 for further details.

### 6.3.3 Results and outcomes

In order to assess the performance of the proposed methods, we consider two conventional state-of-the-art methods that do not exploit RISs, namely MMSE and ZF precoding (see [PHS05] [SSH04], respectively). We evaluate the performance of RISMA, MMSE, and ZF as the radius of the network increases for a fixed number of UEs, which are uniformly distributed within the considered circular area, and as the power budget at the BS increases. As depicted in Figure 6-5, RISMA allows to effectively extend the coverage of wireless networks and always outperforms conventional methods in terms of system sum-rate, except when the dimension of the network is very small and the power budget at the BS is very high. Moreover, we demonstrate how with even few quantization bits the achieved performance (Lo-RISMA) is nearly as good as the ideal case (RISMA) and always superior to the reference schemes (see [MDS21] for more details).

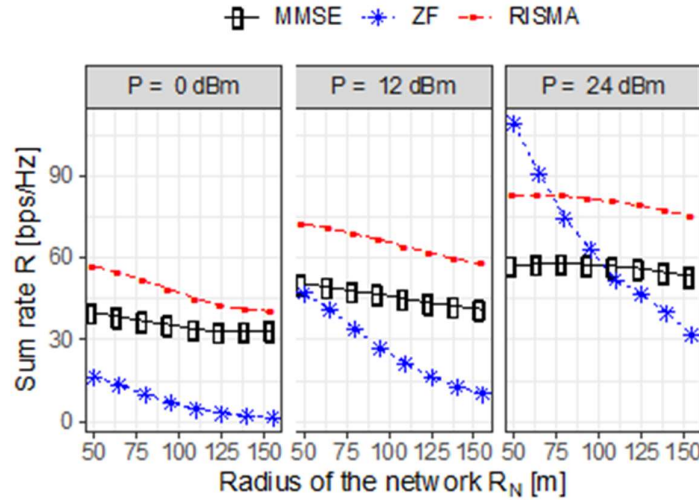


Figure 6-5: Average sum rate obtained with the proposed RISMA algorithm and with conventional MMSE and ZF precoding versus the radius of the network area and for different values of transmit power.

### 6.3.4 Relation to other RISE-6G contributions

This contribution provides an upper bound on the achievable performance of RIS-aided wireless networks with static deployments, centralized optimization and out-of-band losses CCs. It can thus be used as benchmark to assess the performance of other WP4 contributions.





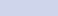





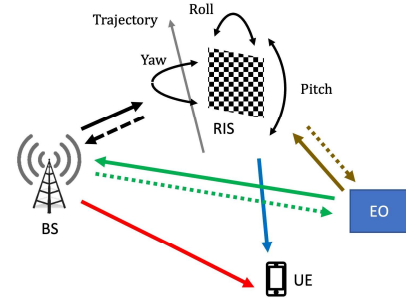


## 6.4.2 Overall system description

### Deployment scenario

The considered deployment scenario is depicted in Figure 6-7, where a BS serves a given target UE via a nomadic nearly-passive RIS. Moreover, both the BS and the RIS can communicate with an external operator (EO) that may be in charge of maneuvering the RIS (e.g., on board a UAV). The optimization of both BS and RIS configuration is assumed to be done centrally in the network. When the EO is deployed, the BS exploits the associated control link to request an update on the RIS position and orientation. In the absence of such EO, this information is obtained by communicating directly with the RIS.

Arrows	Used Interface	Nature of transactions (and order in messages sequence)
	EO-to-RIS	1a) RIS control data (position update)
	RIS-to-EO	2a) RIS control data (position update ACK and orientation estimate)
	BS-to-EO	3a) RIS control data (updated position and orientation request)
	EO-to-BS	4) RIS control data (updated position and orientation request)
	BS-to-RIS	1) RIS control data (updated position and configuration) 3b) RIS control data (updated position request) 5) RIS control data (updated RIS configuration) 7) User data
	RIS-to-BS	2) RIS control data (position and configuration update ACK and orientation estimate) 4a) RIS control data (updated position and orientation estimate) 6) RIS control data (configuration update ACK)
	BS-to-UE	7b) User data
	RIS-to-UE	7a) User data



**Figure 6-7: Physical scenario of deployment and nature of transactions.**

### Methodology and control considerations

In [DMS22], we explore two relevant uses cases, namely a static and a nomadic UAV scenario. In the former, we assume that due to low mobility of ground UEs, a the UAV is kept in a fixed location in space, which is only seldom updated. However, due to adverse atmospheric conditions (e.g., wind, rain, and humidity), the UAV is subject to unwanted perturbations, which result in undesired roll, yaw, and pitch of the surface of the on-board RIS, which is further exacerbated since the latter performs instantaneous passive signal reflection. UAV movement counteractions are automatically taken but still orientation oscillations or location perturbation may result in an instantaneous RIS misconfiguration, leading to misalignment of the reflected beams and degraded overall achievable rate. In this regard, in [MSL23] we study the problem of ensuring that each RX obtains a sufficiently high SNR, by taking into account the undesired rotations of the surface of the RIS caused by perturbations on the UAV. The expression of the SNR is averaged over the possible oscillations of the UAV and the resulting problem is based on semidefinite relaxation and Monte Carlo sampling, denoted as RiFe. However, RiFe requires to be solved every time the statistics of the perturbations are no longer valid which, given the need to use semidefinite programming, can be excessively time-consuming when the statistics change rapidly. Hence, we further propose a more practical solution denoted as Fair-RiFe, which fixes the RIS configuration as a weighted sum of the direction of arrival corresponding to the sampling points within the target area. Such weights are then optimized by allocating the available power proportionally to the distance from said points to the RIS. As the UAV is in a fixed position, the RIS and BS precoders can be updated only when needed, i.e., when the perturbation statistics evolve due to a change of atmospheric conditions. Our proposed enhanced control architecture provides two ways to deal with such a scenario, which are characterized by an *intermittent* and *regular* reconfiguration rate, respectively. This can be done by having the UEs in the service area periodically send updates to the network with the current perceived QoS, or by proactively sending updates on the UAV perturbation statistics when a relevant change is detected. This approach leads to higher power consumption at the UAV due to continuous monitoring and increased communication overhead. On the other hand, it allows to quickly react to varying environmental conditions and minimize network downtime. Lastly, note that both aforementioned approaches can be realized under *coupled* or *feedback-based* maneuvering.

In the case of nomadic UAV, i.e., when the UAV is subject to desired movements in space (e.g., following a predefined trajectory), the drone movements lead to a continuous position and orientation change of the on-board RIS which, if not properly addressed, could lead to severe beam misalignment, and potentially to complete service disruption. The UAV maneuvering can be either *coupled* with the rest of the centralized network optimization (e.g., the BS and RIS configurations) or *feedback-based* from the EO (e.g., a member of first responder teams). Such design choice clearly influences the degree of control signalling required in the network and the resulting system performance. Indeed, the need for continuous communication adaptation, specific of the nomadic UAV scenario, results in a control architecture design that has to sustain a relatively high reconfiguration rate, i.e., *regular* or *frequent*. This implies a potentially high control overhead to frequently transmit the RIS configuration to the RIS.

Note that this contribution assumes the existence of a lossless out-of-band CC with either the RIS, EO, or both, depending on the aforementioned design choices in terms of UAV maneuvering.

### Signaling and data flow

In Figure 6-8, we distinguish three cases of UAV maneuvering and point out the different signalling required to allow efficient UAV-RIS deployment. Specifically, when the UAV maneuvering is coupled, i.e., centrally controlled in the network, the associated overhead is kept at a minimum since the BS obtains the updated RIS position and orientation directly from the RIS, which in turns reads these values from the on-board sensors. In the cases of feedback-based maneuvering, the BS needs to query the EO for information on the RIS position and can then subsequently perform optimization of its configuration. Lastly, in the case of *disjoint* maneuvering, we assume that EO maneuvering the UAV-RIS is not connected to the BS. Hence, in this case the position and orientation updates are obtained via direct communication with the RIS. Note that this case can be classified as *shared RIS*, according to Table 4.

In Figure 6-9, we provide an example of one full transmission frame for the three aforementioned cases of UAV maneuvering.

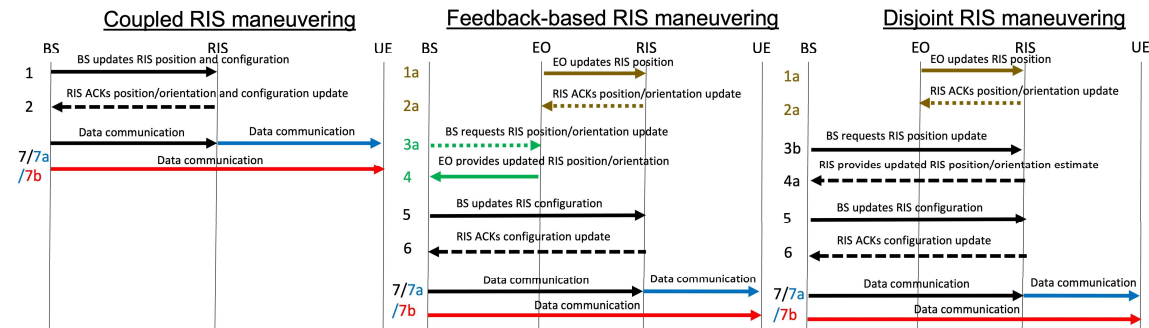
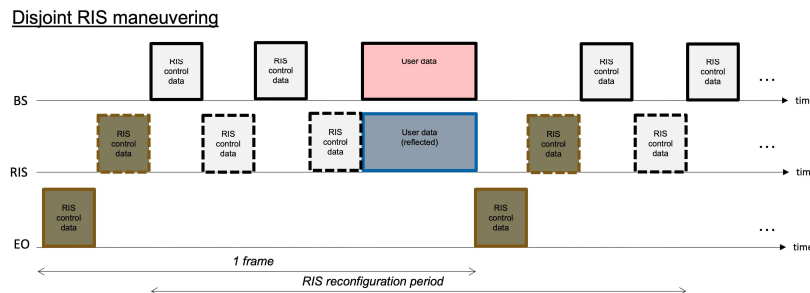


Figure 6-8: Message sequence chart of nomadic RIS for different maneuvering options.



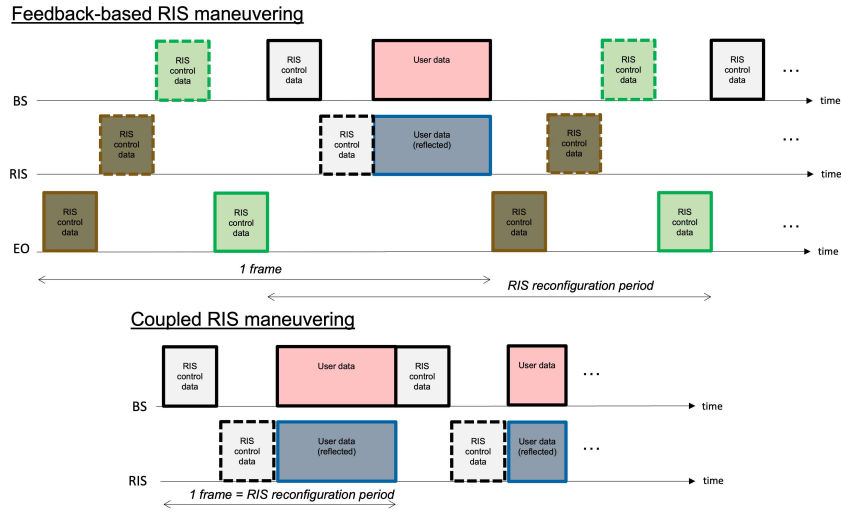


Figure 6-9: Frame structure for nomadic RIS and different maneuvering options.

### 6.4.3 Results and outcomes

For the case of static UAV subject to perturbations on its position and orientation, we evaluate the performance of RiFe against an agnostic method that ignores said perturbations and optimizes the RIS by assuming the known nominal UAV position. In Figure 6-10, we show the benefits of RiFe in terms of average minimum SNR over multiple independent perturbation realizations in the target area of interest for different RIS sizes.

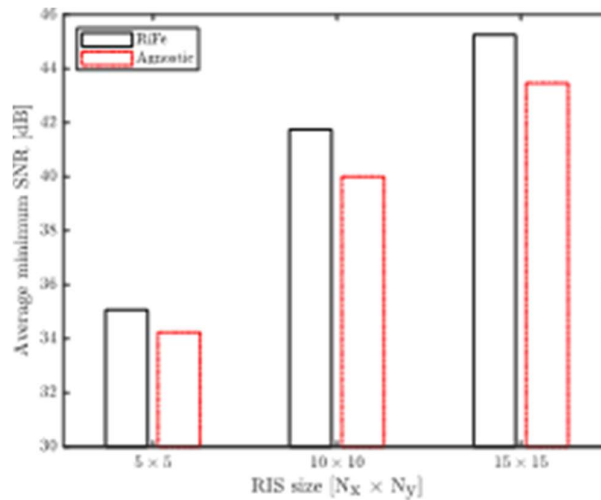


Figure 6-10: Average minimum SNR over the target area obtained with RiFe and with an agnostic solution for different number of RIS elements.

Moreover, for the case of nomadic UAV with an EO handling the maneuvering, we compare two different schemes, namely our proposed enhanced control architecture dubbed as *Adaptive* and the standard state-of-the-art control framework namely *Fixed* versus the UAV speed over a given predefined trajectory. In Figure 6-11 we show both the achievable rate and reconfiguration overhead (computed as the fraction of time spent in exchanging control messages) for the two considered schemes under *frequent* and *regular* reconfiguration rates. The proposed adaptive scheme manages to obtain significantly lower overhead at a small cost in achievable rate for low UAV speeds, while it obtains higher rate at the cost of increased overhead for faster UAV speeds.



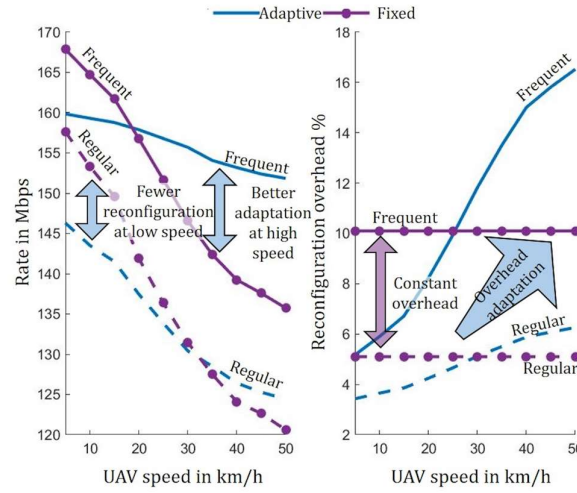


Figure 6-11: Achievable rate and associated reconfiguration overhead for a nomadic UAV scenario with EO.

#### 6.4.4 Relation to other RISE-6G contributions

This contribution provides design guidelines and insights on nomadic RIS deployments, specifically in the case of A2G networks. Moreover, it provides architectural and control signaling considerations for various relevant use cases and scenarios. The associated deployment problem of such *aerial RIS* may be studied alongside conventional RIS deployment as in other WP4 contributions.

### 6.5 Multi-UE channel estimation framework

#### 6.5.1 Motivation and context

As previously discussed, one of the fundamental challenges with the adoption of RISs is the accurate and efficient CE, due to the fact of the large number of antenna/antenna-like elements involved. To better accommodate the novel ideas developed in the project for improved CE in terms of algorithmic and deployment considerations, a generalised architecture in terms of deployment, control and signalling is presented in this contribution.

## 6.5.2 Overall system description

### Deployment scenario

The generic system is presented in terms of a BS and multiple UEs in the presence of a reflecting RIS. This system can capture both single- and multiple-antenna transceivers, and can be easily extended to multiple RISs.

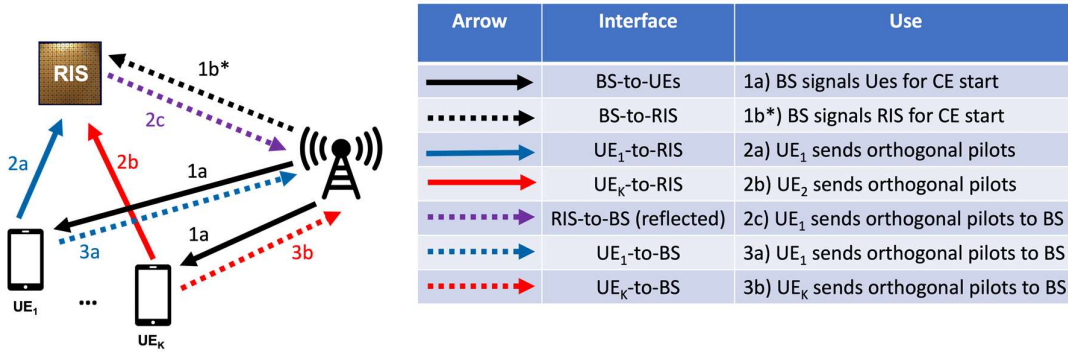


Figure 6-12: General deployment and signal diagram for CE with a reflecting RIS.

### Methodology and control considerations

Using a reflective RIS, the usual CE procedure involving multiple UEs, involves the following steps, as illustrated in Figure 6-12:

1. The procedure is initialised by the BS, which informs all  $K$  UEs, as well as the RIS controller that the procedure is starting. The “Start” messages contain the appropriate parameters (number of frames, pilot structure, frequency-division scheme and allocation, etc.).
2. The UEs send UL orthogonal pilots using  $T_1$  frames. The RIS cycles through predefined CE configurations at every frame. The pilots are reflected by the RIS toward the BS.
3. After  $T_1$  frames have elapsed, the RIS turns OFF. The UEs continue to transmit UL pilots for  $T_2$  frames, that are then sensed directly by the BS.

### Signaling and data flow

Using the collected channel pilots, the BS performs an optimisation procedure, commonly on the NMSE metric, in order to estimate the involved links. Note that up to Step 2), only the cascaded channel (including the direct link) may be estimated under this methodology, in general. Additionally, Step 3) allows specifically for the direct channel to be estimated, which may then be removed from the cascaded channel. Still, the individual UE-RIS and RIS-BS links cannot be estimated independently, but for the use of more advanced signal processing techniques (which is the focus of D4.4) or more intricate system deployment (included as novel contributions in this Deliverable). The time and block diagrams of this procedure are given in Figure 6-14 and Figure 6-13.

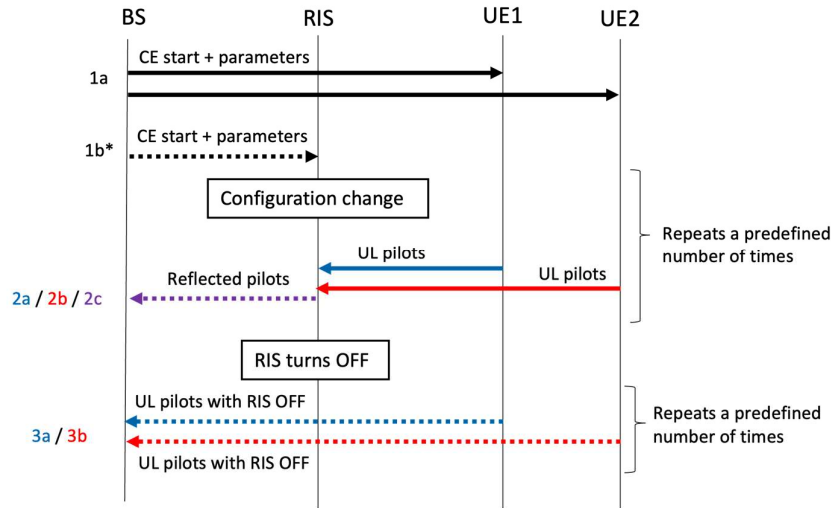


Figure 6-14: Time diagram of the signalling process of the general CE framework with reflecting RISs.

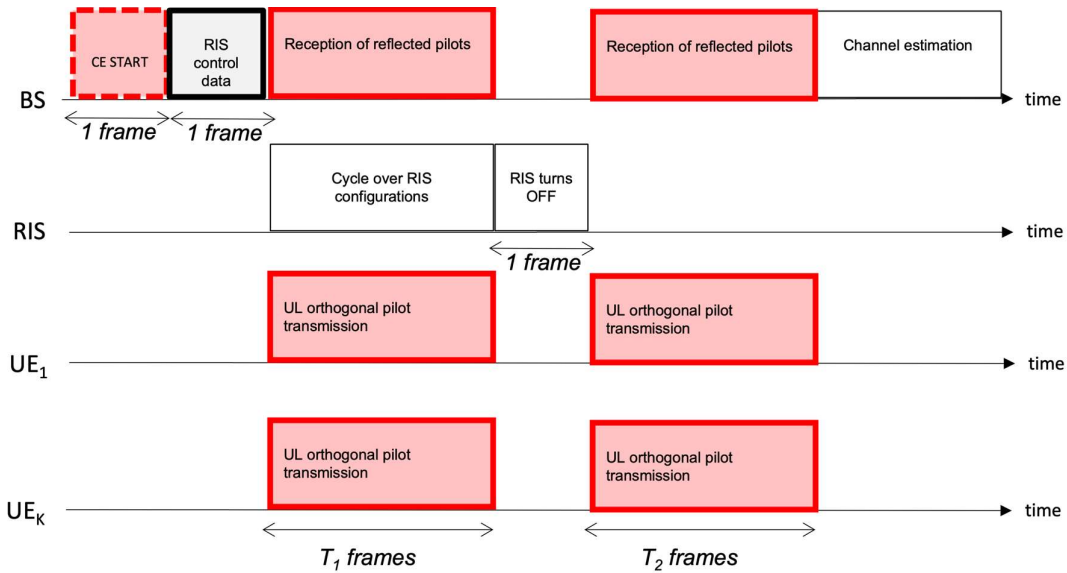


Figure 6-13: Block diagram for the general CE procedure with reflecting RISs.

### 6.5.3 Results and outcomes

This contribution is primarily intended as a detailed explanation of the general CE process under the RISE-6G vision and doubles as harmonisation point for deployment, signalling, and algorithmic contributions, therefore its outcomes are dependent on the respective application. In the scope of D4.2, multiple CE techniques will be presented [WHG22], [ZZD22] to showcase the applicability of this framework.

### 6.5.4 Relation to other RISE-6G contributions

Further contributions in this Deliverable will showcase alternatives regarding system components and protocol aspects, while D4.4 will present algorithmic solutions by referencing the following architecture.

In particular, the contribution in Section 6.13 modifies this deployment framework by utilising a simultaneously reflecting and sensing RIS. Additionally, contributions that present deployment strategies and assume channel knowledge, implicitly suppose this architecture for CE, although those steps have been left out for brevity in the respective contributions.

## 6.6 Centralised multi-UE multi-RIS optimisation within a channel coherence time

### 6.6.1 Motivation and context

To facilitate the various deployment strategies presented in Section 3, a common centralised deployment strategy is presented in this contribution. The intention is to provide a unified framework that can be extended in further contributions, as well to be used as a reference point by the algorithmic strategies to be presented in D4.4.

### 6.6.2 Overall system description

#### Deployment scenario

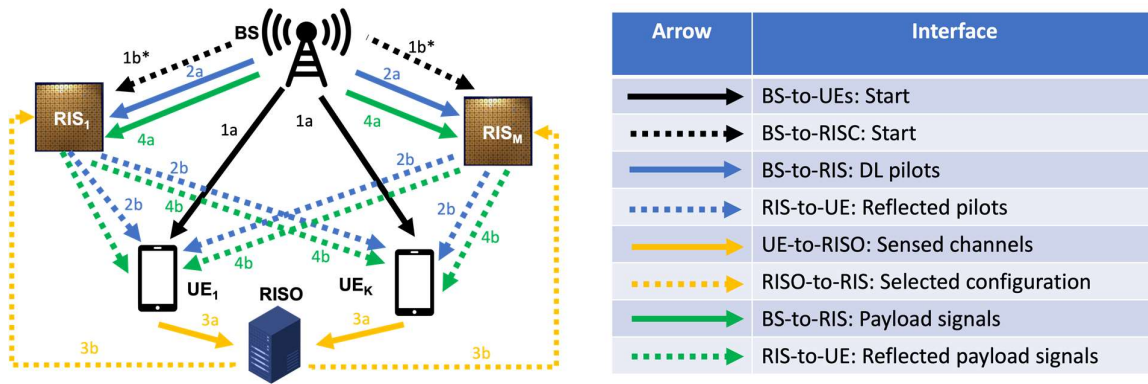
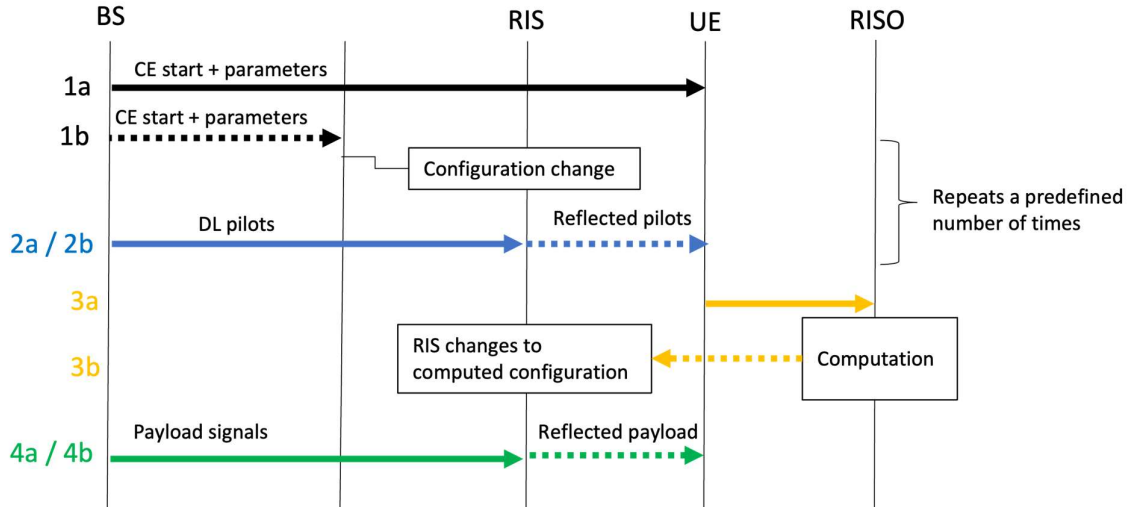


Figure 6-15: System and signal model of the centralised RIS orchestration scheme.

The system considers the general case of  $M$  reflecting RISs and  $K$  UEs alongside a BS as illustrated by Figure 6-15. The RISO is responsible for collecting all available information and solving the optimisation problems that entail RIS configuration selection and potentially adjacent problems such as resource allocation. It is important to note that this scenario is formulated per channel coherence time, i.e., the steps to be presented below are to be repeated when the channel realisations change.

### Methodology and control considerations



**Figure 6-16: Time diagram of the centralised RIS optimisation architecture within a channel coherence time.**

The general procedure within a channel coherence time involves the following steps:

1. **Procedure start:** At the start of the channel frame, the BS is responsible for informing the RISs and the UEs that the procedure is commencing. Appropriate parameters are transmitted and the individual nodes prepare for the pilot exchange sequences.
2. **Channel estimation step:** Based on the formulation of Contribution 6.5, the channels are estimated using the predetermined pilots.
3. **Computation step:** The RISO collects all available CSI observations and determines the configurations of the RISs that better serve the system's objective. Since such multi-RIS problems are in general difficult to solve, the computation time must be taken into consideration by the deployed system to ensure that the benefits gained from the computed configurations are not outweighed by the introduced delay and that the whole operation is constrained within a channel frame.
4. **Payload transmission step:** Now that the system is configured, the normal payload transmissions take place.

### Signaling and data flow

An example of the considered frame structure is provided in Figure 6-17 below. All signalling, computation, and transmission operators are assumed to take place within a channel frame, where the channel is quasi-static. A predefined number of frames is required for the CE and the transmission of the information to the RISO. The computation needs at least one frame to take place, although it may span over possible frames. Nevertheless, the transmission step is intended to occupy the largest portion of the overall coherence time.

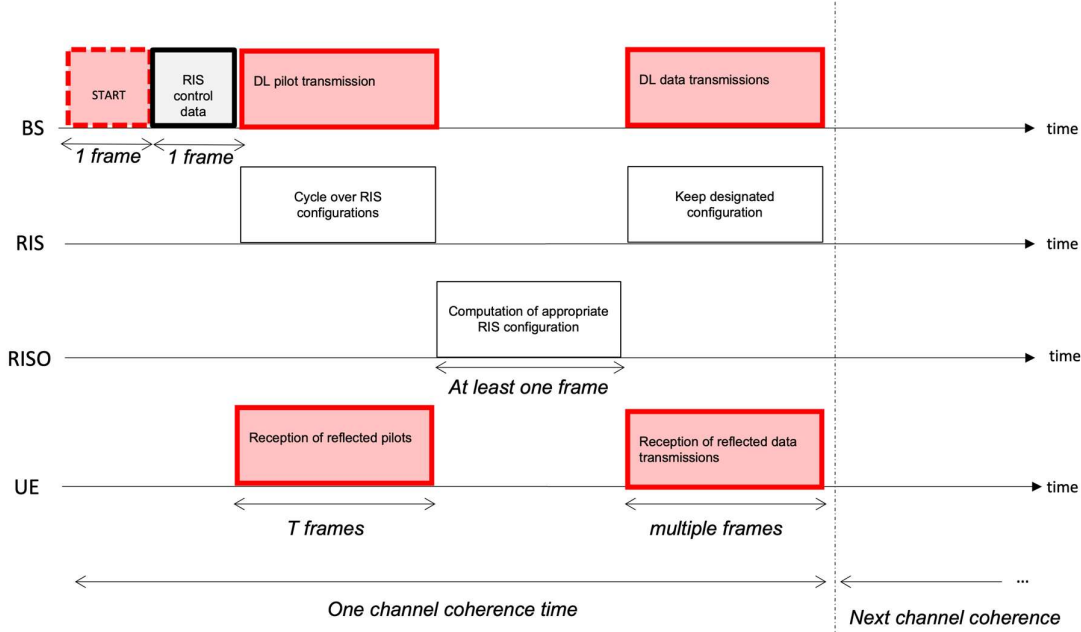


Figure 6-17: Block diagram of a coherence block for the centralised RIS control deployment strategy

### 6.6.3 Results and outcomes

This unified framework for centralised optimisation within a time coherence block provides the backbone of multiple deployment strategies and algorithmic contributions to be presented in this and the next deliverable and addresses the signalling and information-exchange parts that may not be the focus during the control development. As discussed in Section 3, strategies like AI-orchestration (Section 3.4) and Edge-Computing (Section 3.3) take advantage of the proposed framework.

### 6.6.4 Relation to other RISE-6G contributions

Contributions that implicitly utilise the detailed signalling framework include Section 6.3, 6.4, and 6.11. This contribution builds on top of the contribution of Section 6.5, that describes the CE process in more detail, but it is also presented in a general way to incorporate more generic beam-training frameworks and RAN structures (see Section 5). In fact, the beam-sweeping strategy described in Section 5.3.2 uses the exact same signalling, control, and block structure as described above. A different version of the per-channel optimisation is given in Section 6.14, where the system and block structure remain mostly the same, however the CSI collection phase takes place over multiple channel blocks and the process results in a static RIS configuration, instead of being repeated at every time frame. As highlighted in Section 3.5, the proposed framework implies reliable and efficient CCs between the network nodes and the RISO, which may not be readily available. To that end, distributed contributions are proposed (Section 6.12) or contributions that envision self-configuring RISs (Section 0).

## 6.7 Multi-UE codebook-based framework

### 6.7.1 Motivation and context

To avoid CE procedure, a different concept of RIS-aided communication can be obtained when considering codebook-based approaches. The main idea is to select the configuration that provide the

highest SNR for the communication, without estimating the overall channel, in order to reduce the overhead of the system [AXW22], [SCK23].

### 6.7.2 Overall system description

#### Deployment scenario

The deployment scenario is the same as Section 6.5, depicted in Figure 6-12.

#### Methodology and control considerations

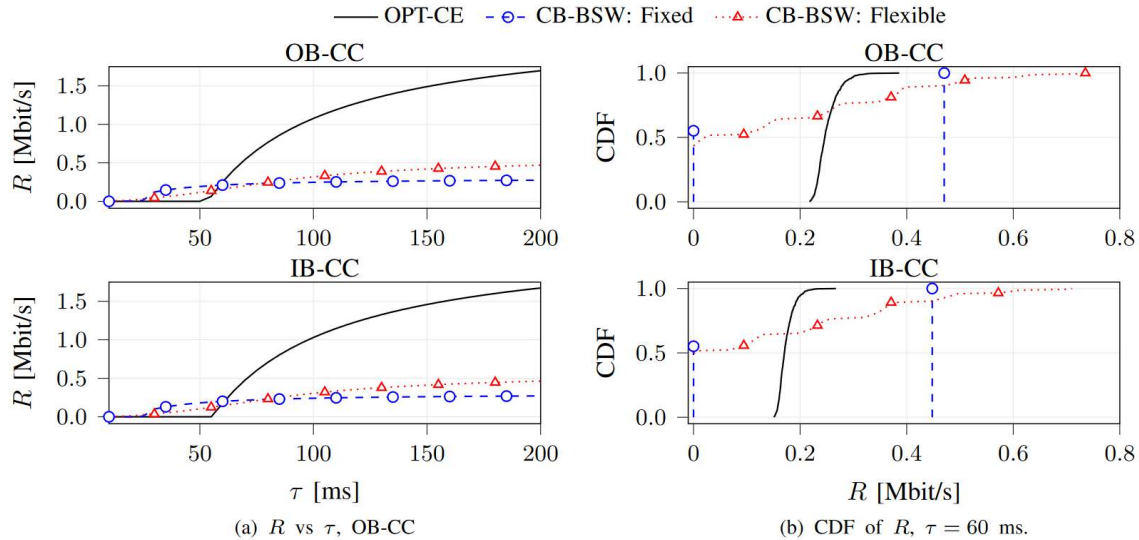
Using a reflective RIS, instead of the usual CE procedure, another possibility is searching for the configuration providing enough gain for the UEs from a discrete set of configuration, namely the *configuration codebook*. The procedure of this method is the similar to the one given in Section 6.7, with the following modifications:

1. The procedure is initialised by the BS in the same way as in Section 6.7.
2. The UEs send UL orthogonal pilots using  $T_1$  frames, and the RIS cycles through predefined CE configurations (from a codebook) at every frame, as in Section 6.7.
3. After  $T_1$  frames have elapsed, the BS select the best configuration in the codebook for each UE. This is already the configuration that will be selected for the transmission of the data afterwards.

Differently from the CE-based approach of Section 6.7, no optimization is involved. This can be seen as *fixed rate transmission*, in which the data rate is set *a priori* and there is a possibility that an outage occurs if the actual communication channel capacity is lower than the selected rate. Nevertheless, this framework is able to reduce the time. The time and block diagrams of this procedure can be derived by Figure 6-14 and Figure 6-13 with minor modifications.

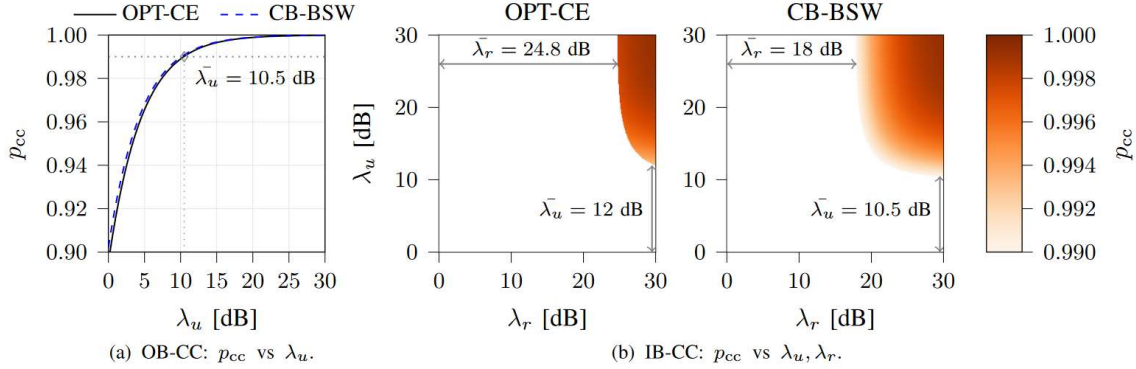
### 6.7.3 Results and outcomes

This contribution is primarily intended as a detailed explanation of the general codebook-based process. Nevertheless, in Figure 6-18, the results comparing the performance of CE-based and codebook-based as a function of the overall frame duration are shown in a single UE setting [SCK23]. Both out-of-band and in-band channel are tested, while their impact is negligible in terms of generated overhead. It can be seen that the CE-based approach generally achieves better performance, but it requires a higher frame length, i.e., a higher coherence time. On the other hand, Figure 6-19 shows the value of the SNR needed to obtain a reliable CC for both out-of-band and in-band cases. In general, the codebook-based is more resilient because it needs less control information to be sent to the RIS. More details in [SCK23].





**Figure 6-18: Performance comparison between CE-based (OPT-CE) and codebook-based (CB-BSW).**



**Figure 6-19: Impact of CC reliability on the overall performance for out-of-band (OB-CC) and in-band (IB-CC) CCs. The values of  $\lambda_r$  and  $\lambda_u$  represent the average SNR of the control messages at the RIS RX and UEs needed to achieve a certain probability of correct control  $p_{cc}$ .**

#### 6.7.4 Relation to other RISE-6G contributions

The codebook-based framework can be exploited in various applications, particularly suited for low coherence time scenario or scenarios that constraint the use of in-band CCs. In this regard, this information can be exploited by other RISE-6G methods that not require the acquisition of instantaneous CSI or focus on different metric, for instance, the localisation procedures described in D5.2 and D5.4. Indeed, it is possible to map the best configuration with a region of space where the user presumably is, and use this information as a first rough estimation of the position, to be refined afterward. The general considerations provided here can be extended considering multi-antenna devices or sensing capabilities of the RIS.

### 6.8 Random access algorithm for RIS-aided communications

#### 6.8.1 Motivation and context

An important open question is how to design an access protocol for multiple uncoordinated UEs, while taking advantage of the possibility to configure the RIS. The aim of this section is to illustrate a random-access protocol based on the spatial dimension given by the RIS, presented in [CSL22], [CSL23]. For simplicity of presentation, we consider a single-input single-output (SISO) scenario, but the same scheme can be applied to multi-antenna BSs.

#### 6.8.2 Overall system description

##### *Deployment scenario*

We consider a scenario where a set of uncoordinated UEs cannot be served by a BS due to blockages. To overcome this problem, a network operator can deploy a RIS to extend the coverage area of the BS and offer network access to the UEs affected by the blockages. The scenario considered can be seen in Figure 6-20.

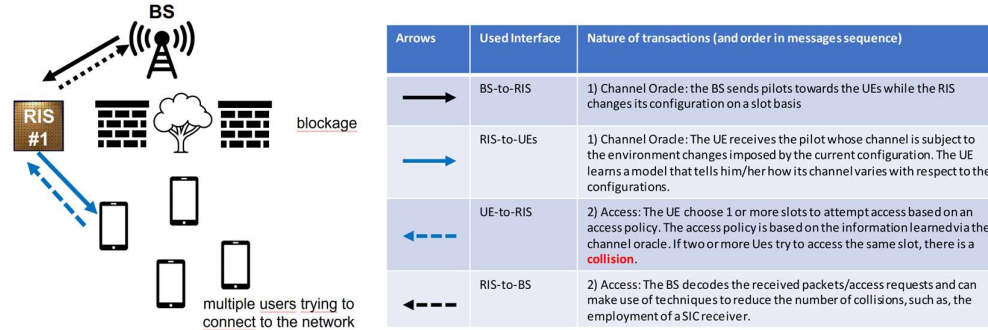


Figure 6-20: Physical scenario of deployment and nature of transactions.

### Methodology

The proposed protocol operates by dividing the communication channel into multiple subchannels, with the RIS used to selectively reflect signals towards different spatial regions. In particular, the protocol is divided in two main phases: 1) the channel oracle, 2) the access. In each of those phases, the RIS sweeps through pre-defined sets of configurations, named *codebooks*, loading every configuration in each slot. The BS and UEs acts as follows.

1. During the channel oracle phase, the BS sends DL pilot signals per each configuration change; the UEs listen to the received signal and estimate a model of the channel under the different configurations.
2. During the access phase, the UEs try to access to the network sending access signals on different slots using the knowledge obtained by the previous phase. If more than a UE select the same slot a collision occurs and the access does not occur.

Optimistically, the knowledge provided by the channel oracle phase mixed with the spatial dimension generated by the RIS should help the UEs to select access slot without incurring in collisions. Note that the codebooks of channel oracle and access are different and design to provide different aims. In particular, the channel oracle codebook is designed to maximize the estimation accuracy of the channel while minimizing the overall duration, while the access codebook is optimized for minimize the number of collisions. More details on the design principles and optimization of the codebooks are given in [CSL23].

### Control considerations

The proposed protocol relies on *explicit control* from the BS. In particular, the BS needs to inform the RIS about the codebooks used during the operation phases, the slot time, acquired by PHY frame synchronization with the BS. To minimize the number of control messages, it is possible to store the codebooks in a look-up table at the RIS and command it to start the beam sweeping. Hence, the function can be implemented directly in the RISC and RISA, without explicit need of controlling the change of each configuration from the BS. Note that [CSL22] and [CSL23] assume *out-of-band CC* because it is more robust to interference and easier to present. Nevertheless, the system can be implemented using *in-band CCs*, taking care of designing a low-rate communication information to inform the RIS to start the beam sweeping procedure.

### Signaling and data flow

The message sequence chart corresponding to the scenario from Figure 6-20 is shown in Figure 6-21.

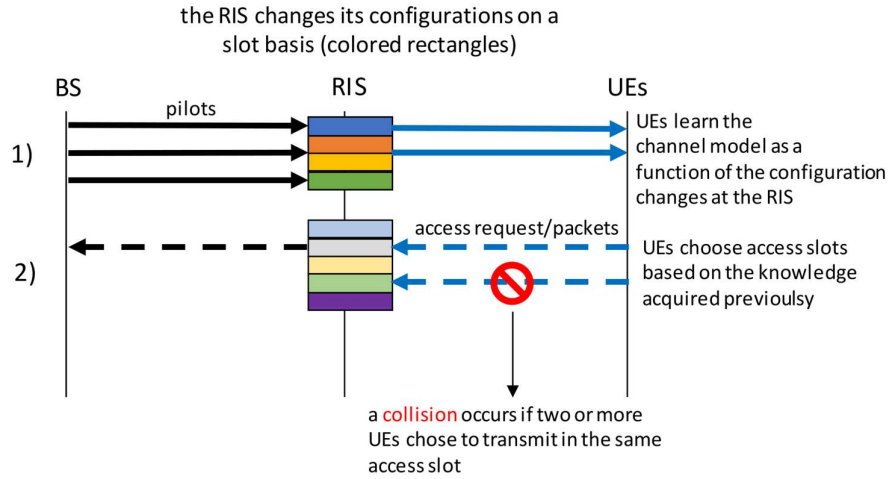


Figure 6-21: Message sequence chart of random access algorithm for RIS-aided communications.

The signaling related to the methodology explained is given in Figure 6-22. It is worth noting that the overall procedure needs to be performed within a coherence time of the channel to avoid that the estimated channel in the channel oracle phase results outdated during the access phase.

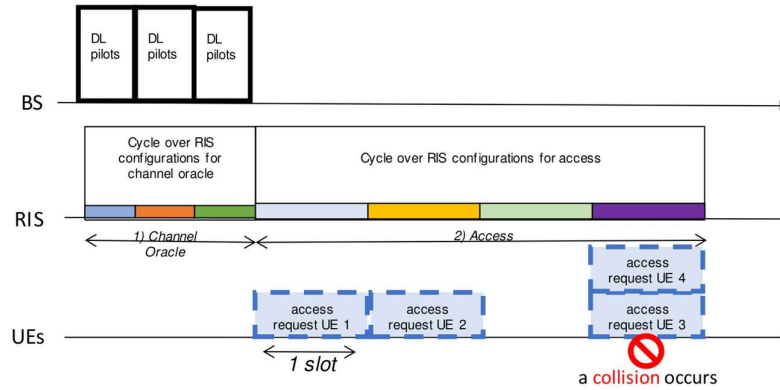


Figure 6-22: Time diagram for random access procedure in RIS-aided networks.

### 6.8.3 Results and outcomes

A results in terms of throughput provided by the proposed protocol with respect to the legacy protocols is given in Figure 6-23. Disregarding access policy used (see details in [CSL23]), our proposed random access protocol always outperforms the baseline. On average, our best results are obtained by the R-GSCAP access policy that provides a throughput 66.18% higher than the baseline. Other results can be seen in [CSL22], [CSL23].

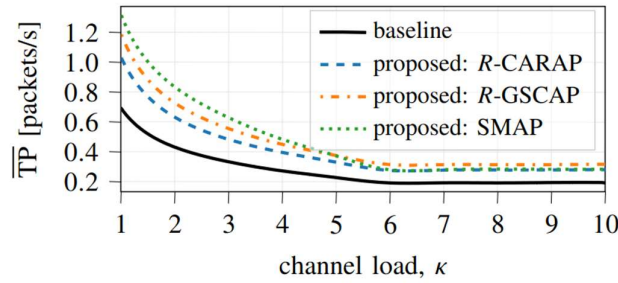


Figure 6-23: Expected overall throughput vs. the channel load (i.e., UE active during an access).

#### 6.8.4 Relation to other RISE-6G contributions

The proposed random-access is a basic building block to let uncoordinated UEs access the network. Moreover, the procedure retrieves information on the CSI of the UE for every configuration of the RIS involved in the access phase. At the end of the procedure, the BS is informed on which configuration each UE prefers for transmission. This information can be broadcasted as an input to other optimisation procedures, such as the algorithms described in detail in deliverables D4.2 and D4.4 of WP4.

### 6.9 Multiple access protocol for combinations of static and mobile UEs

#### 6.9.1 Motivation and context

The ongoing visions of wireless networks are provisioning massive numbers of connections, heterogeneous data traffic, high spectral efficiency, and low latency services. These services are spurring research activities that are focused on defining a next generation multiple access (NGMA) that can accommodate massive numbers of UEs in different resource blocks, thereby achieving higher spectral efficiency and better connectivity compared to conventional multiple access schemes. This contribution concerns a multiple access scheme for NGMA in wireless communication systems assisted by multiple RISs. In this regard, considering the practical scenario of static UEs operating together with mobile ones, a multiple access framework for RIS-assisted communications is proposed [ZSA23], along with a design of a medium access control (MAC) protocol incorporating RISs.

#### 6.9.2 Overall system description

##### *Deployment scenario*

The deployment scenario entails a multi-UE, multi-RIS system. Different mobility profiles of UEs are explicitly considered in practical scenarios (e.g., in smart industries where fixed sensors and mobile robots co-exist.) and improve the efficiency of the MAC protocol and reduce the complexity of the RIS configuration in multi-UE communication scenario by exploiting UEs' mobility profiles: Users having similar mobility profiles are grouped together to enhance interplay of RIS configuration and MAC protocol. Furthermore, existing (either static or mobile) and new (mobile) UEs are considered. Each UE is equipped with a single antenna and the BS is equipped with multiple antennas. Each RIS is equipped with a controller connected to the BS. The RISs are assumed to operate in non-overlapping frequencies, and that each RIS may be used by one UE at a time.

##### *Methodology and control considerations*

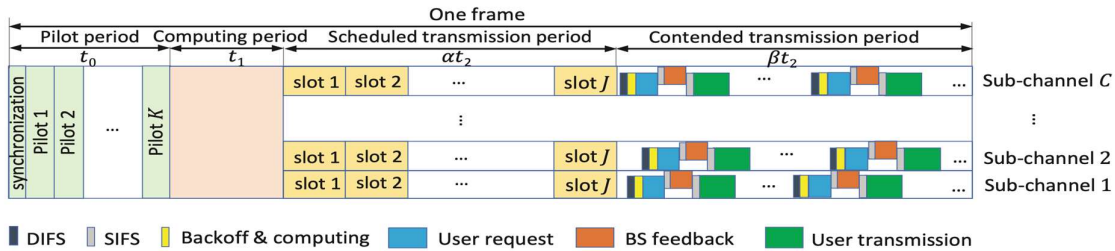
The considered deployment scenario is the one detailed in Section 6.6, i.e., a multi-RIS, multi-UE scenario. The proposed multiple access framework, whose signaling is detailed in Figure 6-24, which combines two aspects: 1) the MAC protocol, and 2) the configuration mode of multiple RISs. These two interact with each other according to the dynamic wireless environments. The MAC protocol is designed and optimized on a frame-by-frame basis, and each frame is divided into three periods: a pilot period,  $t_0$ ; a computing period,  $t_1$ ; and a transmission period,  $t_2$ . The latter consists of the scheduled and the

contended transmission periods, the proportion of each is  $\alpha$  and  $\beta$ , respectively. In a frame, based on pilot transmissions and optimizing computation, the proposed MAC protocol switches between the scheduled and the contended modes (i.e., static UEs are scheduled to communicate with the BS via  $M$  RISs, while mobile UEs are allowed to contend for communications with the BS via the same RISs.). If only static or only mobile UEs have to be served in a frame, the proposed MAC protocol will become a pure scheduled mode or a pure contended mode. The ratio of  $\beta/\alpha$  is optimized by the BS during the computing period. In addition, centralized optimization is used for scheduled transmissions, while distributed optimization is used for contended transmissions.

### Signaling and data flow

1. **MAC Design:** MAC protocol that integrates the centralized and distributed implementations into a frame is presented, as illustrated in Figure 6-24. The pilot period is further divided into  $K$  pilot slots according to the number of existing UEs. Based on the received pilot transmissions, the BS estimates the CSI of static UEs and calculates their RIS configuration and MAC protocol parameters during the computing period. Assume that the scheduled transmission period contains  $J$  data slots and that  $C$  sub-channels may be utilised. The BS coordinates the multiple access of static UEs, following that, the static UEs transmit their data to the BS via RISs based on the scheduled results. During the contended transmission period, mobile UEs compute the RIS configuration and contend for their access based on their CSI. Specifically, to facilitate both static (scheduled) and mobile (contended) UEs, the protocol involves the following steps in order:

1. **Pilot transmissions** (all UEs participating) for the BS to acquire all needed CSI.
2. **Computing and feedback** (performed individually by the BS). It involves the following operations:
  - a. **User classification** to either mobile or static based on the acquired CSI.
  - b. **Resource Allocation:** The BS first computes the duration of the scheduled transmission period and that of the contended transmission periods, namely  $\alpha$  and  $\beta$  ratios. Then, the BS allocates  $M$  RISs and  $J$  data slots to static UEs over the  $C$  non-overlapping sub-channels.
  - c. **RIS phases configurations** are computed so that the rates of the scheduled UEs are maximised.
  - d. **Feedback** messages are broadcasted so that all UEs being communicated their scheduled periods and sub-channels.
3. **Scheduled transmissions of static UEs** for the predetermined period, using the computed RIS configurations and UEs' allocations to sub-channels.



**Figure 6-24: The MAC protocol of the proposed NGMA framework as a frame structure.**

4. **Contended transmission for mobile UEs.** As the designated contended transmission period begins, the unscheduled mobile UEs start their multiple access and compute the RIS configuration by themselves based on the estimated CSI, which is calculated according to the sensing of each mobile UE on each sub-channel. In contrast to the scheduled transmission of

static UEs, mobile UEs have to negotiate with the BS for their channel access and RIS configuration, which is based on the distributed coordination function scheme by performing the following actions:

- a. **Backoff and computing:** A mobile UE senses the state of the sub-channels. Once a sub-channel is sensed to be idle, waits for an inter-frame space, the mobile UE starts backoff on this sub-channel and computes the RIS configuration.
- b. **Request:** Once the backoff and computing are finished at the contended sub-channel, the mobile UE sends a request-to-send packet included its RIS configuration information to the BS on its occupied sub-channel.
- c. **Feedback:** If the requested RIS is available for the mobile UE on its occupied sub-channel, the BS allows the RIS controller to configure the RIS reflection parameters, and replies a clear-to-send packet to the mobile UE.
- d. **Transmission:** Once the clear-to-send feedback is received at the mobile UE, it then transmits the data to the BS via the configured RIS on its occupied sub-channel.

### 6.9.3 Results and outcomes

Given the dynamic switching between the scheduled mode and the contended mode, our MAC protocol is capable of maintaining the target rate via RISs at a low cost. Additionally, the fairness of the static and mobile UEs having poor channel conditions can be maintained by scheduling and effective contention, respectively. In fact, the proposed contribution has the following advantages: (i) *Complexity reduction*. By implementing centralized and distributed operations for static and mobile UEs instead of harnessing centralized operation for all UEs, the computational complexity of RISs can be substantially reduced in the computing period and the contended transmission period, respectively. (ii) *RIS utilization improvement*. Upon considering dynamic wireless environments, each period of a frame can be adjusted to improve the utilization of RISs. (ii) *Service fairness improvement*. The RISs can serve new mobile UEs in the contended period of the current frame, thereby providing fairness for the UEs. As illustrated in the numerical evaluations conducted in the corresponding publication [ZSA23], the proposed framework is able to fully utilize the presence of RIS in massive UE scenarios and outperform scheduling-only and contention-only schemes.

### 6.9.4 Relation to other RISE-6G contributions

This contribution is related to the multiple access procedure presented in Section 6.8. It is designed to account for multiple RISs and massive numbers of UEs with different mobility profiles, thus a more involved framework and access procedures are developed. At the same time, the protocol relies on efficient scheduling and RIS configuration algorithms – which are the focus of Deliverable 4.4.

## 6.10 A Self-Configuring RIS Solution Towards 6G

### 6.10.1 Motivation and context

In [ADS22], we envision the novel concept of self-configuring RIS, i.e., an *autonomous* RIS device that automatically optimizes its configuration without any specific CC with the BS, i.e., having an implicit CC. To this goal, sensing capabilities are required and a quasi-active RIS (HRIS) needs to be employed. However, scheduling the HRIS operation modes concurrently with communication protocols creates challenges that needs to be addressed. Indeed, the sensing process requires shaping the propagation environment; this may exert a negative impact on the network operation if the sensing operation of the HRIS happens simultaneously to the sensing operation of the BS, for example during CE. Therefore, a detailed feasibility study and orchestration framework are required to effectively have self-configuring HRIS in place, while still ensuring conventional network operations. In [CDS23], we propose an orchestration framework to determine the optimal operation modes of HRISs and presents the self-configuring trade-off, an engineering trade-off that defines the applicability of self-configuring HRISs in



massive multiple inputs multiple outputs (MIMO) networks. The main architectural considerations are summarized here.

### 6.10.2 Overall system description

#### Deployment scenario

The considered scenario is a mMIMO communication scenario in which multiple single-antenna UEs are served by a single multi-antenna BS. A HRIS is deployed to increase the coverage of the BS, helping the communication with the edge UEs. Both direct and reflected links are considered. The deployment scenario is shown in Figure 6-25.

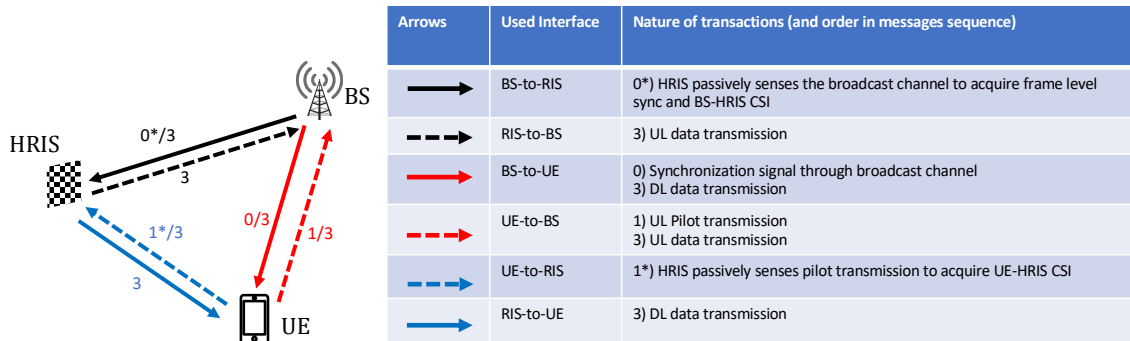


Figure 6-25: Physical scenario of deployment and nature of transactions.

#### Methodology and control considerations

The HRIS relies on *implicit CC*, and no specific control message is sent to control the device. The HRIS has two modes of operation:

1. Probing mode: the sensing mode of the HRIS. In this mode, the HRIS continuously changes configurations and sense the environment to acquire the local CSI;
2. Reflection mode: the communication mode of the HRIS. In this mode, the HRIS has loaded the locally optimized configuration to help the mMIMO communication towards the UEs.

Concurrently, the BS and UEs have two operation phases:

1. Channel estimation: the UEs send pilot sequence; the BS processes them to acquire the E2E CSI
2. Data transmission: the UEs/BS transmit UL/DL data.

Once the RIS is in reflection mode, it provides additional high gain multipath components between the BS and the UEs, which can be detected by the standard channel sounding. Hence, the BS will implicitly exploit the presence of RIS in a transparent manner to the network. This requires that the HRIS reflection mode overlaps the CE phase of the BS. Moreover, at least one CE phase needs to be performed when the HRIS is in probing mode, so that the local channel can be estimated by means of the transmitted sequences. In general, there exists a trade-off between the accuracy of the CSI acquisition at both BS and HRIS and the overall communication performance generated by the time expended in the two operation modes. The higher the time in probing mode, the higher the CSI acquisition accuracy at the HRIS, and thus the higher the SNR boost provided by the HRIS, but the lower the time left for CSI acquisition at the BS. This leads to a lower accuracy of the CSI and thus to worse degraded communications performance. Vice versa, a low duration probing mode might prevent the HRIS to enhance the communication performance.

#### Signaling and data flow

The sequence of messages exchanged is given in Figure 6-26. It is worth noting that the HRIS is still connected to the CC of the BS as it was a UE. In this way, the HRIS can obtain frame level synchronization and BS position estimation resulting transparent to the BS.



The time diagram of the operations is given in Figure 6-27, which shows the organization of the phases and operation modes described in the Methodology section.

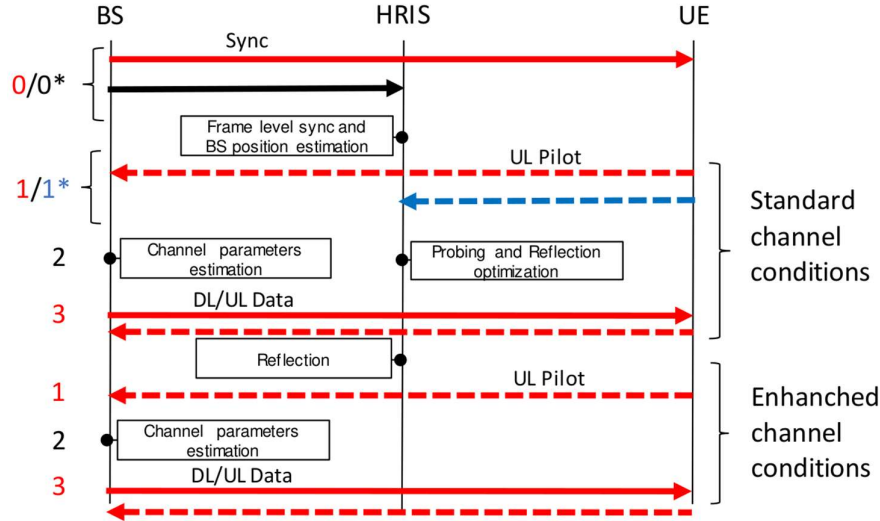


Figure 6-26: autonomous RIS implicit CC message sequence chart.

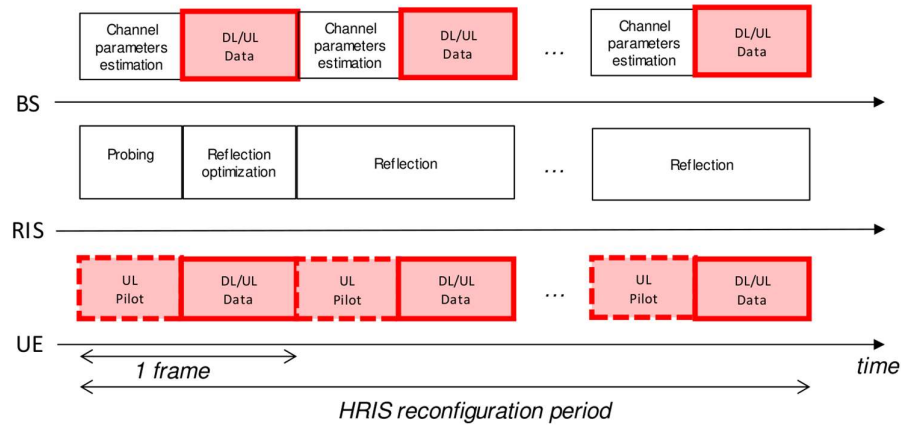
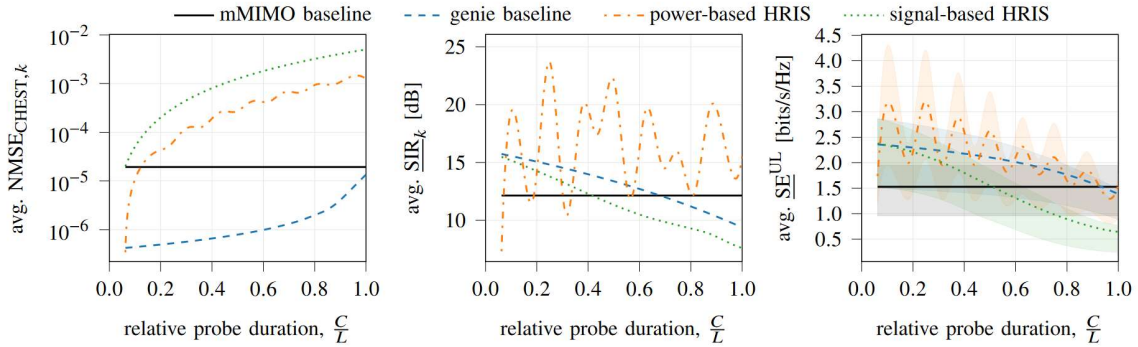


Figure 6-27: autonomous RIS implicit CC frame structure.

### 6.10.3 Results and outcomes

The study evaluates the proposed framework using two HRIS hardware architectures, power-based and signal-based HRISs, which differ in their hardware complexity. The results shown in Figure 6-28 indicate that the self-configuring HRIS can significantly improve network performance when using the proposed framework, when the probe duration is less than half of the overall frame duration. More details can be found in [CDS23].



**Figure 6-28: Network performance as a function of the probe/reflection trade-off. In order: NMSE of the CE at the BS; Average signal-to-interference-ratio; Average SE achieved.**

#### 6.10.4 Relation to other RISE-6G contributions

The proposed contribution gives a generalized approach to deal with the performance evaluation of autonomous RIS with implicit CC. The developed framework can be extended to specific hardware and needs. Moreover, the contribution shows a basic trade-off that needs to be taken into account when using autonomous RISs; moreover, this method can be considered when deciding the deployment of RISs, where choosing an autonomous RIS can help to alleviate the overhead associated with the RIS CC.

### 6.11 RIS-Empowered MEC

#### 6.11.1 Motivation and context

This section is dedicated to the interplay between RISs and MEC, two key technological enablers of the 6G vision. The proposed RIS-Empowered MEC paradigm plays a key role in improving network performances, thanks to the double benefit of computation and communication aspects, to be tackled and optimized jointly. In particular, a strong performance boost can be achieved by empowering MEC systems with RISs, with the aim of enabling applications running at the edge of the wireless network with the required quality of service in terms of latency, energy, and accuracy. The goal of this section is to summarize and describe the main achievements of RISE-6G project in this context. In the following, we present three different contributions, based on the same architecture and deployment scenario.

#### 6.11.2 Overall system description

The first contribution proposed in this section devises a novel methodology for MEC empowered by multiple RISs [DMC21]. The architecture considers an AP endowed with an ES via a highspeed backhaul link, multiple UEs, and multiple nearly passive RISs. Hinging on the presence of several RISs, this architecture aims to enable edge computing services to UEs through a dynamic optimisation of radio (i.e., power, transmission rates, sleep mode and duty cycle) and computation resources (e.g., CPU clock frequencies, etc.), jointly with the optimal selection of RIS's phase profiles.

The method has also been extended in the second proposed contribution [AMD22], to incorporate MIMO communications and robustness to intermittent mmWave links. In this setting, we are specifically interested to mmWave communications that imply a higher sensitivity to the presence of blockages. The main goal is to explore how effective is the use of an RIS to counteract the complexity brought when going higher in frequency and to minimize UE's transmit power, with guaranteed finite E2E delay of the offloading service. In these first two contributions, we suppose that the AP assigns orthogonal channels to its connected UE, thus preventing interference among them, while simultaneously served.

The last contribution [MFC21] of this section focuses on the intersection between the possibility of adapting wireless propagation as per end UEs' convenience according to specific service requirements, enabled by RISs, and the possibility to bring a powerful distributed computing environment at the wireless edge, enabled by the MEC. In particular, we leverage on the recently developed Lorentzian model for

RIS reconfiguration parameters, which allows the optimization of the wireless communication through frequency dependent RIS response profiles. From the UE perspective, the goal is to minimize the power spent by the device for processing data locally and then transmit information units in order to enable a desired computation offloading task, within a maximum required service delay.

### Deployment scenario

The proposed RIS-empowered MEC contributions are based on the following deployment scenario. The third contribution is based on the exact represented scenario, consisting of a single AP/ES (named as BS), a single RIS and a single UE requiring offloading its tasks. The second contribution allows simultaneous multiple UEs for computation offloading, each one interacting with the single RIS and the single BS, when possible, as for the single-UE case. The first proposed methodology considers a MEC system endowed with multiple passive RISs and multiple UEs, where again this scenario applied whenever a UE is connected to the BS and an available RIS.

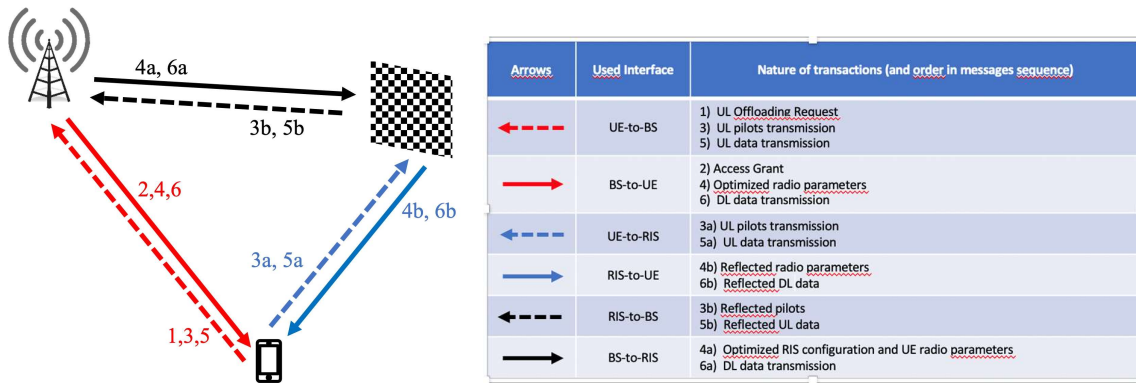


Figure 6-29 Physical scenario of deployment for RIS-Empowered MEC

### Methodology and control considerations

In the proposed RIS-empowered MEC contributions, the time is divided in slots, whose duration is designed with respect to the channel coherence time. The computation offloading procedure starts after a first phase during which the UEs are granted by the BS (here intended as the ensemble of AP and ES) to access the wireless network, following their requests. Each time slot is divided in two portions: the first one is dedicated to CE, control signalling and then to perform the proposed optimization of radio resources and of the RIS(s) configuration; the second part consists of the actual task offloading, which involves the optimization of computation resources, the UL data transmission, the data processing and the DL of results. The overall procedure is detailed as follows:

1. At the beginning of the slot, UE(s) perform a computation offloading request, which is acknowledged by the BS, if sufficient resources are available.
2. UE(s) send pilot signals to the BS, directly (when possible) and (or) reflected by the RIS(s).
3. The BS performs the estimation of UE(s)-BS and UE(s)-RIS(s)-BS channels, and the joint optimisation of radio resources and RIS(s) configuration parameters. The first proposed strategy [DMC21] is the only one that optimizes also DL communication resources. The BS sends the optimisation results to the UE(s) and to the RIS(s) via a dedicated out-of-band CC.
4. The UE(s) upload data to enable the computation offloading, directly to the BS if possible and (or) through the RIS(s). In the third proposed method [MFC21], the UE performs a local optimisation of CPU clock frequencies and then a partial data processing, before the UL transmission. The BS performs the optimal allocation of computation resources for each

connected UE. Then, after the remote data processing for all required computations, the BS sends results back to the intended UE(s), directly and (or) through the RIS(s).

### Signaling and data flow

Examples of the proposed message sequence chart is shown in Figure 6-30, while the time-diagram of the operations is presented in Figure 6-31. The following message exchanges can be applied to all the proposed three methodologies, considering for each UE a RIS static deployment scenario, during each time-slot, where the system optimization is carried out in a centralized manner within the network. The overall procedure (signalling, computation and transmission) is performed within a coherence time of the channel, corresponding to the slot.

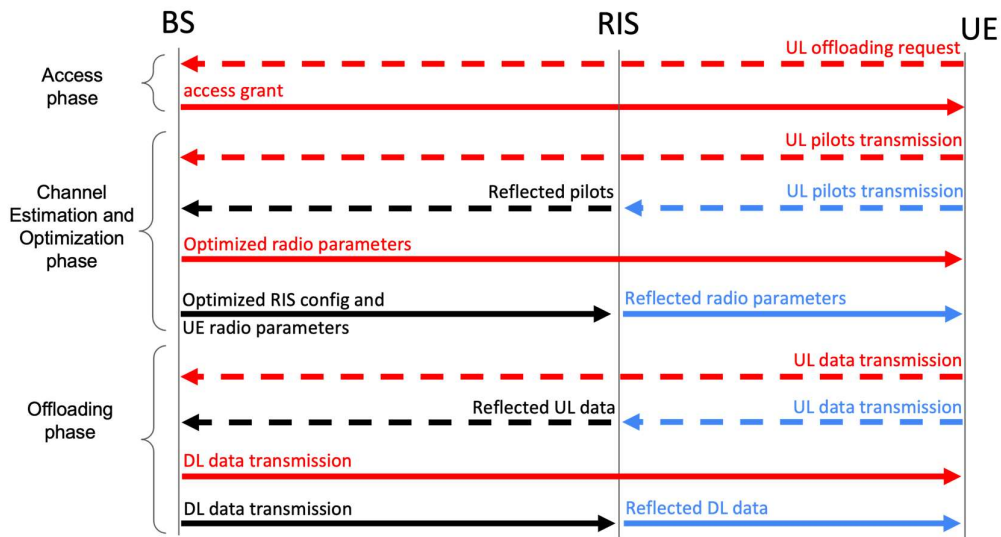
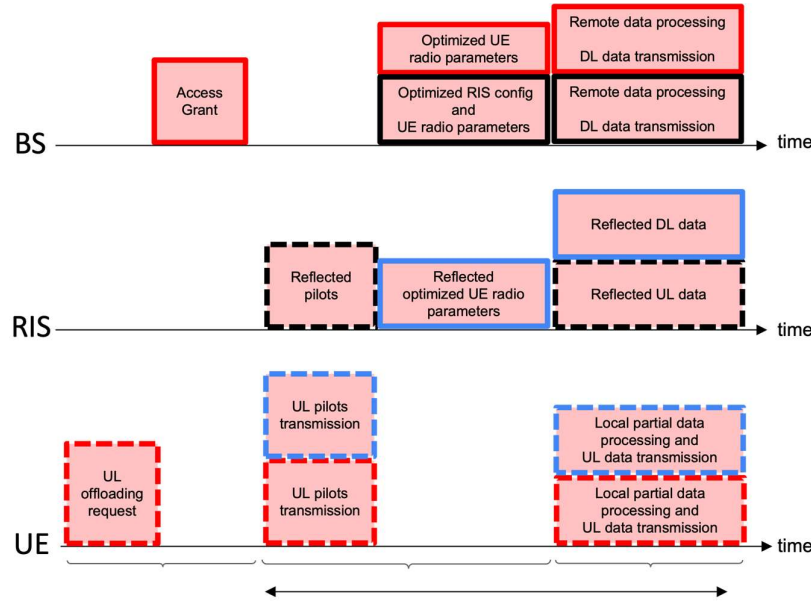


Figure 6-30 Message sequence chart for RIS-Empowered MEC



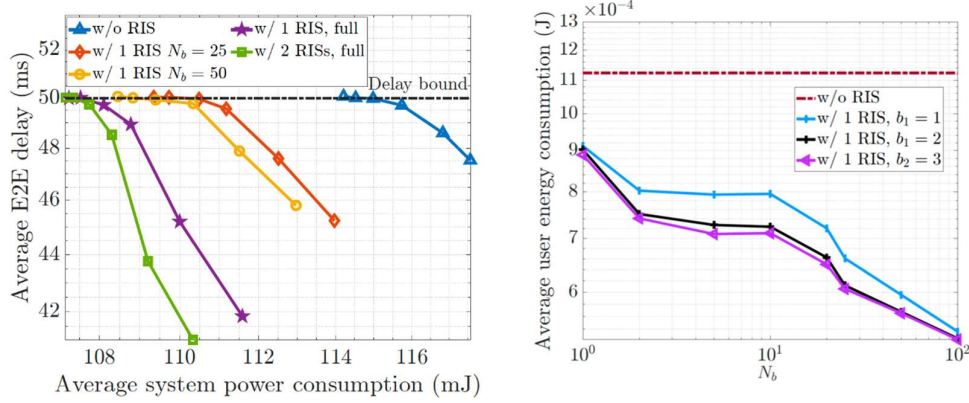
**Figure 6-31 Time diagram for RIS-Empowered MEC**

### 6.11.3 Results and outcomes

In this section, we illustrate the potential advantages introduced by our methodologies proposed in the context of MEC enhanced with RIS' technology. To show the results of the first contribution [DMC21], we consider a scenario composed by 5 edge devices, 1 AP and 2 RISs with 100 elements each. We assume that an obstacle obscures the direct communication between the UEs and the AP, with an additive pathloss attenuation equal to  $30dB$ . In Figure 6-32(Left), we illustrate the E2E delay as a function of the average energy spent by the overall system, for the Lyapunov trade-off parameter  $V$  increasing from right to left. By increasing  $V$ , each curve reaches a different value of the average energy consumption, while converging to a desired delay bound (in this case set to  $50ms$ ). The performances are evaluated for different scenarios. All RIS-Empowered strategies clearly outperform the one without RIS (blue curve), in terms of energy-delay trade-off. In case the optimization of the phase-shift parameters is performed for each single element of the RIS (violet and green curves), we can achieve the largest gain. When RIS' elements are optimized in groups of 2 ( $N_b = 50$ ), or in groups of 4 ( $N_b = 25$ ), the complexity of the proposed greedy strategy is clearly reduced, but at the cost of increased energy consumption. In Figure 6-32(Right), we explore the performance in terms of energy consumption in the UE-centric case ( $\sigma = 1$ ), as a function of the number of blocks  $N_b$ , for different number on bits  $b_i$  used for RIS' optimization. As expected, by increasing the number of blocks, the energy consumption decreases thanks to the larger degrees of freedom in optimizing the RISs. Also, increasing the number of bits yields a further reduction in the energy consumption.

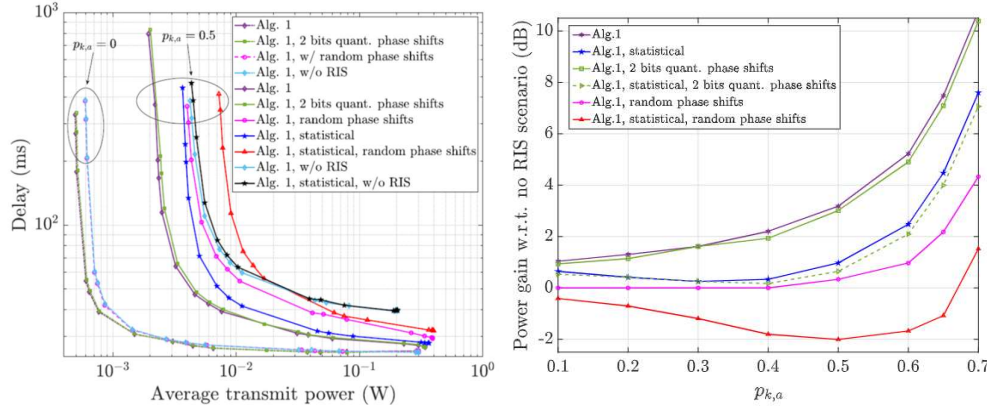
The scenario of our second contribution [AMD22] is composed by 6 edge devices, 1 AP and 1 RIS with 64 elements, with 4 antennas at either at the TX and the RX. In Figure 6-33(Left), we assess the performance of the proposed methodology in striking the best trade-off between energy consumption and average delay for different blocking conditions. We compare strategies with instantaneous knowledge of blocking states (named simply Alg. 1), strategies with statistical blockage knowledge (with probabilities  $p_{k,a}$ ), both of them with and without RIS and considering also random RIS' phase shifts and different quantization bits. All scenarios with optimized RIS outperform the case without RIS, although with negligible gain in the absence of blocking. This suggests that the benefits of the RIS are more significant in case of high blocking probability of the direct link. The method illustrates also very good performance if the RIS phase shifts are quantized with 2 bits, which is typical of practical scenarios.





**Figure 6-32 (Left) Average E2E delay versus Average system energy consumption, for different scenarios. (Right) Average UE Energy consumption versus number of blocks composing the RIS, for different number of quantization bits.**

We illustrate in Figure 6-33(Right), the gain in terms of average transmit power of each strategy with respect to the no-RIS case, as a function of the direct link blocking probabilities, for a fixed E2E delay bound of 150ms. As can be seen, as  $p_{k,a}$  increases, the gain notably increases also for quantized phases. Conversely, in case of statistical blockage knowledge, the gain is visible only for higher blocking probabilities, being the channel knowledge well-matched to the real channel states.



**Figure 6-33 (Left) Delay-Energy trade-off for different offloading strategies. (Right) Average transmit power versus AP blocking probability**

We assess the performance of our third proposed strategy through a scenario composed of 1 UE device, 1 AP and 1 RIS with 100 elements. Time is divided in slots of equal duration, during each slot Rayleigh fading SISO channels are generated. We compare the RIS-aided performance with the Lorentzian model and our frequency selective-aware optimization, termed as *Lorentzian RIS*, with two benchmarks: i) the case without the RIS, termed as *no RIS*; ii) the frequency flat RIS case, termed as *flat RIS*, in which the RIS response does not follow the realistic Lorentzian model, but it is flat across all frequencies. In Figure 6-34(Left), we show the trade-off between the average E2E delay and the power consumption for two different average delay thresholds, namely 100ms and 80ms. As we can notice, for all curves, the average E2E delay increases as the power consumption decreases, until approaching the delay constraint. However, the *no RIS* case exhibits the worst performance in terms of delay-power trade-off, as it achieves higher delays for a fixed power consumption. At the same time, the best performance is achieved by the

*Lorentzian RIS*. Moreover, focusing on the highest delay (points on the left side of the plot), which is indeed the service requirement, we can notice how the proposed method achieves the lowest power consumption, while a slight gain with respect to the *no RIS* case is achieved by the *flat RIS*. Finally, in Figure 6-34(Right), we plot the complementary distribution function of the delay, also known as survivor function, for the highest value of  $V$ , validating the ability of our algorithm to guarantee the probabilistic constraint, as shown by the intersection of the curves between the maximum allowed delay  $D_{max}$  and the reliability threshold  $\epsilon$ .

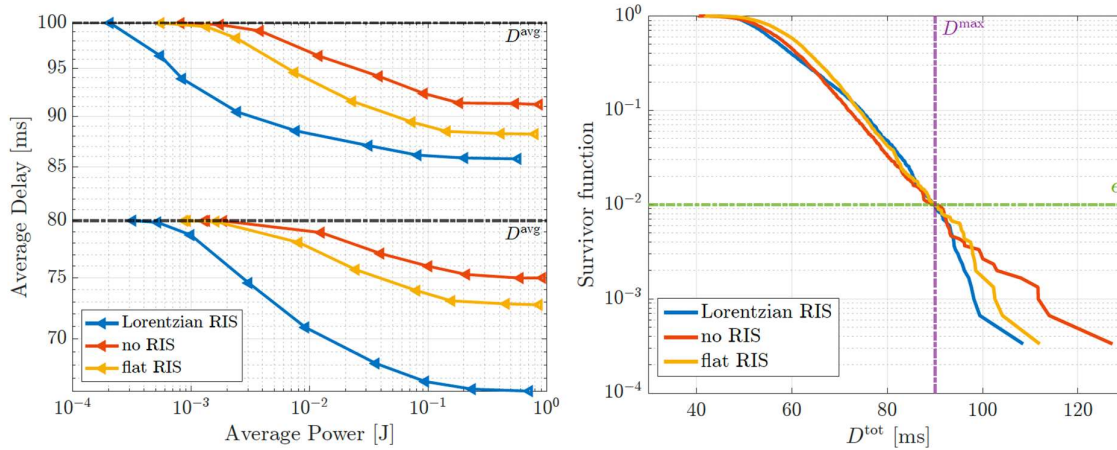


Figure 6-34 (Left) Average power consumption versus average delay, for different strategies. (Right) Survivor function.

#### 6.11.4 Relation to other RISE-6G contributions

The proposed RIS-Empowerd MEC strategies can be generalized considering more sophisticated channel models or the definition of specific applications running at the ES. The strategies hinge on the CE methods developed in WP4. The investigated trade-offs rely on the control of the RIS in terms of hardware parameters, as discussed in WP4.

### 6.12 Reconfigurable Intelligent Surfaces With Outdated Channel State Information: Centralized vs Decentralized Deployments

#### 6.12.1 Motivation and context

We investigate the performance of an RIS-aided wireless communication system subject to outdated CSI that may operate in both the near and far-field regions [ZZD22]. In particular, we take two RIS deployment strategies into consideration: (i) the centralized deployment, where all the reflecting elements are installed on a single RIS and (ii) the distributed deployment, where the same number of reflecting elements are placed on multiple RISs.

#### 6.12.2 Overall system description

##### Deployment scenario

As illustrated in Figure 6-35, we consider a SISO system in which a fixed single-antenna BS communicates with a single-antenna mobile UE with the assistance of  $M$  passive reflecting elements, with each element being capable of independently adjusting its phase shift to reflect the incident signals towards desired directions. Two strategies for deploying the  $M$  reflecting elements are considered: the



centralized and distributed deployments. As far as the centralized deployment is concerned, the  $M$  reflecting elements are installed on one RIS. As far as the distributed deployment is concerned, on the other hand, the  $M$  elements are placed on  $L$  ( $L \geq 2$ ) RISs, where the  $l$ -th RIS is equipped with  $M_l$  reflecting elements.

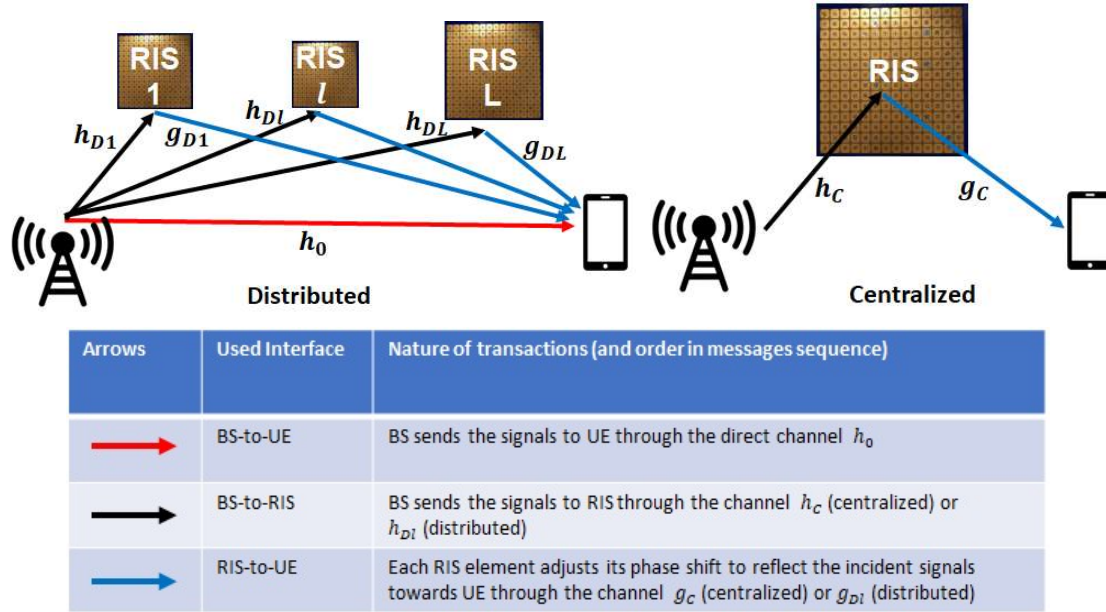


Figure 6-35: Physical scenario of deployment and nature of transactions.

### Methodology and control considerations

In this work, the channel from the BS to the RIS is assumed to be perfectly estimated because the BS and the RIS are assumed to be at fixed locations. Due to the UE mobility, it is not usually possible to perfectly estimate the CSI at the BS and the RIS (e.g., due to the acquisition delay and the feedback overhead). Therefore, we focus our attention on the impact of outdated CSI on the system performance. The correlation coefficient between the outdated channel estimate and the actual channel, can be calculated based on Clarke's fading spectrum.

After CE, the phase shifts at the RIS can be designed such that the outdated direct channel (from the BS to the UE) and the outdated cascaded channel (from the BS to the RIS and from the RIS to the UE) are co-phased.

Then, the received signal is obtained by the sum of the direct signal and the signal reflected by the RIS (centralized) or the sum of the signals reflected by all the  $L$  RIS (distributed).

To analyze the performance of the centralized and distributed RIS-aided systems in near field and far field based on the received SNR, we introduce approximated expressions of the ergodic capacity (EC) based on the Gamma approximation (see details in [ZZD22]).

### Signaling and data flow

The UE sends pilot signals to BS directly or through RIS, to allow the BS to estimate the direct channel and the cascaded channel. Due to the UE mobility, the expressions of the BS-UE channel and the RIS-UE channel consider the impact of the outdated CSI. Then, the phase shifts at the RIS can be designed such that the outdated direct channel and the outdated cascaded channel are co-phased.

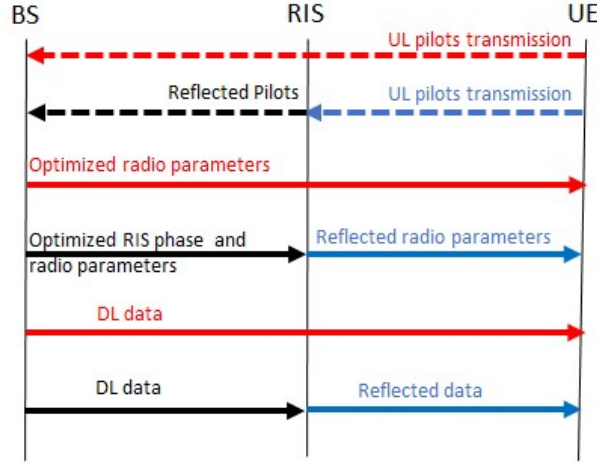


Figure 6-36: Message sequence chart for CE with RIS

### 6.12.3 Results and outcomes

We compare the analytical results against Monte Carlo simulations. In Figure 6-37, the accuracy of the Gamma approximation as well as the tightness of the upper and lower bounds for the EC are examined. It can be observed that the Gamma approximation provides an almost perfect match with the simulated results (see details in [ZZD22]).

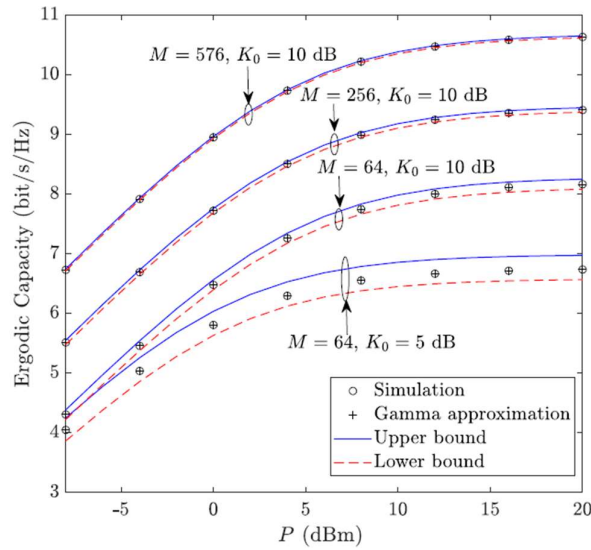


Figure 6-37: EC versus P for different values of  $K_0$  for centralized and distributed RIS deployments.

### 6.12.4 Relation to other RISE-6G contributions

For both deployment strategies, we derive accurate closed-form approximations for the EC, and we introduce tight upper and lower bounds for the EC to obtain useful design insights. Our analysis reveals that the system performance improves with the transmit power, the Rician-K factor, the outdated CSI coefficient, and the size of the reflecting elements. Furthermore, the numerical results show that a distributed RIS-aided system usually outperforms a centralized RIS-aided system, and that they provide almost the same EC if a single RIS is deployed near the TX or near the RX. This study justifies the

deployment of distributed RISs in scenarios where the CSI is often outdated (such as with medium/high UE mobility) and could be used as a motivation to extend other RISE-6G relevant methods to the distributed RIS case.

### 6.13 Channel estimation with simultaneous reflecting and sensing RIS

#### 6.13.1 Motivation and context

Since large numbers of reflecting elements are involved during the transmission process of RISE networks, the problem of CE is getting increasingly difficult and requires a considerable overhead in terms of pilot signals and involved computations. Even more so, common reflective RISs allow only for the E2E channel to be estimated. This poses fundamental limitations to the application of many algorithmic frameworks that usually make assumptions about the availability of CSI on individual communication links. Those limitations, however, can be overcome by the deployment of a RIS empowered with both reflecting and receiving functionality. Those quasi-active RISs not only control the impinging waveform but are also capable of sensing and processing signals using some active elements (i.e., elements with enabled RF-chains) [ZSA23].

#### 6.13.2 Overall system description

##### Deployment scenario

This contribution concerns the process of CE in a quasi-active-RIS-empowered system. An indicative application considering an UL multi-UE scenario was studied, as illustrated in **Erreur ! Source du renvoi introuvable.**

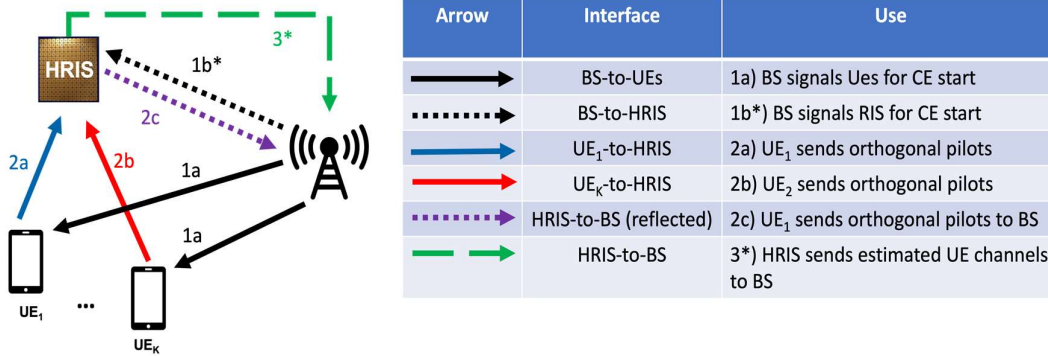


Figure 6-38: Deployment and signaling of a quasi-active RIS (HRIS) for CE of partial wireless links (\* denotes over-the-air interface).

##### Methodology and control considerations

The participating UEs send UL pilots utilizing orthogonal frequency resources. In that, a (controllable) portion of the impinging RF signal is absorbed by the active RF-chains to perform the local analog combining and digital processing, before being forwarded (out-of-bound) to the BS which plays the role of the estimation endpoint. Since the BS receives both the reflected pilots, as well as the sensed UEs-RIS channel, it is able to gain knowledge of all partial links of the communication system. The control needed for this methodology involves synchronisation and allocation protocol operations, as is typical in CE frameworks as well as an out-of-band one-way channel from the RIS to the BS. A lower bound of the number of power signals needed for ideal channels has been derived, and the estimation-MSE of the individual links has been expressed as functions of the quasi-active RIS parameters, given the received pilots. Therefore, the estimation procedure is facilitated using standard numerical optimization algorithms.

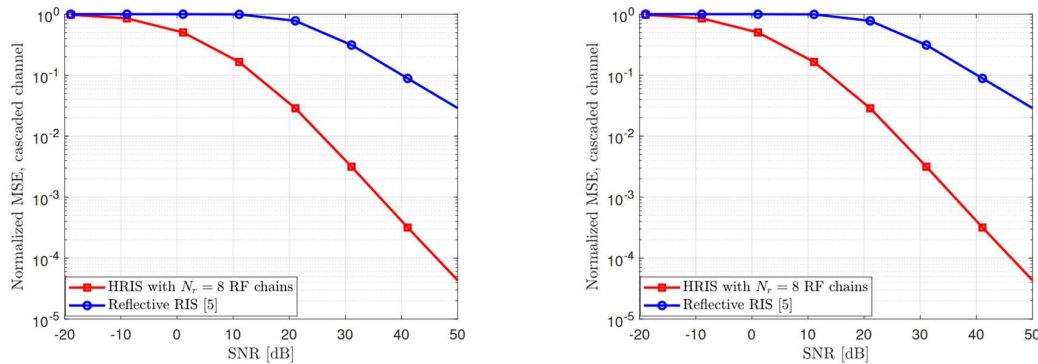
### Signaling and data flow

The signaling operations involved in this contribution are similar to that of Contribution 6.5. The respective Figure 6-14 describes the signalling operations of the current deployment strategy, with the only difference being in step 3: There is no need for the HRIS to turn off to perform estimation for the direct link, as the communication is assumed to be happening via the RIS-reflected path (i.e. the direct link is attenuated). Instead, in step 3 of this approach, the HRIS computes the partial channels locally and forwards the information to the BS.

The data flow is split in terms of  $T$  frames. At each frame, the RIS selects a new configuration.  $B$  orthogonal pilots are transmitted by the UEs. The RIS senses a portion of the received signals and performs an initial estimate of the channels. The rest of the signal is reflected so that the BS also receives the pilots. After the final frame is completed, the RIS controller performs its final estimate of the channel, which is then transmitted using a dedicated link to the BS.

### 6.13.3 Results and outcomes

In the high SNR regime, and considering the ideal case of negligible noise presence, the lower number of pilots needed for accurate recovery of the individual channel links is proved to be inversely proportional to the ratio of the total number of RIS elements versus the number of RF-enabled elements, resulting in an intuitive benefit in terms of pilot overhead when quasi-active RISs with a reasonable number of active elements are deployed. A practical consideration of the methodology is to determine the power splitting parameter of the surface. It has been observed that a trade-off in the accuracy of the BS-RIS versus UE-RIS links exists when the ratio of the reflected signal is lower than 50%, while no substantial improvements are observed after that value. As we can notice from Figure 6-38, when comparing estimation results of the quasi-active RIS methodology over a benchmark approach utilizing a reflective RIS and setting the number of pilots to equal lengths for both cases, the quasi-active approach results in multiple orders of magnitude lower error in the estimation of the cascaded channel in the high-SNR regimes.



**Figure 6-38: CE performance of the proposed methodology utilising a quasi-active RIS. (left) Trade-off of estimation errors between the BS-RIS and the BS-UE links across different configurations. (right) Estimation of the cascaded channel over increasing SNR values [ZSA23].**

### 6.13.4 Relation to other RISE-6G contributions

The benefits of this approach are illustrated by the fact that the number of pilots needed for effective CE can be hugely decreased when quasi-active RISs with only a small number of RF-enabled elements are considered. As a sidenote, quasi-active RISs can also be configured to act in reflect-only or receive-only mode, if desired, and as a result they can be deployed with negligible control and energy overheads when their sensing functionality is not needed. This work should be considered together with other relevant RISE-6G contributions that consider the CE procedure with nearly-passive RISs, in order to study the underlying trade-offs in terms of performance and overhead/power consumption at the deployment stage.

## 6.14 Static RIS tuning in rich scattering environments

### 6.14.1 Motivation and context

Rich scattering occurs in wireless environments in which many scattering objects appear. When those scatterers move through time the state of the channel changes dynamically in unpredictable patterns. In such cases, the standard methodology of measuring each channel realisation and optimising the RIS configuration at every channel frame is not only challenging, but additionally provides more limited boost in terms of enhanced spectral efficiency. This contribution presents an alternative methodology which involves estimating the channel statistics over time and setting the RIS configuration so as it maximises the expected value of the target KPI.

### 6.14.2 Overall system description

#### Deployment scenario

The overall deployment system considers a simplified scenario with a static DL multi-antenna TX/RX pair and an RIS, placed on a *dynamic, high-reverberating* environment due to the presence of perturbing and moving objects that create rich scattering, as illustrated Figure 6-39.

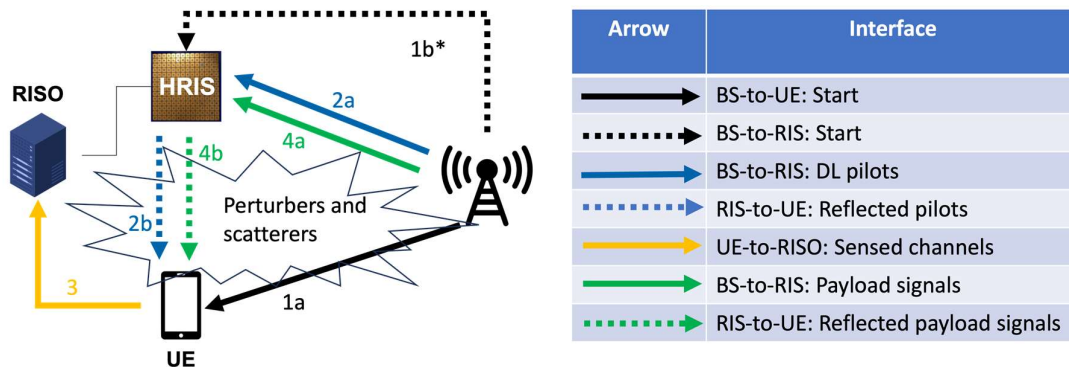


Figure 6-39: Deployment architecture of the static RIS tuning methodology.

#### Methodology and control considerations

The system involves four phases, whose time evolution and messaging is depicted in Figure 6-40:

1. **Channel sounding and measurement phase:** Using the CE procedure presented in the contribution of Section 6.5, the channel responses are sensed over an enlarged period that spans multiple channel frames.
2. **Optimisation:** Based on the acquired information, the system performs an algorithmic-defined optimisation to attain the RIS configuration that maximises the expected value of the objective. Note that other parts of the network may be optimised altogether, therefore the RIS components is utilised in Figure 6-39.
3. **RIS configuration:** The network controller informs the RIS about the selected profile and the RIS switches to the selected phase shifts. The phase shifts stay constant for the duration of the deployment.



4. **Payload transmissions:** The system proceeds to normal transmission mode. The selected RIS tuning is designed to guarantee on average high/designated KPI values, despite the effect of individual channel realisations.

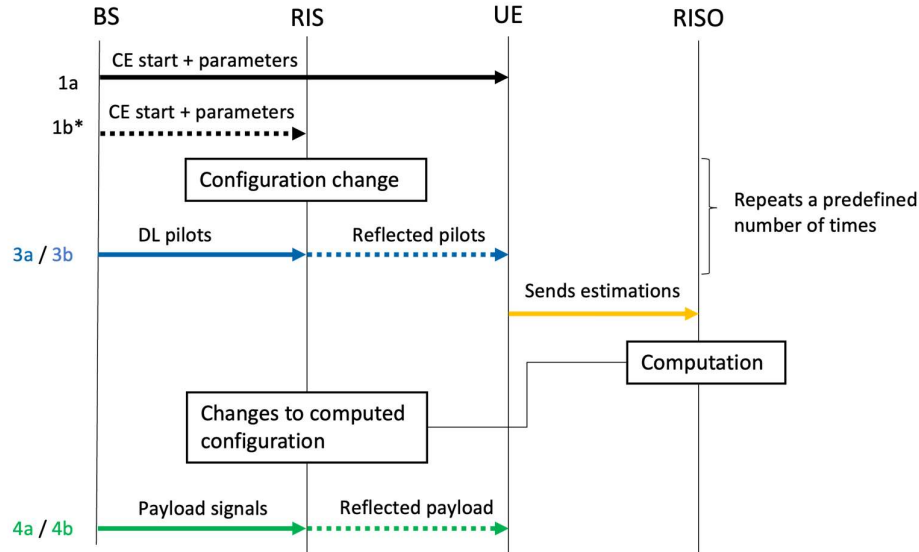


Figure 6-40: Time diagram of the static RIS optimisation deployment strategy.

### Signaling and data flow

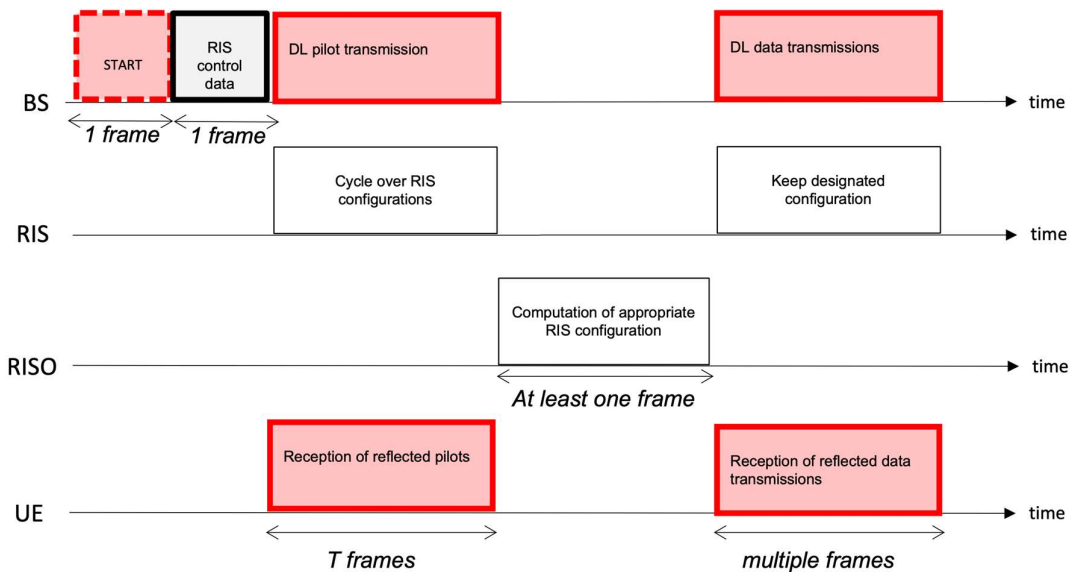


Figure 6-41: Data flow of the static RIS tuning methodology.

The signalling requirements for this operation are minimal, and are restrained in the first three phases, allowing for full utilisation of the channel resources for communication. As illustrated in Figure 6-41, the





main overhead of this methodology lies in the extended channel sounding phase, the duration of which should be long enough to accurately capture the statistics of the reverberating environment.

### 6.14.3 Results and outcomes

The described contribution provides a system overview of a solution for rich scattering environments. Under D4.4, algorithmic advancements based on deep learning, physics-based modelling, and discrete optimisation will be presented [TKB22] to showcase its effectiveness.

### 6.14.4 Relation to other RISE-6G contributions

This contribution has a close correspondence to the per-slot optimization framework proposed in the contribution of Section 6.6. In this approach, the specific problem of rich-scattering has been considered which leads to a static optimization problem, since in such conditions, a static (i.e. non-reconfigurable) RIS configuration is a more practical approach. To that end, the signalling and block-diagram methodologies are similar, with their main two differences being that, in this contribution, the channel measurement phase spans several channel frames, and that the process is not repeated after its end.

## 6.15 Autonomous RIS solution with Energy harvesting and Self-configuration

### 6.15.1 Motivation and context

Major impairments for commercially viable RISs are the need for a complex and fast CC to enable adaptation of RIS configuration to the channel condition changes, and the need for an extensive and capillary grid to supply power to each deployed RIS. In [ADS23], we extend the concept of self-configuring RIS proposed in [ADS22], by proposing a novel RIS design that combines the self-configuration capabilities of the RIS with the potential of EH. The novel solution, dubbed as ARES: an Autonomous RIS with Energy harvesting (EH) and Self-configuration solution, leverages an HRIS solution that combines the power detection capabilities of HRISs with EH, as we will detail shortly. The CSIs obtained are used both for communication purposes and EH operations, i.e., they are used for the optimization of the HRIS reflection properties and the maximization of the absorbed power. ARES is the first fully-autonomous RIS solution enabling a seamless installation of HRIS devices throughout the service area, without requiring modifications to the deployed mobile network and the power distribution system.

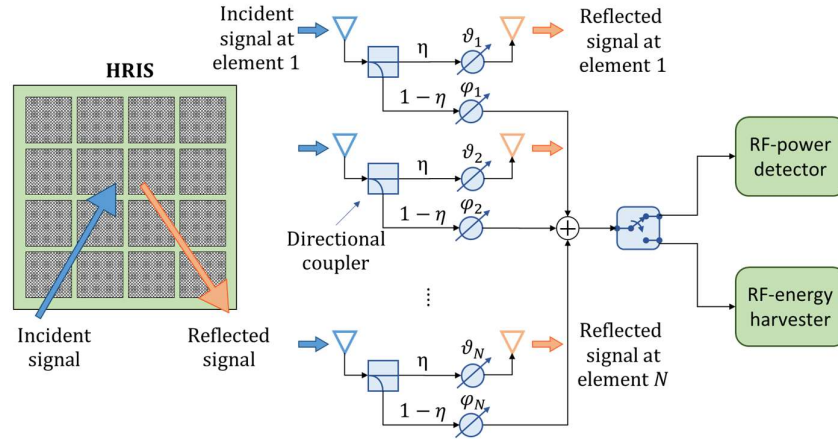
### 6.15.2 Overall system description

#### *Deployment scenario*

The considered playground is a MIMO communication scenario in which a multi-antenna BS serves multiple single-antenna UEs. An HRIS is deployed to improve channel conditions and increase communication performance between BS and UEs and is in line with the deployment scenario depicted in Figure 6-25.

#### *Methodology and control considerations*

Figure 42 depicts the proposed HRIS hardware architecture, which extends the architecture proposed in [ADS22] to enable EH. A directional coupler splits the incident signal into the reflection and absorption branches of the RF circuits of the HRIS. The portion  $\eta$  of the signal is fed into the reflection branch and re-irradiated according to the reflection configuration  $\vartheta$ . While portion  $1 - \eta$  of the incident signal is directed to the absorption branch. The proposed hardware allows tuning the absorption properties of the HRIS using the absorption configuration  $\varphi$ . Following [ADS22], an RF combiner sums the signal components absorbed by each HRIS element. We place an RF switch downstream of the RF combiners. The switch allows us to steer the absorbed signal either towards the RF-power detector or the RF-energy harvester, which are used for directional power sensing and EH, respectively. A rechargeable battery collects the harvested energy and feeds the active components of the HRIS hardware.



**Figure 42: Reference diagram of HRIS with EH capabilities.**

In line with contribution 6.10, the HRIS is not receiving any specific control message from the BS and relies only on the implicit CC. Moreover, it operates according to the probing and reflection modes described in Section 6.10.2. However, it exploits the CSI available locally from the probing mode, to optimize both the reflection and the absorption configuration of the HRIS.

The operational steps are detailed as follows:

1. Probing mode: the RF switch steers the signal to the power detector, and the HRIS absorption configuration is continuously changed to directionally sense pilot transmissions from UEs and from the BS and acquire local CSI.
2. Local CSI is used to optimize the reflection configuration as per [ADS22] and the absorption configuration to maximize the absorbed power.
3. Reflection and harvesting mode: the reflection ( $\theta$ ) and absorption ( $\varphi$ ) configurations are set on the corresponding phase shifter bank. The RF switch steers the signal to the RF-energy harvester.

While the HRIS is in reflection and harvesting mode, it boosts channel conditions to increase communication performance. At the same time, it collects the fraction of the signal absorbed by the directional coupler to feed the battery with energy to operate the device. Operation phases of the BS follow the description in contribution 6.10.

### **Signaling and data flow**

The signaling and data flow of this contribution is the same as the one described in Section 6.10.2.

### **6.15.3 Results and outcomes**

The study evaluates the feasibility of EH for operating the devices by considering both the harvested and the consumed power. We consider a number of PIN diodes forming each phase shifter that is equal to the phase quantization level  $Q$ . Subsequently, we model the consumed power as a function of the active PIN diodes corresponding to the desired reflection and absorption pattern. While absorbed power is a function of the absorption configuration  $\varphi$  and the traffic level, which is modeled through the factor  $\zeta \in [0,1]$ . The results shown in Figure 43 indicate that radio frequency (RF) EH is feasible for operating the HRIS device.

The battery charge/discharge process is modelled with an irreducible Markov Chain, and the lifespan of the HRIS is evaluated considering a minimum level of energy available to operate the HRIS, below which the battery is considered to be in a loss of charge state. Figure 44 shows the LoC probability as a function of the battery size. The higher the battery size lower the LoC probability. More details can be found in [ADS23].

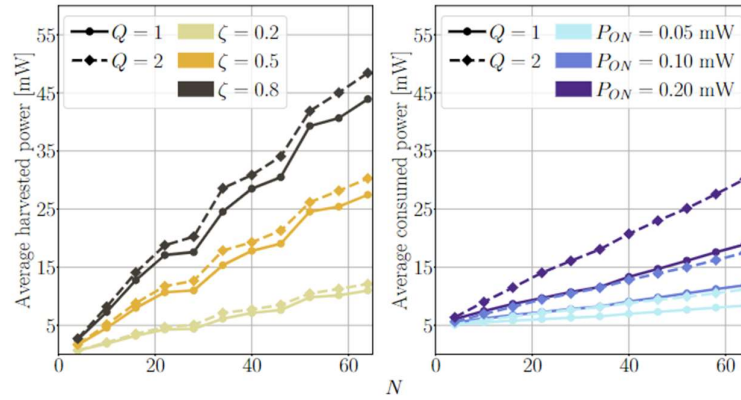


Figure 43: EH performance as a function of the number of HRIS elements  $N$ . The average harvested power is shown with different levels of traffic  $\zeta$  and different phase shifters quantization levels  $Q$ . The average consumed function is shown with different values of energy consumption of the PIN diodes  $P_{ON}$  and different phase shifter quantization levels  $Q$ .

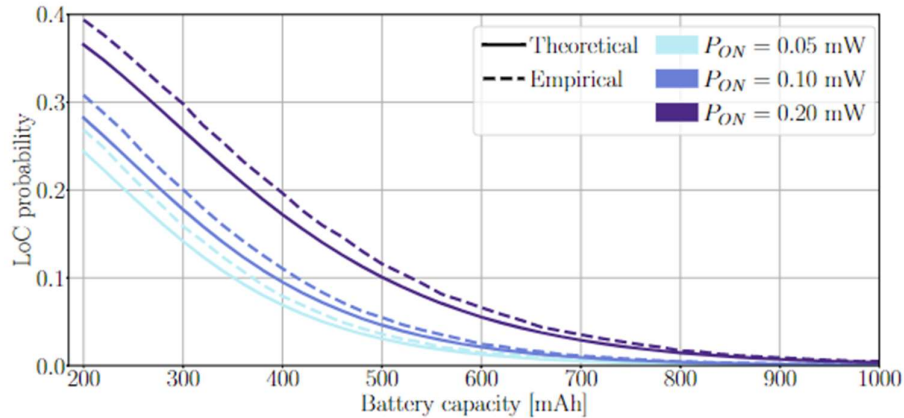


Figure 44: Loss of charge probability against the battery capacity.  $N = 40$  meta-atoms,  $Q = 2$ . The scenario includes  $K = 75$  users with traffic  $\zeta = 0.5$ .

#### 6.15.4 Relation to other RISE-6G contributions

The contribution demonstrates the feasibility of EH solutions to support the energy demand required to operate the RIS. The proposed solution further facilitates the deployment of autonomous RISs, which in addition to not requiring an explicit CC, are also free from the need for a power supply or periodic maintenance for battery substitution in the case of battery-powered RIS. Thus providing an additional degree of freedom to the RIS deployment. This work thus further strenghtens the case of using autonomous RISs and sheds light on the implications of using the technology as oppsoed to centralised RISs (as in most of the other relavant RISE-6G contributions), and should thus be considered in the deployment stage.



## 7 Conclusions and outlook

In this deliverable, we have provided RISE-6G proposals and guidelines on architectural elements related to deployment and control signaling in RIS-aided networks. Indeed, the integration of such novel devices, capable of providing boosted coverage areas in both UL and DL, enhancing connectivity and reliability, and enabling edge computing services thanks to the possibility of shaping the wireless propagation environment on-demand, requires novel architectural building blocks designed to tailor associated specific KPIs (e.g., rate, latency, etc.). We have provided a comprehensive view and the associated taxonomy related to the RIS deployment, network performance evaluation, and CC considerations.

In terms of deployment, we have addressed the problem of deploying RISs in a static or nomadic fashion (e.g., by mounting them on the facade of buildings or by mounting them on moving objects such as UAVs, respectively). Specifically, we have provided solutions to the deployment problem and associated RIS optimization in both cases, and provided several notable examples of realistic scenarios and use cases. Among them, we have identified four main design choices for the RIS deployment problem: 1) boosted communication and enhanced coverage, 2) static or nomadic RIS, 3) edge computing-aware schemes, and 4) AI-based solutions. A study on the different technical challenges and opportunities of both centralised and distributed RIS deployments has been provided.

Regarding the CC design, we have investigated the use of RISs in both a controlled and autonomous manner. In the former case, i.e., when there is an explicit CC between the RIS and the network, we have provided in-depth investigation of the joint BS and RIS configuration optimization. In this regard, RIS control can be executed via both in-band or out-of-band CCs. In-band CCs require a reliable communication between RISC and RISs, impacting on the choice of resource allocation and RIS configuration. This constraint is relaxed for the out-of-band channel, leading to a simpler control design. Whereas, to alleviate the burden of the control signaling to be exchanged between the RIS and the network (e.g., for CE operations), RISs can act autonomously to perform self-optimization based on locally available CSI, which is enabled to endowing the structure with basic sensing capabilities, thus making it a hybrid structure. In this case, the RIS is indirectly discovered and exploited by the BS as a high-power path towards the UE (implicit CC).

Motivated by the above, in this deliverable we have provided key design elements on the protocol structure necessary to support robust RIS operation, including the UE initial access. In this regard, a crucial part is the CE procedure, which is key to both the BS and RIS optimization. The associated CSI is then exploited for communication purpose, along with measurements of the current optimisation metrics and KPI, which require novel, specific control protocols. Both aspects directly impact the resource allocation problem, which is designed to account for both operations, and the overall RAN structure, as detailed in this deliverable.

In conclusion, it is the recommendation from this deliverable that the RISE-6G architecture should support all the aforementioned alternatives and define the interfaces and signals between the different entities in the architecture (UE, BS, RIS, RISA, RISC, ES, etc.). At a minimum, the RISE-6G architecture should support: (i) Synchronization among RISs, BSs, and UEs and the associated control signaling; (ii) Acquisition of the RIS-aided CSI; (iii) a RISC that adapts the configuration of the RIS in either a controlled or autonomous fashion.

## References

[AAS21]	I. Alamzadeh, G. C. Alexandropoulos, N. Shlezinger, and M. F. Imani, "A reconfigurable intelligent surface with integrated sensing capability," <i>Nature Scientific Reports</i> , vol. 11, no. 20737, pp. 1–10, Oct. 2021.
[ADS22]	A. Albanese, F. Devoti, V. Sciancalepore, M. Di Renzo, and X. Costa-Pérez, "MARISA: A Self-configuring Metasurfaces Absorption and Reflection Solution Towards 6G," in <i>IEEE INFOCOM 2022 - IEEE Conference on Computer Communications</i> , 2022.
[ADS23]	A. Albanese, F. Devoti, V. Sciancalepore, M. Di Renzo, A. Banchs, and X. Costa-Pérez, "ARES: Autonomous RIS solution with Energy harvesting and Self-configuration towards 6G." <i>IEEE Transactions on Mobile Computing</i> , under revision, 2023, [online] <a href="https://arxiv.org/abs/2303.01161">https://arxiv.org/abs/2303.01161</a> .
[AES22]	Albanese, A., Encinas-Lago, G., Sciancalepore, V., Costa-Pérez, X., Phan-Huy, D.-T., & Ros, S., "RIS-Aware Indoor Network Planning: The Rennes Railway Station Case," in <i>Proceedings of the IEEE International Conference on Communications (ICC) 2022</i> .
[AJH20]	S. Alfattani, W. Jaafar, Y. Hmamouche, H. Yanikomeroglu, A. Yongac oğlu, N. D. Đ'ao, and P. Zhu, "Aerial platforms with reconfigurable smart surfaces for 5G and beyond," <i>IEEE Communications Magazine</i> , no. January, pp. 96–102, 2020.
[AJS22]	Alexandropoulos, G. C., Jamali, V., Schober, R., & Poor, H. V. (2022, June). Near-field hierarchical beam management for RIS-enabled millimeter wave multi-antenna systems. In <i>2022 IEEE 12th Sensor Array and Multichannel Signal Processing Workshop (SAM)</i> (pp. 460-464).
[AMD22]	F. Ezzahra Airod, M. Merluzzi, P. Di Lorenzo, and E. Calvanese Strinati, Reconfigurable Intelligent Surface Aided Mobile Edge Computing over Intermittent mmWave Links, in <i>Proceedings of the IEEE International Workshop on Signal Processing Advances in Wireless Communication (SPAWC)</i> , 2022.
[APV21]	N. Awarkeh, D. -T. Phan-Huy and R. Visoz, "Electro-Magnetic Field (EMF) a-ware beamforming assisted by Reconfigurable Intelligent Surfaces," 2021 IEEE 22nd International Workshop on Signal Processing Advances in Wireless Communications (SPAWC), 2021, pp. 541-545.
[APV221]	N. Awarkeh, D.-T. Phan-Huy, R. Visoz, M. di Renzo "A Novel RIS-Aided EMF-Aware Beamforming Using Directional Spreading, Truncation and Boosting," accepted to EuCNC 2022.
[APV222]	N. Awarkeh, D.-T. Phan-Huy, M. di Renzo "A Novel RIS-Aided EMF Exposure Aware Approach Using an Angularly Equalized Virtual Propagation Channel," accepted to EuCNC 2022.
[ASA21]	G. C. Alexandropoulos, N. Shlezinger, I. Alamzadeh, M. F. Imani, H. Zhang, and Y. C. Eldar, "Hybrid reconfigurable intelligent metasurfaces: Enabling simultaneous tunable reflections and sensing for 6G wireless communications," <i>IEEE Communications Magazine</i> , under revision, 2021, [online] <a href="https://arxiv.org/abs/2104.04690">https://arxiv.org/abs/2104.04690</a> .
[ASC21]	A. Albanese, V. Sciancalepore, and X. Costa-Pérez, "SARDO: An Automated Search-and-Rescue Drone-based Solution for Victims Localisation," <i>IEEE Transactions on Mobile Computing</i> , pp. 1–12, 2021.
[ASH22]	G. C. Alexandropoulos, K. Stylianopoulos, C. Huang, C. Yuen, M. Bennis, and M. Debbah, "Pervasive machine learning for smart radio environments enabled by reconfigurable intelligent surfaces," <i>IEEE Proceedings</i> , 2022.
[AV20]	G. C. Alexandropoulos and E. Vlachos, "A hardware architecture for reconfigurable intelligent surfaces with minimal active elements for explicit channel



	estimation," in Proc. IEEE International Conference on Acoustics, Speech, and Signal Processing, Barcelona, Spain, 4–8 May 2020, pp. 9175–9179.
[AXW22]	An, J., Xu, C., Wu, Q., Ng, D. W. K., Di Renzo, M., Yuen, C., & Hanzo, L. Codebook-Based Solutions for Reconfigurable Intelligent Surfaces and Their Open Challenges. <i>IEEE Wireless Communications</i> , 2022.
[BSD14]	S. Barbarossa, S. Sardellitti, and P. Di Lorenzo, "Communicating while computing: Distributed mobile cloud computing over 5G heterogeneous networks," <i>IEEE Signal Proc. Mag.</i> , vol. 31, no. 6, pp. 45–55, 2014.
[CSL22]	V. Croisfelt, F. Saggese, I. Leyva-Mayorga, R. Kotaba, G. Gradoni and P. Popovski, "A Random Access Protocol for RIS-Aided Wireless Communications," <i>2022 IEEE 23rd International Workshop on Signal Processing Advances in Wireless Communication (SPAWC)</i> , Oulu, Finland, 2022, pp. 1-5, doi: 10.1109/SPAWC51304.2022.9833984.
[CSL23]	Croisfelt, V., Saggese, F., Leyva-Mayorga, I., Kotaba, R., Gradoni, G., & Popovski, P. "Random Access Protocol with Channel Oracle Enabled by a Reconfigurable Intelligent Surface." in <i>IEEE Transactions on Wireless Communications</i> , 2023 doi: 10.1109/TWC.2023.3268765. <i>arXiv preprint arXiv:2210.04230</i> .
[CDS23]	Croisfelt, V., Devoti, F., Saggese, F., Sciancalepore, V., Costa-Pérez, X. and Popovski, P., 2023. "An Orchestration Framework for Open System Models of Reconfigurable Intelligent Surfaces." <i>arXiv preprint arXiv:2304.10858</i> .
[DMC21]	P. D. Lorenzo, M. Merluzzi, E. C. Strinati, and S. Barbarossa, "Dynamic edge computing empowered by reconfigurable intelligent surfaces," <i>EURASIP Journal on Wireless Communications and Networking</i> , vol. 2022, no. 1, Dec. 2022.
[DMS22]	F. Devoti, P. Mursia, V. Sciancalepore and X. Costa-Pérez, "Taming Aerial Communication with Flight-assisted Smart Surfaces in 6G Era", in <i>IEEE Vehicular Technology Magazine</i> (to appear), 2023.
[GRT21]	R. Gupta, D. Reebadiya, S. Tanwar, "6G-enabled Edge Intelligence for Ultra - Reliable Low Latency Applications: Vision and Mission," <i>Computer Standards &amp; Interfaces</i> , vol. 77, pp. 103521, 2021.
[HHA20]	C. Huang, S. Hu, G. C. Alexandropoulos, A. Zappone, C. Yuen, R. Zhang, M. Di Renzo, and M. Debbah, "Holographic MIMO surfaces for 6G wireless networks: Opportunities, challenges, and trends," <i>IEEE Wirel. Commun.</i> , vol. 27, no. 5, pp. 118–125, Oct. 2020.
[HJU09]	R. Hunger, M. Joham, and W. Utschick, "On the MSE-duality of the broadcast channel and the multiple access channel," <i>IEEE Trans. Signal Process.</i> , vol. 57, no. 2, pp. 698–713, Feb. 2009.
[HYS20]	H. Lu, Y. Zeng, S. Jin and R. Zhang, "Aerial Intelligent Reflecting Surface: Joint Placement and Passive Beamforming Design With 3D Beam Flattening," in <i>IEEE Transactions on Wireless Communications</i> , vol. 20, no. 7, pp. 4128-4143, July 2021
[JAB22]	M. Jian, G. C. Alexandropoulos, E. Basar, C. Huang, R. Liu, Y. Liu, and C. Yuen, "Reconfigurable intelligent surfaces for wireless communications: Overview of hardware designs, channel models, and estimation techniques," <i>TUP and ITU Intelligent and Converged Networks</i> , vol. 3, no.1, pp. 1-32, March 2022.
[MCK22]	M. Merluzzi, F. Costanzo, K.D. Katsanos, G. C. Alexandropoulos, P. Di Lorenzo, Power Minimizing MEC Offloading with QoS Constraints over RIS-Empowered Communications, in <i>Proceedings of the IEEE Global Communications Conference (GLOBECOM)</i> , 2022.
[MDB21]	Mattia Merluzzi, Paolo Di Lorenzo, and Sergio Barbarossa, "Wireless edge machine learning: Resource allocation and trade-offs," <i>IEEE Access</i> , vol. 9, pp. 45377–45398, 2021.
[MFC21]	E. Moro, I. Filippini, A. Capone and D. De Donno, "Planning Mm-Wave Access Networks With Reconfigurable Intelligent Surfaces," <i>2021 IEEE 32nd Annual</i>





	International Symposium on Personal, Indoor and Mobile Radio Communications (PIMRC), 2021, pp. 1401-1407.
[MSB18]	M. Mozaffari, W. Saad, M. Bennis, Y. H. Nam, and M. Debbah, "A tutorial on UAVs for wireless networks: Applications, challenges, and open problems," <i>IEEE Communications Surveys and Tutorials</i> , vol. 21, no. 3, pp. 2334–2360, 2018.
[MSG21]	P. Mursia, V. Sciancalepore, A. Garcia-Saavedra, L. Cottatellucci, X. C. Pérez and D. Gesbert, "RISMA: Reconfigurable Intelligent Surfaces Enabling Beamforming for IoT Massive Access," in <i>IEEE Journal on Selected Areas in Communications</i> , vol. 39, no. 4, pp. 1072-1085, April 2021, doi: 10.1109/JSAC.2020.3018829.
[MDS21]	P. Mursia, F. Devoti, V. Sciancalepore and X. Costa-Pérez, "RISe of Flight: RIS-Empowered UAV Communications for Robust and Reliable Air-to-Ground Networks," in <i>IEEE Open Journal of the Communications Society</i> , vol. 2, pp. 1616-1629, 2021.
[MSL23]	Mo, L., Saggese, F., Lu, X., Wang, Z. and Popovski, P., 2023. Direct Tensor-based Estimation of Broadband mmWave Channels with RIS. <i>IEEE Communications Letters</i> .
[NTH19]	A. Ndikumana, N. H. Tran, T. M. Ho, Z. Han, W. Saad, D. Niyato, and C. S. Hong, "Joint communication, computation, caching, and control in big data multi-access edge computing," <i>IEEE Transactions on Mobile Computing</i> , pp. 1–1, 2019.
[PHS05]	C B Peel, B M Hochwald, and A L. Swindlehurst, "A Vector-Perturbation Technique for Near-Capacity Multiantenna MultiUE Communication - Part I: Channel Inversion and Regularization," <i>IEEE Trans. Commun.</i> , vol. 53, no. 1, pp. 195–202, Jan. 2005.
[PSZ21]	X. Pang, M. Sheng, N. Zhao, J. Tang, D. Niyato, and K.-K. Wong, "When UAV Meets IRS: Expanding Air-Ground Networks via Passive Reflection," <i>IEEE Wireless Communications</i> , vol. 28, no. 5, pp. 1–7, 2021.
[SAH22]	K. Stylianopoulos, G. C. Alexandropoulos, C. Huang, C. Yuen, M. Bennis, and M. Debbah, "Deep contextual bandits for orchestrating multi-UE MISO systems with multiple RISs," <i>IEEE International Conference on Communications</i> , Seoul, South Korea, 16–20 May 2022.
[SCK23]	Saggese, F., Croisfelt, V., Kotaba, R., Stylianopoulos, K., Alexandropoulos, G. C., & Popovski, P. (2023). A Framework for Control Channels Applied to Reconfigurable Intelligent Surfaces. <i>arXiv preprint arXiv:2303.16797</i> .
[SSH04]	Q. H. Spencer, A.L. Swindlehurst, and M. Haardt (2004). Zero-forcing methods for downlink spatial multiplexing in multiUE MIMO channels. <i>IEEE Transactions on Signal Processing</i> , 52(2), 461–471.
[SSH22]	K. Stylianopoulos, N. Shlezinger, P. del Hougne, and G. C. Alexandropoulos, "Deep-learning-assisted configuration of reconfigurable intelligent surfaces in dynamic rich-scattering environments," <i>IEEE International Conference on Acoustics, Speech, and Signal Processing</i> , Singapore, 22–27 May 2022.
[TKB22]	R. A. Tasci, F. Kilinc, E. Basar, and G. C. Alexandropoulos, "A new RIS architecture with a single power amplifier: Energy efficiency and error performance analysis," <i>IEEE Access</i> , 2022.
[WHA21]	L. Wei, C. Huang, G. C. Alexandropoulos, C. Yuen, Z. Zhang, and M. Debbah, "Channel estimation for RIS-empowered multi-UE MISO wireless communications," <i>IEEE Transactions on Communications</i> , vol. 69, no. 6, pp. 4144–4157, June 2021.
[WHG22]	L. Wei, C. Huang, Q. Guo, Z. Yang, Z. Zhang, G. C. Alexandropoulos, C. Yuen, and M. Debbah, "Joint channel estimation and signal recovery for RIS-empowered multi-UE communications," <i>IEEE Transactions on Communications</i> , under revision.
[XH21]	F. Xin and Y. Huo. "An Overview of Low latency for Wireless Communications: An Evolutionary Perspective," 2021 Online: <a href="https://arxiv.org/abs/2107.03484">https://arxiv.org/abs/2107.03484</a>
[XYH22]	X. Cao, B. Yang, C. Huang, G. C. Alexandropoulos, C. Yuen, Z. Han, H. V. Poor, and L. Hanzo., "Massive Access of Static and Mobile Users via Reconfigurable



**Document:** H2020-ICT-52/RISE-6G/D4.3

**Date:** 30/06/2023

**Status:** Final

**Security:** Public

**Version:** 1.0

	Intelligent Surfaces: Protocol Design and Performance Analysis," in IEEE Journal on Selected Areas in Communications, vol. 40, no. 4, pp. 1253-1269, April 2022, doi: 10.1109/JSAC.2022.3145908.
[ZZD22]	Y. Zhang, J. Zhang, M. Di Renzo, H. Xiao and B. Ai, "Reconfigurable Intelligent Surfaces With Outdated Channel State Information: Centralized vs. Distributed Deployments," in IEEE Transactions on Communications, vol. 70, no. 4, pp. 2742-2756, April 2022, doi: 10.1109/TCOMM.2022.3146344.
[ZSA23]	H. Zhang et al., "Channel Estimation With Hybrid Reconfigurable Intelligent Metasurfaces," in IEEE Transactions on Communications, vol. 71, no. 4, pp. 2441-2456, April 2023, doi: 10.1109/TCOMM.2023.3244213.